Title

Eutrophication to Aquaculture: Understanding Anthropogenic Nutrients and Kelp Suitability in Coastal Waters

Author

Hoel, Paige

Publication Date

2024

Peer reviewed|Thesis/dissertation

UNIVERSITY OF CALIFORNIA
Los Angeles

Eutrophication to Aquaculture: Understanding Anthropogenic Nutrients and Kelp Suitability in Coastal Waters

A dissertation submitted in partial satisfaction
of the requirements for the degree
Doctor of Philosophy in Atmospheric and Oceanic Science

by

Paige Hoel

2024

ABSTRACT OF THE DISSERTATION

Eutrophication to Aquaculture:
Understanding Anthropogenic Nutrients and Kelp Suitability
in Coastal Waters

by

Paige Hoel
Doctor of Philosophy in Atmospheric and Oceanic Science
University of California, Los Angeles, 2024
Professor Daniele Bianchi, Chair

Coastal oceans are among the most dramatic, engaging, and dynamic locations the Earth has to offer. The Southern California Bight (SCB) is among those locations, full of iconic coastlines, economically important fisheries, marine protected areas, ports and shipping lanes, a national park, and a massive tourism industry (Crosset et al., 2013). The SCB homes a diverse array of ecosystem types, ranging from rocky inner-tidal reef systems to giant kelp forests (Dailey et al., 1993). The SCB also supports a coastal population of 23 million (Ahn et al., 2005), making this a region of high human influence. Wastewater, rivers, and other sources of anthropogenic nutrients-enter this coastline in impressive quantities daily, heavily influencing the nutrient balance of coastal ecosystems. This dissertation provides a comprehensive analysis of anthropogenic nutrient influence in the context of micro and macro algae, first through a study of wastewater distribution, then through the impacts of kelp health through a nutrient stressed event. We also explore which regions would be most ideal to support kelp farming operations, amidst this anthropogenic influence.

In Chapter 2, we present a mechanistic analysis of components of oceanic wastewater discharge in the SCB. Our goal was to understand productivity in the nearshore coastal area

(0-15 km of coastline) and examine how it changes with and without chemical and physical components of the major wastewater plumes. We accomplish this by using five different scenarios of a wastewater model examining the mechanisms of buoyancy and inorganic nitrogen composition of outfall plumes. In this Chapter I demonstrate that the primary factors within treated wastewater that influence the productivity are the form of dissolved inorganic nitrogen and the buoyancy of the emitted plume. I show that the effects of increased buoyancy and nutrients on biomass are non-additive. Furthermore we identify a highly seasonal cycle in the influence of outfall scenarios on biomass in the surface ocean, with the largest impacts on NPP seen in the winter, when stratification in the water column is minimal.

In Chapter 3, we illuminate the influence of anthropogenic nutrient inputs on the recovery and growth of giant kelp forests in the SCB. To do this we examine kelp forests before and amidst the 2014-2016 marine heat wave (MHW) an event which caused a large loss of kelp forest area. From this study we identify a significant positive relationship of anthropogenic nutrients and kelp forest area maintained through the 2014-2016 MHW. Additionally, we find that during this period there are large portions of the SCB that would be nutrient limited if not for anthropogenic inputs.

In Chapter 4, we highlight the optimal locations in the SCB to cultivate giant kelp, and analyze the anthropogenic nutrient influence in these optimal locations. As demand for aquaculture, and in particular macroalgal cultivation, grows in the SCB, so has need for siting optimal locations. Our suitability analysis utilizes highly resolved biogeochemical models to find optimal nutrient (DIN), sunlight (PAR), and water temperature, as well as locational factors such as distance to port and depth in a rigorous spatial analysis framework, which builds upon others from this region. Our suitability results identifies highly suitable regions in the Santa Monica Bay and the Santa Barbara Channel. We find that of these two regions those located in Santa Monica Bay have the least potential interference with current kelp forest areas.

The dissertation of Paige Hoel is approved.

Kyle C. Cavanaugh

Tina Irene Treude

Kristen A. Davis

Daniele Bianchi, Committee Chair

University of California, Los Angeles

2024

To the ocean . . .

to the shores that stole my heart

the waves that captured my wonder

and to the others who worship it as I do.

TABLE OF CONTENTS

LIST OF FIGURES

LIST OF TABLES

ACKNOWLEDGMENTS

This dissertation would not be possible without the mentorship of my advisor, Daniele Bianchi. I am deeply appreciative for his guidance and patience through my scientific journey. I am appreciative of Allison Moreno, whos mentorship brought me to where I am today. I am grateful for the effort and guidance of my collaborators and committee. Beyond my immediate academic family I attribute much of my success to the Center for Diverse Leadership in Science (CDLS), which has empowered me to grow my skills as a teacher, and have given me a sense of community through the isolating ocean of a PhD.

I have been lucky enough to serve aboard two oceanographic cruises amidst my graduate student career. I would like to thank the crew and scientists aboard the University of Washington R/V Thomas G. Thompson on the GO SHIP A20 cruise (March - April 2021), in addition to the crew and scientists aboard the NOAA R/V Okeanos Explorer expedition EX-22-03 (March 2022).

Beyond my oceanographic endeavors, I owe my success to many communities and relationships. First and foremost, my parents, Kristen and Erik Hoel, who have shown me the meaning of lifelong learning and love, and my brother, Grant Hoel, another lifelong learner and more importantly my goofball companion. To my best friend, Brennen, who has made me believe in, above other things, myself. And finally to the North County Ocean Swimmers, who are as crazy as ocean lovers come.

VITA

2014–2018	B.S. (Earth Science) High Honors Distinction B.S. (Physical Geography), University of California, Santa Barbara
2018–2019	Scientific Visitor, National Center for Atmospheric Research
2019–2022	M.S. (Atmospheric and Oceanic Sciences), UCLA.
2020–2024	Teaching Fellow, Atmospheric and Oceanic Science Department, UCLA.
2019–present	Research Assistant, Atmospheric and Oceanic Science Department, UCLA.

PUBLICATIONS

Hoel, P., Cavanaugh, K., Davis, K., Freider, C., Renolyds, A., & Bianchi, D. Navigating Coastal Complexities: Advanced GIS Analysis for Kelp Aquaculture Suitability in the Southern California Bight, *in preparation for Sustainability Science 2024*

Hoel, P., Moreno, A., & Bianchi, D. Mechanisms controlling lower trophic ecosystem response to ocean outfall discharges: role of nitrogen form and freshwater volume, *in review Regional Studies in Marine Science 2024*

Hoel, P., Freider, C., Cavanaugh, K., & Bianchi, D. Anthropogenic nutrient sources influence kelp canopies during a marine heat wave, *in review Marine Pollution Bulletin 2024*

Hoel, P., Fredston, A., & Halpern, B. An Evaluation Framework for Risk of Coastal Marine Ecological Diversity Loss From Land-Based Impacts, *Frontiers in Marine Science 2022*

Hoy, S., Peliks, M., Freitas, D., Gillespie, T., Wilkins, C., **Hoel, P.**, ... & Egan, K Mapping Data Acquisition and Processing Summary Report: EX-22-03, Puerto Rico Mapping and Deep-Sea Camera Demonstration (Mapping and Tech Demonstration)., *NOAA technical report 2023*

CHAPTER 1

Anthropogenic impacts on micro- and macro-algae in the SCB

The injection of large quantities of nitrogen into the ocean, primarily throughout the widespread use of agricultural use of fertilizers, has led widespread eutrophication, an exaggeration of phytoplankton growth due to excess nutrients (Vitousek et al., 1997). The most significant effects of this issue occur at river mouths and urbanized coastal areas where point sources (like waste water effluent and storm drains) and non point sources (such as runoff from agriculture or construction) introduce dissolved inorganic nitrogen (DIN) to marine environments(Carpenter et al., 1998). The increase in DIN and subsequent blooms of algae, can have negative impacts on the diversity of the region, especially when harmful species of phytoplankton dominate (Vitousek et al., 1997). This proliferation can lead to a reduction or depletion of oxygen (hypoxia) (Rabouille et al., 2001), a reduction in resource use efficiency (Chai et al., 2020), and ultimately lead to the complete loss of aquatic animals (Howarth et al., 2011).

In this introductory chapter we provide a comprehensive overview of the influence of anthropogenic nutrients within the Southern California Bight (SCB), and the ecological and economic role of giant kelp in this region. We also discuss the changes in nutrient dynamics triggered by the 2014-2016 marine heat wave (MHW). This chapter sets the stage for subsequent chapters by giving the necessary background and context crucial for the research conducted within this dissertation.

1.1 Anthropogenic influence in the SCB

Human activities significantly influence nutrient levels in the southern California Bight (SCB), substantially impacting regional productivity and ecosystem health. Research indicates that phytoplankton biomass in 0-15 km coastal band of the SCB is doubled due to nutrients from anthropogenic sources (Kessouri et al., 2021a), including wastewater effluent, and to a lesser extent, runoff from infrequent rain events (Sutula et al., 2021a). In this zone, the contributions of nitrogen from anthropogenic sources are equivalent to natural nitrogen sources (Howard et al., 2014), especially during non-upwelling periods, highlighting the substantial role of anthropogenic nutrients.

The dynamics of these nutrients are not only influenced by their quantity, but also by their form. Unlike the nitrate predominantly brought to the surface by natural upwelling, anthropogenic sources typically contribute ammonium- a form of inorganic nitrogen that is highly bioavailable, and more readily uptaken by phytoplankton. This difference in nutrient form can lead to faster development of blooms, and favor phytoplankton species that thrive on ammonium, potentially altering community compositions and accelerating eutrophication processes.

These combined interactions pose significant challenges in disentangling the combined effects of large quantities of DIN, growth of biomass, and changes in water clarity on the pelagic health of the SCB. Furthermore, the situation is often complicated by other factors such as climate change, local pollution, and natural variability (Paerl et al., 2014), which intertwine to degrade ocean health. Comprehensive ecosystem models demonstrate that the SCB has experienced a deterioration in ocean health due to these compounded factors (Halpern et al., 2009). It is evident that left unchecked, anthropogenic nutrients will continue to change the health of ecosystems in the global ocean and the SCB. Mitigation, management, and reduction strategies of human nutrient inputs to the coastal ocean are needed.

1.2 Giant kelp in the SCB

Giant kelp (*Macrocystis spp.*) is a keystone species that dominates kelp forests along the west coast of South America and North America (Schiel, 2015). In the SCB, giant kelp is highly resilient, and forms the basis of a highly bio-diverse community, with over 200 species of algae, invertebrates, fishes, and mammals commonly found within kelp forests (Graham, 2004; Dailey et al., 1993). Kelp is a highly productive species, growing up to 45m long. Kelp plants can live 2-3 years, while fronds live 4-6 months (Reed et al., 2008). Kelp is a relatively ephemeral species which often experiences mortality during large storms and events characterized by a significant wave height (Reed et al., 2011, 2008). Kelp grows in a wide range of temperatures globally. In southern California, optimal growth is documented between temperatures of 14 °C and 20 °C (Zimmerman & Kremer, 1986). As a result the cold nutrient rich water delivered from the California Current System (CCS) and water supplied from wind driven upwelling make a suitable temperature range for giant kelp in the SCB. Beyond their optimal growth temperature, kelp begin to die off around 20 °C as juveniles and 23 °C as adults (Schiel, 2015; Cavanaugh et al., 2019).

Giant kelp exhibits remarkable resilience and can capitalize on episodic supplies of nutrients. Seasonally, growth is highest in the spring, when nutrients are ample and there is less shading due to algal canopies (Reed et al., 2008). Growth is typically lowest in the winter, when nitrate is plentiful but light is limited. In the summer and fall, despite the low mean nitrate concentration, there is no noticeable decline in growth rate (Brzezinksi et al., 2013). Previous observations suggest that only when nitrate reaches concentrations below 1-2 µmol L^{-1} is growth not sustained in southern California (Brzezinksi et al., 2013). More recent findings, however, show that during periods of low nitrate availability, typically co-occurring with high SST in the SCB, sources of nitrogen unrelated to temperature such as ammonium and urea, can continue sustaining kelp growth (Brzezinksi et al., 2013). Unlike further north in the CCS, which can experience widespread deforestation due to purple urchins (otherwise known as "urchin barrens"), the SCB rarely experiences prolonged or massive deforesta-

tion via biological influences (Steneck et al., 2002), likely due to ecosystem controls upon predators and herbivores that can potentially damage kelp plants.

Kelp maintains a low capacity to store nutrients (Zimmerman & Kremer, 1984). Laboratory and field studies suggest that giant kelp can maintain a healthy structure under nutrient limitation for up to 2-3 weeks until its growth is impacted (Reed et al., 2016). During periods of diminished nitrogen supply, kelp compensates by decreasing its tissue nitrogen content. Conversely, kelp's ability to grow in periods of high nutrient availability is well documented (Zimmerman & Kremer, 1984).

Over the past century, the use of kelp has expanded from a food source to include applications in medicines, fertilizers, bio-plastics, textiles, and bio-fuel (Buschmann et al., 2017; Frieder et al., 2022). Seaweed aquaculture, the fastest growing component of global food production (Duarte et al., 2017), is projected to significantly benefit global food security as it expands. Within the century demand for kelp has also developed as a tool for anthropogenic nutrient remediation (Buschmann et al., 2017) as well as a mechanism for carbon dioxide sequestration (Duarte et al., 2017; Froehlich et al., 2019). Kelp farming is in its infancy in the United States compared to the major producers of seaweed such as Asia and Europe (Delaney et al., 2016). The US Department of Energy recently invested over 21 million USD to develop macroalgal farming for biofuel and carbon remediation (Rugiu et al., 2021), while the US Department of Agriculture has also invested in companies for kelp cultivation as a food source (Lawrence, 2023). In addition to these public investments, private development of kelp farming in the US has gained traction in the northeast United States (Fantom, 2023; Piconi et al., 2020).

Beyond its obvious importance as a keystone species in the SCB, attention is being drawn to kelp for these practical benefits. In the SCB, natural kelp has had a rich history of research (LTER et al., 2022; Cavanaugh et al., 2011; Bell et al., 2015, 2020a; Bell & Siegel, 2022), and this region is gaining momentum as a potential location for the kelp farming industry (Kübler et al., 2021; Morris Jr, 2021).

1.3 The 2014-2016 MHW

Between 2014-2016 the west coast of North America experienced a significant anomaly in sea surface temperatures (SSTs), sometimes referred to as "the Blob". SST in southern California reached 6.2 °C above average (Gentemann et al., 2017), resulting in marked stratification. This stratification impeded upwelling of denser, nutrient rich deep water, critical for supporting California Current ecosystems. The diminished nutrients led to lower phytoplankton production and a proliferation of gelatinous zooplankton. These modifications to primary and secondary producers caused shifts higher up in the food chain, impacting fish (Rogers et al., 2021), birds, and mammals (Gentemann et al., 2017).

The marine heat wave (MHW) triggered kelp mortality across the SCB, with significant fluctuations in effects over time and space (Cavanaugh et al., 2019). During this event, large declines in canopy coverage were seen in the summer and fall of 2015, and recovery was small in the winter and spring of 2016. Studies on the recovery of kelp forests to this MHW in the SCB displayed high variation, and provided further evidence that giant kelp is not only resilient in the SCB, but also may be adapted to local nutrients and conditions (Cavanaugh et al., 2019).

Occurrence of MHW have increased, a trend that is expected to continue as a result of climate change (Laufkötter et al., 2020). As these events become more common it is imperative to understand how keystone species such as giant kelp will respond. This knowledge is essential not only for predicting future impacts on kelp forests but also for managing and potentially mitigating the effects of anthropogenic nitrogen inputs on these vital ecosystems. The resilience of giant kelp during the MHW provides a unique opportunity to study how nutrient dynamics under stress conditions influence kelp ecosystems and their broader ecological roles.

1.4 Science Questions and outline

In this initial chapter, we summarized the mechanism of eutrophication and its influence

on phytoplankton and kelp within the SCB. We reviewed how the presence of kelp has played a pivotal role in the environment, and may play a larger role in our economy as demand grows for its cultivation for many purposes, from carbon dioxide sequestration to human consumption. The SCB, and the kelp within it, is not impervious to natural nutrient disruption, this becoming evident in the 2014-2016 MHW. This MHW disrupted all levels of the food chain, and resulted in a non uniform die-off of kelp. The pattern and cause of the kelp die off remain poorly understood, as the nutrient decrease was relatively uniform throughout the Bight.

We begin our study of anthropogenic influences in the coastal zone of the SCB by investigating the impact that wastewater, the primary point source of anthropogenic nutrients, has throughout the SCB. Specifically, we explore how nitrogen in wastewater and the volume of freshwater released influence coastal ecosystems. We use a numerical model to quantify the changes in net primary production surrounding large publicly owned treatment works (POTWs).

Specifically, we aim to answer the following questions:

1. What is the effect of outfall freshwater volume on NPP and phytoplankton biomass in the nearshore coastal zone?

2. How does nitrogen form affect the impact of outfall water on the coastal environment?

To this end, we develop a series of idealized scenarios utilizing an ocean biogeochemical model of the SCB, each intended to modify the standard nutrient and/or physical properties of typical wastewater, and compare this to our control. We find that nutrient form plays a large role in the magnitude of productivity stimulation, with ammonium based DIN scenarios generating 40% more productivity than nitrate based scenarios. Furthermore, we find that more diluted scenarios will distribute productivity over a wider area than concentrated ones with an equivalent amount of nutrients. Concentrated scenarios had a higher influence in embayed regions.

In Chapter 3, in order to better understand the nuances of the relationship of giant kelp

(*Macrocystis pyrifera*) forests with anthropogenic nutrients in the SCB, we study the spatial distribution of kelp amidst the 2014-2016 MHW. This period provides an insight to the role of anthropogenic nutrient sources in mitigating the effects of reduced natural nutrient availability.

Specifically, we delve into the patterns of kelp forests and their nutrient dependencies amidst a MHW. This exploration is structured around the following key questions:

1. What was the extent of nutrient limitation in kelp forest canopy areas during the 2015-2016 MHW?

2. What was the influence of anthropogenic DIN sources in kelp forest canopy areas during the 2015-2016 MHW?

To answer these questions we use a coupled physical-biogeochemical model to understand the magnitude and composition of nutrients throughout the SCB. To understand the patterns of kelp forest area we use a data-set of kelp area and distribution based on satellite imagery. We find that anthropogenic sources supply DIN adequate for kelp growth throughout our study regions during periods in which natural supplies would fall below growth thresholds. We also find that kelp forests with greater days of anthropogenic influence during the MHW sustained a greater percentage of area relative to their pre-MHW area.

In Chapter 4, to address the burgeoning interest in macroalgal farming and its potential societal benefits, we develop a GIS-based farm suitability framework. This model not only builds upon existing frameworks, but also leverages high resolution nutrient data, offering a refined tool for site selection in the SCB.

The objectives for our GIS suitability summary in Chapter 4 are as follows:

1. Create a GIS framework for selecting suitable oceanic macroalgal farming locations and apply it to a case study in the SCB

2. Examine the influence of anthropogenic nutrients among other variables within the highest suited regions

3. Consider ecological interactions by identifying potential overlap with current kelp forest area within the SCB

In our suitability model, we create kelp growth and location sub-models, and analyze the results from multiple iterations with different variable importance ranks. Our analysis led to the identification of two primary clusters of highly suitable locations for giant kelp farming in the SCB: one in Santa Barbara Channel, and the other within Santa Monica Bay. Of these highly suitable sites the Santa Barbara regions had the highest chance of interaction with current kelp forests, suggesting careful management is needed to balance development and conservation. Conversely, highly suitable locations within the Santa Monica Bay were notable for having a higher proportion of nutrients from anthropogenic sources, pointing toward their dual potential for aquaculture and anthropogenic remediation.

In Chapter 5, I summarize the work conducted within this thesis. I draw attention to the implications of my results and discuss future work needed.

CHAPTER 2

Mechanisms controlling lower trophic ecosystem response to ocean outfall discharges: role of nitrogen form and freshwater volume

This chapter contains the submitted manuscript Hoel et al. (2024b), with formatting changes.

2.1 Introduction

Eutrophication of coastal ecosystems is a global environmental issue (Paerl et al., 2014) driven in large part by an increase in anthropogenic nutrient loading to the coast (Cloern, 2001). Anthropogenic nutrient inputs can have detrimental effects on coastal ecosystems, including harmful algal blooms (Cloern, 2001), hypoxia (Breitburg et al., 2018; Kessouri et al., 2021a), ocean acidification (Cai et al., 2011), and shifts in ecosystem structure (Diaz & Rosenberg, 2008; Doney et al., 2012; Nixon & Buckley, 2002). In estuaries and semi-enclosed seas, the effects of anthropogenic nutrient loading on coastal eutrophication are well studied (Salbitani & Carfagna, 2021; Smith et al., 1999; Vitousek et al., 1997). However, in open embayments and open coastlines, the fate and effects of anthropogenic nutrient inputs have not been examined in the same detail, particularly under the assumption that strong currents and rapid mixing disperse nutrients away from the coast before eutrophication symptoms manifest (Tuholske et al., 2021).

Ocean outfalls, a primary means of disposal of municipal and industrial wastewater in coastal communities around the world (Roberts et al., 2010), are designed to take advantage of this vigorous ocean circulation. Wastewater effluents are discharged via outfall pipes typi-

cally below the euphotic zone and are engineered for maximum dilution (Roberts et al., 2010). However, few studies have characterized the effect of anthropogenic nutrients discharged via ocean outfalls on coastal eutrophication (Uchiyama et al., 2014). Observational techniques like remote sensing and dye release have become more prevalent in recent years, mostly to detect wastewater plumes (Hunt et al., 2010; Wang et al., 2022). These techniques, however, have limitations in their vertical and temporal resolution, especially because nutrients from wastewater plumes can be dispersed far-field of the dye signature. In addition, these techniques cannot disentangle the relative influence of wastewater versus oceanic sources of nutrients on primary production (Kessouri et al., 2021a). Kessouri et al. (2021a) used high resolution biogeochemical models to study the fate of anthropogenic nutrients and their impacts on productivity in the coastal zone. The results shed light on the combined anthropogenic effect on coastal regions, including outfalls, but do not disentangle two major effects of outfalls: introduction of nutrients in a coastal, potentially oligotrophic environment, and increased freshwater volumes, which may alter buoyancy and circulation. In order to gain a comprehensive understanding of wastewater influence on productivity, it is important to disentangle the mechanisms that control nutrient load and dispersion in the euphotic zone, and quantify resulting changes in production in the surrounding environment.

In municipal wastewater, dissolved inorganic nitrogen (DIN) is the largest nutrient constituent, generally in the form of ammonium and nitrate (Mateo-Sagasta et al., 2015). In municipal wastewater discharges, primary or secondary treated effluent DIN is typically in the form of ammonium (Sutula et al., 2021b). Debate has emerged over whether converting DIN to nitrate is environmentally less impactful, albeit at a greater cost, because of reduced toxicity, and because nitrate is taken up on longer timescales than ammonium (Glibert et al., 2016; L'Helguen et al., 2008; McLaughlin et al., 2017; Salbitani & Carfagna, 2021). The volume of wastewater released also causes a significant modification to the immediate area, with warmer temperatures and lower salinity, resulting in a buoyant anomaly (Ramos et al., 2007; Reifel et al., 2013; Washburn et al., 1992), which could entrain deep, nutrient-rich water to the euphotic zone. Numerical models can help tease apart the influence of freshwater input and anthropogenic nitrogen sources on the surrounding productivity. Models have been

used to study the physical fate of wastewater from plumes in idealized conditions (Ho et al., 2021), stratified coastal ocean conditions (Bondur et al., 2018) and in riverine environments (Roberts & Villegas, 2017). However, models have yet to be used to assess the relative influence of buoyancy and nutrients within wastewater plumes, and their consequences for wastewater-driven eutrophication.

The Southern California Bight (SCB) is an ideal location for a modeling study of ocean wastewater inputs in an open embayment. In this region, 19 ocean outfalls discharge treated municipal wastewater effluent from 23 facilities, from a coastal human population of 23 million, roughly doubling the amount of nitrogen from natural oceanic sources (Howard et al., 2014; Sutula et al., 2021b). Robust monitoring programs have quantified terrestrial wastewater inputs to the coastal ocean over time (Sutula et al., 2021b; Howard et al., 2014; Stull, 1995), and changes are documented by a large body of in situ studies (Bond et al., 1973; McLaughlin et al., 2017; Warrick et al., 2007; Reifel et al., 2013). Modeling studies have been conducted and validated in this region (Kessouri et al., 2021a; McLaughlin et al., 2021), and the varied geography and bathymetry provide a diverse physical backdrop for analysis (Dong et al., 2009; Schiff et al., 2019). Upwelling is acknowledged as the primary driver of phytoplankton productivity throughout the Bight. In the coastal band, however, nitrogen from wastewater outfalls and rivers has a distinct, and sometimes dominating, influence (Corcoran et al., 2010; Howard et al., 2014; Kim et al., 2009). For example, wastewater inputs have been shown to change the phytoplankton community structure (Corcoran et al., 2010), e.g., by stimulating blooms of dinoflagellates (Reifel et al., 2013). Furthermore, water reclamation strategies for direct potable reuse in Los Angeles and Orange Counties have already begun to change the volume of wastewater discharged in the SCB (Ho, 2023). Addressing the role of nutrient content, nitrogen form, and freshwater volume on algal productivity could provide further insights on the effects of wastewater inputs, potentially informing coastal water quality management.

To test the influence of wastewater inputs on coastal productivity, we devise a set of idealized modeling experiments that isolate the effects of nutrient form and freshwater volume. These experiments were conducted by focusing on the outfalls of four large publicly owned

treatment works (POTW) in the SCB (Table 2.2), which collectively contribute one billion gallons of wastewater a day to the coastal region (Sutula et al., 2021b). We implement a series of scenarios with a physical-biogeochemical model of the SCB previously used to study coastal eutrophication (Kessouri et al., 2021b,a, 2020), with extensive physical and chemical validation (Deutsch et al., 2021; Kessouri et al., 2021b). Unlike previous work, we focus on the large wastewater outfalls only, rather than considering the additional effect of rivers and other minor point sources. To disentangle the influences of differing nutrient form and freshwater volume, we compare idealized scenarios to a control scenario over a seasonal cycle. We investigate whether freshwater plumes are capable of entraining nutrients to the euphotic zone, and quantify whether freshwater volume correlates with a wider horizontal spread of productivity. To test the influence of nutrient form, we determine whether a scenario that simulates the nitrogen loading from these four POTW, with DIN predominantly as ammonium, stimulates more productivity than one with all DIN as nitrate.

2.2 Material and Methods

2.2.1 Study Area

Our study domain, the SCB, stretches from Punta Colonet, Mexico, to Point Conception, California, and supports a coastal population of 22.7 million people (Crosset et al., 2013). The SCB is a dynamic region with different scales of physical circulation and properties that influence the dispersal of wastewater plumes and their environmental consequences (Di Lorenzo, 2003). A large scale equatorward flow from the California Current System (CCS) influences the SCB year round (Checkley & Barth, 2009). Alongside this flow, alongshore winds strengthen from winter to summer and drive coastal upwelling. In the nearshore region, a southward equatorward jet develops in winter (Di Lorenzo, 2003), while a surface poleward flow develops in summer and fall, producing variable patterns of water transport over the course of the year. The SCB is also influenced by cyclonic and anticyclonic eddies (Chenillat et al., 2018; Dauhajre et al., 2017) that vary by season (Dong et al., 2009). Stratification develops in the summer as the alongshore winds decrease and sea surface temperature

	HTP	JWPCP	OCSD	PLWTP
Depth (m)	60	57	57	94.5
Flow (m^{-3} day^{-1})	1.23*10^6	1.26*10^6	9.05*10^5	6.58*10^5
Temperature (C)	23.9	25.6	25	22.3
Salinity (PSU)	1.5	1.3	3.3	1.5
NH_4^+ (mmol m^{-3})	2053	2174	1864	1979
NO_3^- (mmol m^{-3})	49	7	400	29

Table 2.1: Input values for each of the four large POTW outfalls in the SCB. Values were acquired from 1999-2000 averages of reported terrestrial flux dataset gathered by Sutula et al. (2021b). Flow, temperature, and salinity inform the freshwater component of model scenarios. NH_4^+ and NO_3^- inform the DIN component of model scenarios.

rises in the euphotic zone (Dong et al., 2009).

In the SCB, the majority of wastewater is disposed via four large outfalls that discharge along the upper continental shelf at depths between 60 and 94.5 m, plus a series of minor outfalls that discharge closer to shore and at shallower depths. The four large POTW outfalls alone account for 86% of the wastewater effluent volume discharged into the SCB (Sutula et al., 2021b). The DIN-rich water in these outfalls accounts for 92% of total terrestrial anthropogenic nitrogen loading in the coastal SCB, and 75% of total nitrogen loading when taking into consideration both anthropogenic and non-anthropogenic sources (Sutula et al., 2021b). Not only is the effluent characterized by higher DIN concentration compared to the ambient seawater, but it is also significantly less saline (Table 1), and therefore less dense and potentially more buoyant (Uchiyama et al., 2014). These four large wastewater POTW outfalls consist of the Hyperion Treatment Plant (HTP), located in Santa Monica Bay, Joint Water Pollution Control Plant (JWPCP) in San Pedro Bay, Orange County Sanitation District (OCSD) in Orange County, and Point Loma Water Treatment Plant (PLWTP) in San Diego (Table 2.1).

Both the OCSD and HTP outfall sit approximately 5 miles off-shore on the continental shelf, with multi-port, bottom-mounted diffusers at 60 m and 57 m depth, respectively. The

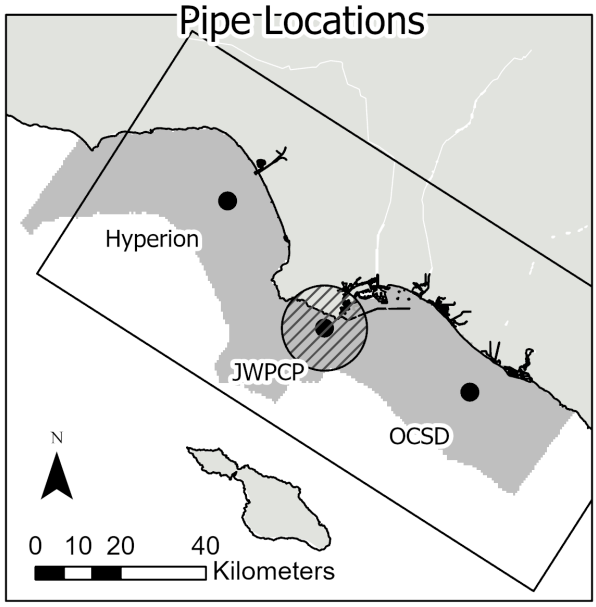

Figure 2.1: Study domain. Locations of the Hyperion, Joint Water Pollution Control Plant (JWPCP), and Orange County Sanitation District (OCSD) wastewater outfalls. The grey shading shows the nearshore coastal region used for the analysis. The black box outlines the domain used to plot maps of net primary productivity (NPP) changes. The grey stippling around the JWPCP outfall indicates the area for the analysis of vertical profiles.

JWPCP outfall is located near San Pedro Bay, at 57 m depth. These three outfalls are in relatively close proximity to one another (within 40 km of each other). The PLWTP outfall is located at a depth of 94.5 m. Our analysis primarily focuses on three outfalls at around 60 m depth (HTP, JWPCP, and OCSD), given their distinct discharge behaviors and influences compared to deeper outfalls (Kessouri et al., 2021a). These shallower outfalls have plumes that more readily reach the surface during winter mixing and upwelling events (Fig. 2.1). Our focus on major outfalls also aligns with the extensive literature on this specific section of the SCB (Kessouri et al., 2021a; McLaughlin et al., 2021; Nezlin et al., 2018; Ahn et al., 2005).

2.2.2 Model Background and Setup

The numerical physical-biogeochemical ocean model used for this study consists of the Regional Ocean Modeling system (ROMS) (Shchepetkin & McWilliams, 2005) coupled to the Biogeochemical Elemental Cycling model (BEC) (Moore et al., 2004). ROMS is a widely adopted regional ocean model with a long history of application to the California Current System (CCS) (Capet et al., 2008a,b,c; Renault et al., 2021; Siedlecki et al., 2021) and specifically the SCB (Dong et al., 2009; Dong & McWilliams, 2007). ROMS captures submesoscale processes occurring at horizontal scales down to hundreds of meters or less (Dauhajre et al., 2017), and is able to resolve the far field transport of wastewater plumes once they are entrained in the water column (Kessouri et al., 2021a; Uchiyama et al., 2014). BEC is a widely adopted ocean biogeochemical model (Moore et al., 2013, 2004; Nissen et al., 2018) that simulates the cycles of nutrients (nitrogen, phosphorus, silicon, iron), carbonate chemistry, oxygen, three phytoplankton groups (small phytoplankton, diatoms, and diazotrophs) and one zooplankton group.

The submesoscale-resolving configuration of ROMS-BEC for the SCB used here is based on progressive dynamical downscaling of a series of nested coast-wide simulations (Deutsch et al., 2021; Kessouri et al., 2020; Renault et al., 2021), and has been extensively validated against in-situ and satellite observations. The model nests begin with a 4 km resolution configuration for the entire CCS, developed and evaluated by Renault et al. (2021) and Deutsch et al. (2021). A second finer resolution nest at 1 km for the southern CCS was developed by Kessouri et al. (2020) and further evaluated by Damien et al. (2023). Finally, a submesoscale-resolving configuration at 300 m resolution was developed for the SCB, as detailed in (Kessouri et al., 2021b). This downscaling approach effectively transfers large-scale physical and biogeochemical patterns to the coastal domain, ensuring accurate representation of submesoscale circulation. This is crucial for capturing the dispersal of wastewater plumes along the continental shelf. The validation provided by Kessouri et al. (2021b) shows that the model captures natural and anthropogenic biogeochemical gradients, making it a valuable tool to study the effects of terrestrial inputs on coastal zone ecosystem and water

quality Kessouri et al. (2021a). We refer the reader to Kessouri et al. (2021b) for specific model rationale, setup, boundary conditions, and forcings. The "parent" models at 4 km and 1 km resolution span the period of 1997-2017. We focus on the years 1999 to 2000 for our study. The model is run at a horizontal resolution of 300 m, with 60 terrain-following vertical levels. The time-step of the model is 30 s and output is saved as 1 day averages. Atmospheric boundary conditions come from a simulation with the Weather Research and Forecast model (Skamarock & Klemp, 2008) run at a resolution of 6 km (Renault et al., 2020). Initial and boundary conditions for oceanic variables are taken from the 1 km-resolution simulation (Kessouri et al., 2020).

The BEC model resolves three phytoplankton functional groups: large phytoplankton (requiring silicon, thus akin to diatoms), diazotrophs, and small phytoplankton. In BEC, the uptake rates for nitrate ($J^{uptake}_{P,NO3}$) and ammonium ($J^{uptake}_{P,NH4}$) for a generic non-diazotroph phytoplankton, P, representing either small phytoplankton or diatoms, are given by:

$$J^{uptake}_{P,NO3} = Q_{N:C} \cdot \frac{V^P_{NO3}}{V^P_{NO3} + V^P_{NH4}} \cdot J^{photo}_{P,C} \tag{2.1}$$

$$J^{uptake}_{P,NH4} = Q_{N:C} \cdot \frac{V^P_{NH4}}{V^P_{NH4} + V^P_{NO3}} \cdot J^{photo}_{P,C} \tag{2.2}$$

Where $Q_{N:C}$ is the phytoplankton nitrogen to carbon ratio, set to the Redfield value of 106:16, and $J^{photo}_{P,C}$ is the the rate of carbon uptake by photosynthesis, calculated in BEC as a function of nutrient limitation (including phosphorus, nitrogen, iron, and, for diatoms, silica), light limitation, a phytoplankton chlorophyll to carbon ratio, and phytoplankton biomass (Moore et al., 2004; Deutsch et al., 2021). The nitrate and ammonium limitation terms V^P_{NO3} and V^P_{NH4} encapsulate saturation dynamics for nutrient uptake, and follow a typical Michaelis-Menten dynamics described by the equations:

$$V^p_{NO_3} = \frac{\frac{NO_3^-}{K_{NO_3}}}{1 + \frac{NO_3^-}{K_{NO_3}} + \frac{NH_4^+}{K_{NH_4}}} \tag{2.3}$$

$$V^{p}_{NH_4} = \frac{\frac{NH_4^+}{K_{NH_4}}}{1 + \frac{NH_4^+}{K_{NH_4}} + \frac{NO_3^-}{K_{NO_3}}} \tag{2.4}$$

Here, the half saturation constants for ammonium and nitrate are respectively K_{NH_4} = 0.01 mmol m^{-3} and K_{NO_3} = 0.5 mmol m^{-3} for small phytoplankton, and K_{NH_4} = 0.1 mmol m^{-3} and K_{NO_3} = 2.5 mmol m^{-3} for diatoms. For each phytoplankton group, the half saturation constant for ammonium is smaller than that for nitrate, reflecting preferential uptake of ammonium (Mulholland & Lomas, 2008). Based on equations 2.1-2.4, the relative uptake of ammonium and nitrate by phytoplankton is controlled by the ratio of nitrate to ammonium in seawater, relative to their half saturation constants. For typical nutrient concentrations found in the SCB, this results in specific ammonium uptake rates that are nearly an order of magnitude larger than nitrate uptake rates. In turn this translates into residence times for ammonium in seawater of the order of a day or less, and of nitrate on the order of several days.

We note that previous studies of wastewater effluent in the SCB found that nitrate was utilized quickly, on the order of one day, at the surface (Reifel et al., 2013), although they may reflect DIN-limited conditions. Recent literature also found high rates of nitrification around SCB outfalls (McLaughlin et al., 2021). Although we do not directly analyze nitrification rates in this analysis, the model does account for this process (Kessouri et al., 2021b), which is reflected in the concentrations of nitrate and ammonium. In our model, higher nitrification rates result in faster conversion of ammonium to nitrate, leading to lower ammonium and higher nitrate concentrations, consistent with observations.

2.2.3 Model Scenarios and Comparisons

We designed a series of idealized model scenarios to disentangle the impacts of wastewater freshwater volume, nutrient content (freshwater plume with nutrients vs. without nutrients), and nutrient form (ammonium vs. nitrate). We focus on inputs from the large POTW outfalls only, because they largely dominate wastewater inputs in the SCB. We run five model configurations with different combinations of these factors (listed in Table 2.2) to

Model Scenarios		
	Freshwater	**DIN**
Control (CTRL)	No freshwater volume	No DIN
Fresh (FRE)	Full freshwater volume in POTW emissions	No DIN
Nitrate (NIT)	Full freshwater volume in POTW emissions	DIN emission in the form of NO_3^-
Nutrient (NUT)	No freshwater volume	Standard DIN emission from POTW outfall (mostly NH_4^+)
Outfall (OUT)	Full freshwater volume in POTW emissions	Standard DIN emission from POTW outfall (mostly NH_4^+)

Table 2.2: Presence of key characteristics in the four mechanistic model scenarios and control scenario. Values for freshwater volume and DIN for each POTW outfall are given in Table 2.1.

identify the effects of wastewater characteristics on nutrient delivery to the euphotic zone, primary production, and the biogeochemistry of the nearshore coastal region.

The Control (CTRL) scenario does not include land-based point sources (POTW ocean outfalls and rivers), and thus removes the effects of wastewater inputs. This simulation, along with the other four, still represents large-scale anthropogenic influences via global atmospheric carbon dioxide forcing, based on the observed record from the Mauna Loa Observatory, and the resulting surface ocean warming and acidification (Deutsch et al., 2021).

The Fresh (FRE) scenario includes only freshwater flux equivalent to the wastewater discharge from the four large POTW without nutrients and other constituents. This scenario

is designed to examine the role of freshwater inputs alone in altering water column stratification, potentially affecting the physical circulation and the delivery of nutrients to surface waters, e.g., by entrainment of ambient nutrients by buoyant plumes.

The Outfall (OUT) scenario simulates realistic wastewater inputs from the four POTW outfalls, with nutrient inputs identical to reported values. Consistent with effluent characteristics (Sutula et al., 2021a), inorganic nitrogen is introduced primarily in the form of ammonium, with a small fraction of nitrate (Table 2.1). The purpose of this simulation is to examine the combined effect of DIN and freshwater.

The Nitrate (NIT) scenario is identical to the OUT scenario, except that nearly all ammonium is converted to nitrate. A negligible amount of ammonium is included for computational reasons (0.01 mmol m^{-3}). The NIT scenario is designed to investigate the effects of the nutrient form on coastal eutrophication by contrast with the OUT scenario, which is essentially dominated by ammonium.

The Nutrient (NUT) scenario includes the full mass loading of wastewater (identical to OUT) scaled to a much smaller volume of water, such that the contribution of freshwater to buoyancy is negligible. The setup of this simulation consists of concentrating the nutrients within wastewater, while decreasing the volume simultaneously by a factor of 100, thus maintaining the observed total nutrient load. To further remove buoyancy effects on the concentrated plume, the salinity and temperature of the wastewater influx match those of the surrounding seawater at the same depth and time. This scenario is designed to identify the effects of DIN addition, independent of the effects of freshwater on wastewater plume buoyancy and dispersal.

The model scenarios are initialized in June 1999, with three months allotted for model spin-up; analysis across the scenarios began in July 1999 and ran until October 2000. Note that 1999 was characterized by La Nina conditions (Wolter & Timlin, 2011), which can impact the productivity and magnitude of the seasonal shifts of nutrients and influence of upwelling within the California Current system. As a consequence, 2000 had a cooler than average sea surface temperatures in the SCB (Schwing et al., 2002).

2.2.4 Analysis

We analyze simulations by focusing on the nearshore band that extends within 15 km from the coast. Within this band, primary production is consistently altered throughout the year by wastewater inputs (Kessouri et al., 2021a). Anthropogenic nutrients enhance productivity in both the nearshore coastal band and offshore; however, their influence in the coastal band is roughly five times larger than in the offshore region. Beyond this nearshore band, the effects of anthropogenic nutrient inputs vary from year to year (Kessouri et al., 2023).

The five idealized scenarios are compared to disentangle the effects of freshwater and DIN form on coastal biogeochemistry (Table 2.2). In order to compare the effects of freshwater, we first consider the difference between the OUT and NUT scenarios. This quantifies the effects of buoyant plumes in the presence of anthropogenic nutrients. We then consider the difference of the FRE and CTRL scenarios to show what the effect of a freshwater addition without DIN would be on the productivity of the nearshore region. To compare the effects of different DIN forms (nitrate vs. ammonium), we consider the difference between the OUT and NIT scenarios.

Previous modeling studies show a significant effect of anthropogenic nutrients on phytoplankton blooms in winter (Kessouri et al., 2021a). Therefore, we focus on this season to best elucidate the differences between scenarios. To accommodate differences in the water column due to the climate regime (Dong et al., 2009; Mantyla et al., 2008; Checkley & Barth, 2009), we analyze the effects across different seasons in addition to annual averages. To analyze vertical patterns in the distribution of salinity, we take an average profile over a 10 km area around the JWPCP. This area is more directly affected by wastewater inputs, and thus is representative of the impacts on NPP and biomass in all scenarios compared to the control case.

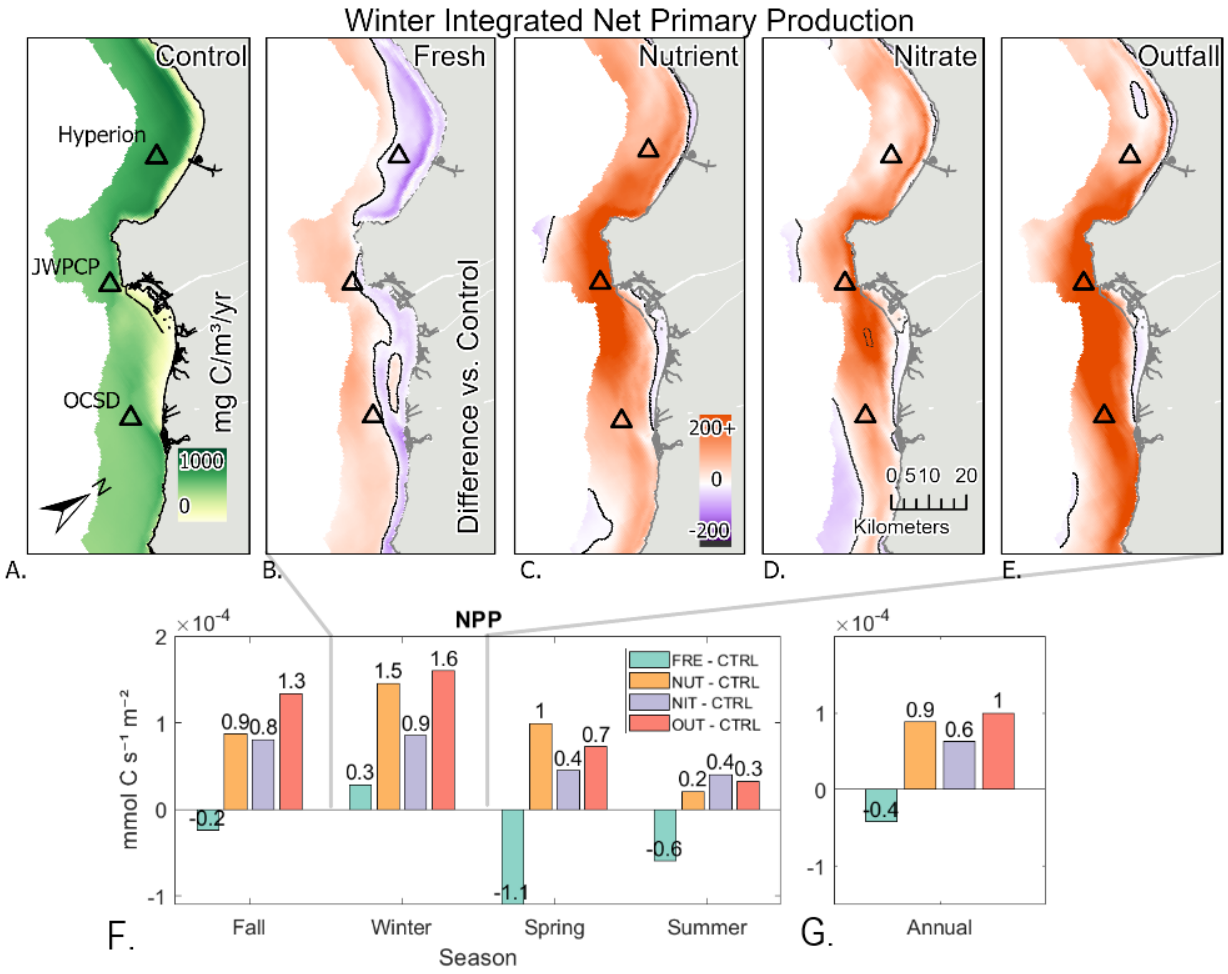

Figure 2.2: Idealized scenario comparison. Panel A shows NPP integrated over the top 100 m of the water column of the control (CTRL) scenario in winter. Panels B-E show the difference between the different idealized scenarios (FRE, NUT, NIT, OUT) and the control (CTRL). In the lower panels, the integrated NPP from each scenarios is compared to control seasonally (F) and annually (G).

2.3 Results

The largest increase in NPP, both in winter and on average over the course of the year, are observed in the OUT (standard nutrient and freshwater volume load; Fig.2.2 E, F) and NUT scenarios (standard load without freshwater; Fig.2.2 C,F). The annual increase in NPP in the NIT scenario (all DIN converted to nitrate with standard freshwater discharge; Fig.2.2 D, F) is substantially less than the OUT and NUT scenarios. A seasonal shift in the relative importance of nitrate to ammonium is observed, with the largest differences between NIT and OUT during the winter, and the smallest in the summer. A slight increase in NPP is seen in the FRE scenario in winter (Fig.2.2 B, F). However, this scenario exhibits a net decrease in annual mean NPP (Fig.2.2 G). The spatial distribution of NPP between these runs remains relatively similar within the nearshore region. Simulations that introduced DIN (OUT, NUT, NIT) show the largest changes in NPP when mixing is high and surface nutrients are still relatively low in fall and winter. In contrast, the influence of wastewater inputs is suppressed in summer. The FRE scenario shows a decrease in NPP in the shallow nearshore region, and a slight increase in the offshore region (Fig.2.2 B). These results reveal that the different wastewater scenarios, particularly the OUT and NUT, significantly influence NPP, both in terms of magnitude and seasonal variation.

Seasonal shifts in the depth of phytoplankton biomass illustrate the biological response to stratification changes. Across all scenarios, biomass decreases at the surface (1-10 m) (Fig. 2.3 A) in late spring compared to the mean, whereas at mid depth (10-50 m), a maximum biomass occurs in June and July (Fig. 2.3 B). The largest differences between the scenarios and the control are observed at the surface from February to April. Changes across scenarios are non-uniform from month to month. There is however consistency in the seasonal cycle of biomass in the OUT and NUT scenarios at depth, and greater variation at the surface. When comparing the distribution of the two scenarios that introduce freshwater and nutrients, the differences between OUT and NIT remain consistent at the surface and at depth (10-50 m). FRE and CTRL exhibit larger differences at 1-10 m throughout the year, with FRE producing greater biomass in Feb and Mar, and less in Jun and Jul. Seasonal

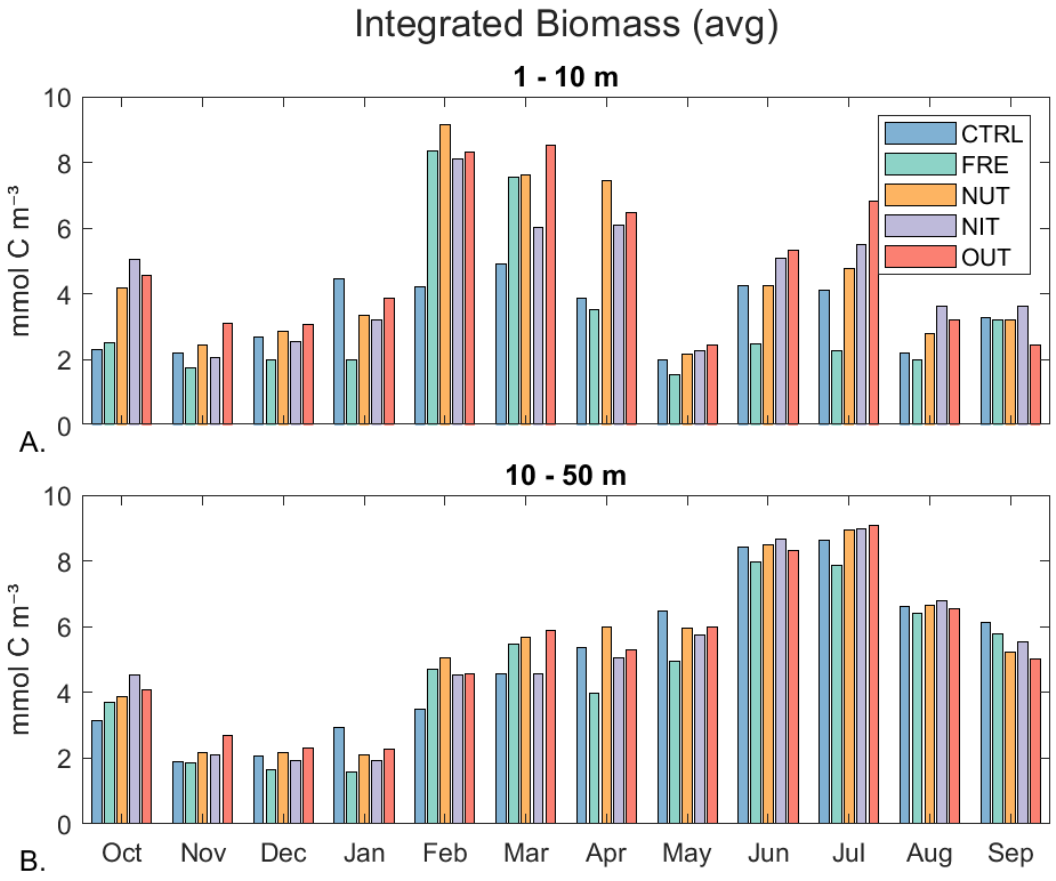

Figure 2.3: Comparisons of monthly average integrated biomass over the top 1-10 m (A) and 10-50 m (B) in the nearshore coastal region of the SCB.

stratification has the largest influence on scenario responses in the top 10 m of the water column.

Scenarios with different nitrogen forms show differences in their horizontal distribution of NPP and biomass. Both scenarios where outfalls introduce nitrogen and freshwater stimulate increases in biomass and NPP, with the ammonium-rich scenario (OUT) producing a greater response (Fig. 2.4 A). Larger concentrations of nitrate (NIT) compared to ammonium (OUT) stimulate less biomass and NPP (Fig. 2.4 D, E), with stronger differences in winter (Fig.2.2 F). Annually, a 40% difference in NPP emerges between NIT and OUT. Comparing NIT and CTRL, ammonium decreases in November and December in the surface and subsurface (1-10 m, 10-50 m), and at depth (50-100 m) annually in the nearshore coastal area (Fig.2.6 C). This dilution in ambient ammonium is supported by a reduction in salinity within a 10 km radius of the outfalls in the NIT, OUT, and FRE scenarios, relative to the NUT scenario (Fig. A.1). These findings demonstrate the importance of the nitrogen form on the spatial distribution and seasonal variability of NPP and phytoplankton biomass changes.

Differences in scenarios with and without freshwater manifest in their horizontal spread of NPP. NUT, with negligible volume of freshwater, shows a larger impact within the shallow region of the Santa Monica Bay, whereas OUT has a greater influence in the southern exposed area (Fig.2.5 A). Similarities in integrated NPP and biomass between OUT and NUT, however, suggest that introduction of freshwater has a small influence on total productivity relative to the nitrogen form. Similarities in total NPP between OUT and NUT are most evident throughout winter and annually in the top 0-100 m of the water column (Fig.2.5 D, E). Both scenarios where DIN is introduced via outfalls in the form of ammonium show high influences on biomass and NPP annually, but exhibit spatial dissimilarities in the horizontal distribution of NPP.

The vertical distribution of ammonium provides information on how horizontal differences of biomass and NPP arise between idealized scenarios. Ammonium concentrations are are highest in the OUT scenario at the surface (1-10 m) (Fig. 2.6 A) throughout the entire year. At mid depths (10-50 m) (Fig. 2.6 B) OUT and NUT show nearly identical concentrations. At depth (50-100 m) (Fig. 2.6 C) NUT shows higher concentrations than OUT. The

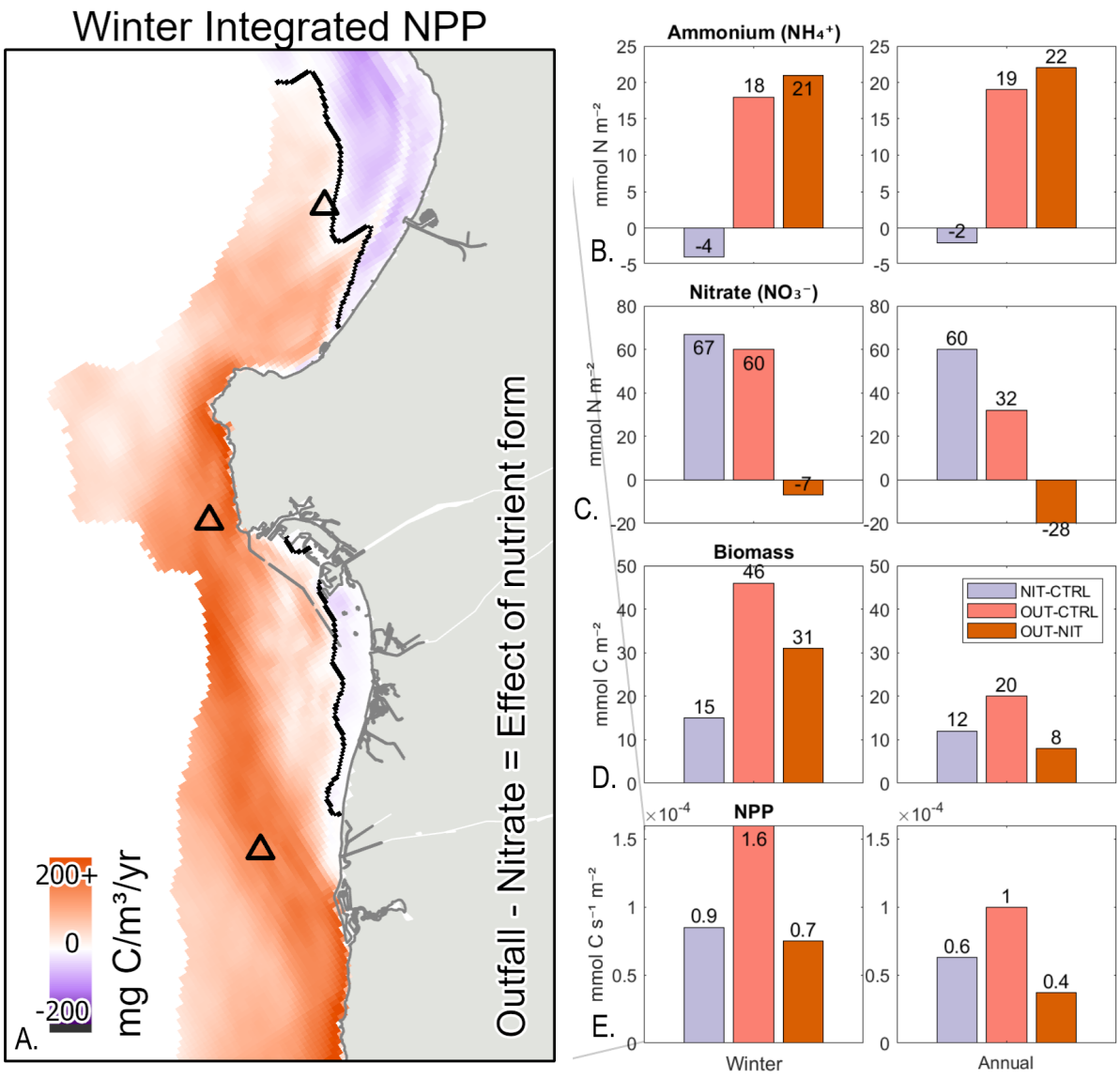

Figure 2.4: Comparison of the effect of the DIN form (ammonium vs. nitrate) on NPP. Panel (A) shows the difference in the vertically integrated NPP in the nearshore region between the OUT and NIT scenarios. The bar charts on the right show the vertically integrated (0-100 m) ammonium (B), nitrate (C), biomass (D), and NPP (E) for winter and as annual means, over the same domain as (A), for the differences between NIT and CTRL (purple, showing the effects of adding nitrate alone), OUT and CTRL (red, showing the effect of adding ammonium alone), and OUT and NIT (orange, showing the amplification in NPP caused by switching from nitrate to ammonium).

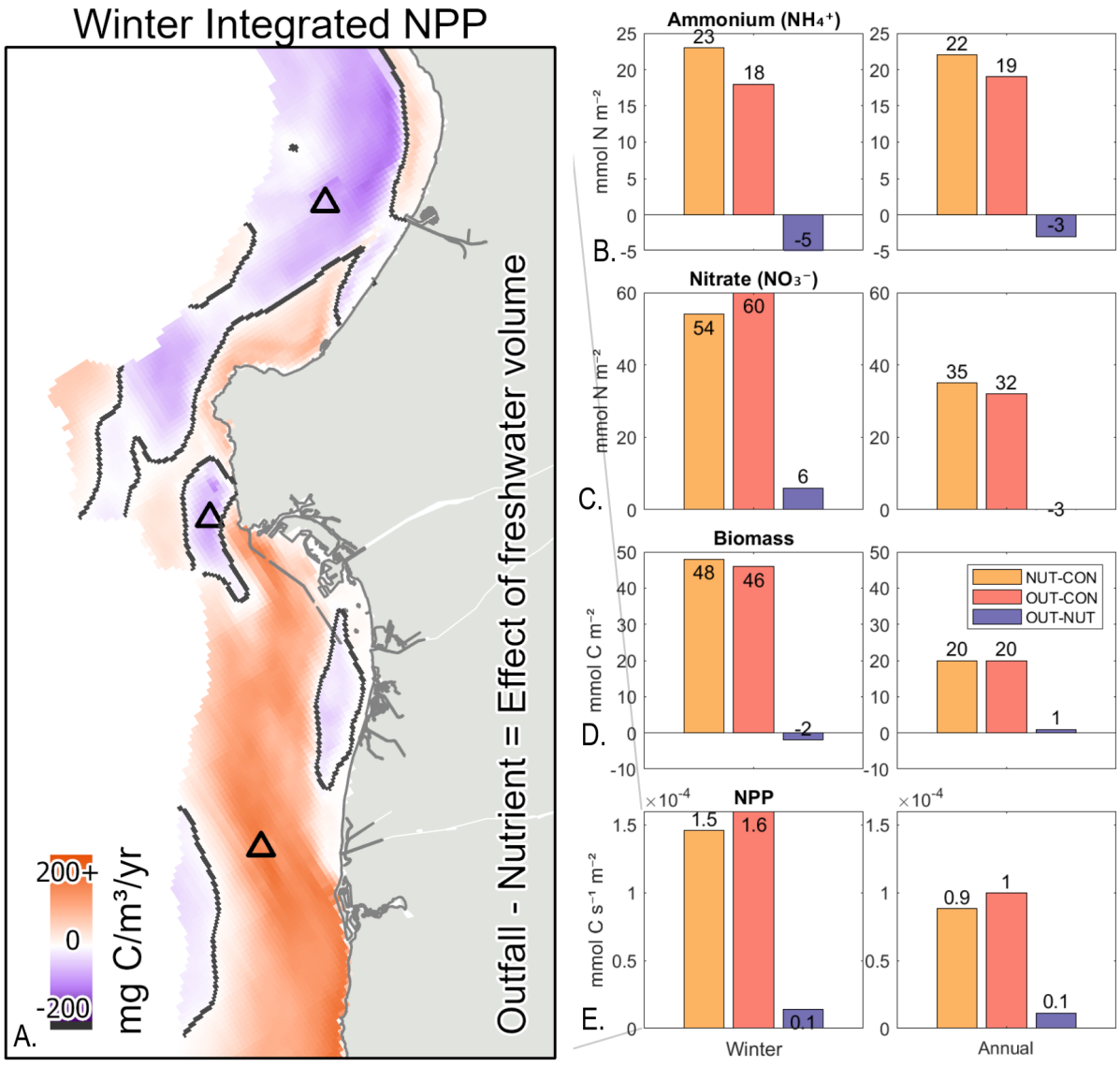

Figure 2.5: Comparison of the effects of freshwater volume on NPP. Panel (A) shows the difference in the vertically integrated NPP in the nearshore region between the OUT and NUT scenarios. The bar charts on the right show the vertically integrated (0-100 m) ammonium (B), nitrate (C), biomass (D), and NPP (E) for winter and as annual means, over the same domain as (A), for the differences between NUT and CTRL (orange, showing the effects of adding nutrients without any freshwater), OUT and CTRL (red, showing the effect of adding nutrients and freshwater), and OUT and NUT (purple, showing the change in NPP caused by introducing freshwater in the presence of nutrients).

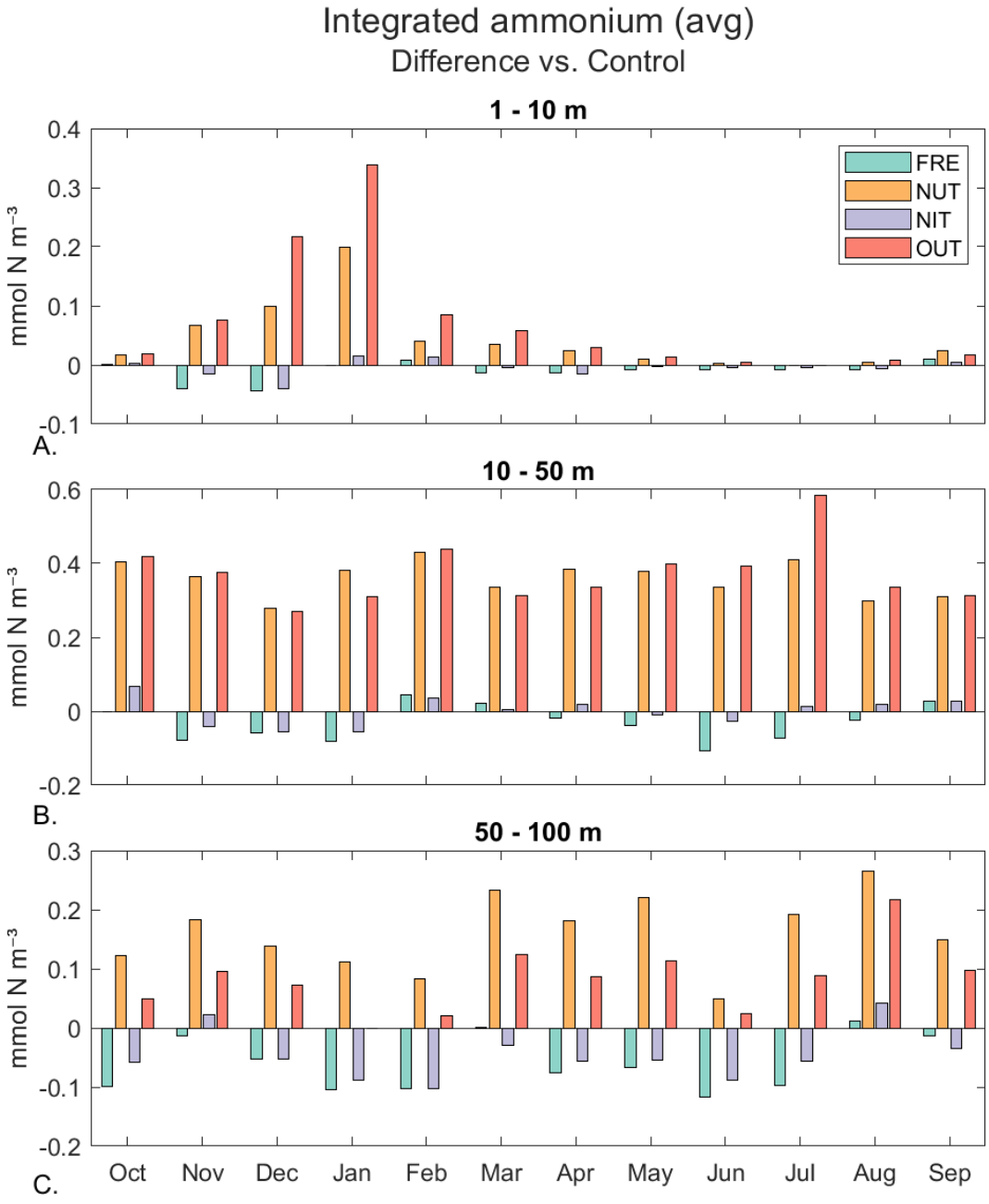

Figure 2.6: Difference in vertically integrated ammonium over the top 10 m (A), 10-50 m (B), and 50-100 m (C) between the FRE (green), NUT (orange), NIT (purple), OUT (red) scenarios and the CTRL scenario.

freshwater (FRE) and nitrate-rich (NIT) scenarios show similar decreases in ammonium at depth over the annual cycle. Differences in ammonium with depth suggest a broader vertical spread of the OUT scenario compared to NUT. The decreases in ammonium at depth for the FRE and NIT scenarios suggest a potential dilution of preexisting ammonium in subsurface waters.

2.4 Discussion

Our simulations show that coastal productivity is altered by removing the effect of freshwater volume on outfalls. We hypothesise that a greater volume of freshwater increases the horizontal spread of NPP and potentially increases the entrainment of wastewater plumes by coastal currents and eddies that facilitate offshore transport (Dong et al., 2009; Kessouri et al., 2023). In contrast, in scenarios with more concentrated wastewater inputs the lower volume of freshwater restricts the dispersion of nutrient-rich wastewater. This in turn results in more intense blooms that remain closer to the emission points, potentially leading to enhanced eutrophication in the adjacent nearshore regions. This effect is illustrated by the larger biomass increase in the Santa Monica Bay for the NUT scenario relative to OUT. This observation aligns with in-situ studies documenting a magnified productivity response to highly concentrated plumes in the Santa Monica Bay (Corcoran et al., 2010; DiGiacomo et al., 2004). In the Santa Monica Bay, we found that freshwater alone reduces NPP, which we interpret as a dilution effect, wherein the injection of freshwater dilutes ambient nutrients, consistent with reduced salinity near the outfalls. This finding is consistent with the study by Corcoran et al. (2010), who found that fresh stormwater plumes diluted upwelled waters high in phytoplankton biomass in the Santa Monica Bay. Additionally, the horizontal dispersal of more concentrated plumes appears to be less effective. Ho (2023) modeled the effects of potable water recycling on NPP in the SCB, finding that progressive declines in water volumes under constant nutrient loading reduced cross-shelf horizontal transport of DIN occurring predominantly via eddies. The spatial differences in NPP between the NUT and OUT scenario show consistent patterns to those discussed by Ho (2023).

Integrated biomass and NPP remained similar between runs with and without the introduction of freshwater. However, the vertical placement of wastewater plumes in the water column affected the fate of the plume and the resulting NPP changes. We explored two possibilities related to the introduction of freshwater: 1) a wider transport via currents and eddies due to the greater proximity of buoyant wastewater plumes to the surface (Ahn et al., 2005; Washburn et al., 2003), and 2) entrainment of nutrients from the surrounding environment by buoyant plumes.

Shoaling of buoyant plumes led to a change in the horizontal transport of anthropogenic nutrients, as wastewater plumes are exposed to currents and eddies of differing intensities at various depths. Such changes are consistent with findings from prior studies, including Hunt et al. (2010), DiGiacomo et al. (2004), Dong et al. (2009), and Kessouri et al. (2023). The role of subsurface currents and eddies warrants more investigation, as a great variability in current velocities can exist withing few tens of meters of depth in the Santa Monica Bay and San Pedro Bay (Uchiyama et al., 2014) .

Our results suggest that entrainment of ambient nutrients and uplift by buoyant plumes are relatively weak. This is consistent with previous studies that indicate a small effect in non-stratified seasons (Nezlin et al., 2016; Washburn et al., 1992). Our finding that plumes with greater buoyancy support increased biomass is consistent with the sensitivity of productivity to light. Plumes situated higher in the water column, where light is more intense, stimulate more productivity compared to deeper plumes.

These findings also complement those of Ho (2023), which observed a reduction in ammonium concentration between 0-100 m with decreased freshwater input. Thus, differences in the vertical and horizontal distribution of wastewater have consequences on coastal productivity, and call for better understanding of nearshore dynamics to better predict the fate of outfall plumes.

Because of the faster uptake timescale for ammonium compared to nitrate, ammonium-rich wastewater inputs stimulate greater coastal productivity than nitrate-dominated inputs. However, the NIT scenario suggests that inputs of DIN as nitrate would still produce an im-

portant increase in primary production. This response is spread out over a larger region, likely reflecting the slower uptake of nitrate relative to ammonium. We note that an increasing body of literature suggests a complex influence of the nitrogen form on phytoplankton assemblages. For example, diatoms species can use a large amount of nitrate even when ample ammonium is available (e.g., Glibert et al. (2016); Zhao et al. (2005)). This species-dependent variability is not captured by the simple formulation of our model. Further studies are needed to evaluate the effect of different nitrogen management strategies on coastal ecosystem and water quality, using a combination of field work and numerical models.

The varied responses of our idealized scenarios to seasonal changes demonstrate that even minor variations in environmental conditions can lead to significant differences in the influence of outfall plumes within the SCB. Although in the OUT scenario, wastewater plumes mostly remain below the surface in the summer (Jones et al., 2002; Carvalho et al., 2002) and reach the surface in the winter (Booth et al., 2014; DiGiacomo et al., 2004; Washburn et al., 1992; Uchiyama et al., 2014), the transition from spring to summer drives somewhat different responses across all four scenarios. DiGiacomo et al. (2004) note anomalous events where plumes reach the surface despite high stratification in the summer, likely because of nearshore submesoscale eddies. This and work of Bondur et al. (2018) agrees with our finding that the response in productivity is heavily modulated by the season and freshwater content of wastewater. In addition to buoyancy, seasonal nutrient variations and upwelling impact the relative influence of the nutrient addition, with nitrate showing a greater relative effect when it is less abundant (and thus more limiting) in summer (Hickey, 1979; Reifel et al., 2013).

Although our findings are relatively consistent across seasons and scenarios, there remain several caveats to our approach. First, our results are based on analysis of relatively short simulations. We expect that inter-annual climate variability would influence the dynamics of wastewater inputs and the corresponding ecological responses (Kessouri et al., 2023; Ho, 2023). Our short time frame did not allow us to determine these impacts. Second, our study focuses on the coastal band. Despite significant differences in the horizontal spread of wastewater influences, the model suggests little difference the annual mean NPP in this

region. However, we did not account for changes in production offshore in the SCB, which, based on recent work, are likely important (Kessouri et al., 2023).

We also acknowledge the shortcomings of using treatment standards from 1999, a period for which the model was validated against observations, and interpret our results as broad illustrations of the influence of wastewater properties. Nonetheless, the broad magnitude of nutrient fluxes has remained similar over the past 20 years, despite changes to management standards (Sutula et al., 2021a). Specifically, Kessouri et al. (2023) indicate a 13% decrease in DIN inputs from 2013-2017 compared to 1997-2000. Due to these limitations, and the idealized nature of the scenarios, our findings should be interpreted as a mechanistic exploration of wastewater influences that should be accompanied by more specific and realistic scenarios to better inform coastal water quality management.

Our study illustrates mechanisms that could enhance or suppress the effects of wastewater nutrient inputs in coastal waters, which would be difficult to observe directly. We conclude that varying the volume and buoyancy of wastewater can significantly alter the horizontal dispersal of anthropogenic nutrients, modulating their environmental consequences. Results from our idealized modeling approach can thus complement and inform studies based on in-situ and remote sensing methods, and expand discussion of wastewater impacts in dynamic coastal environments.

CHAPTER 3

Anthropogenic nutrient sources influence kelp canopies during a marine heat wave

This chapter contains the submitted manuscript Hoel et al. (2024a), without any changes.

3.1 Introduction

Marine heatwaves (MHWs) have been linked to rapid declines in giant kelp (*Macrocystis pyrifera*) forest area throughout the global ocean coastline (Cavanaugh et al., 2019; Filbee-Dexter et al., 2020; Wernberg et al., 2016; Nepper-Davidsen et al., 2019). Climatic events such as El Niño and MHWs lower dissolved inorganic nitrogen (DIN) in the surface waters of important regions for giant kelp, including the Southern California Bight (SCB), as enhanced stratification caused by high ocean temperatures suppresses upwelling of nutrient rich deep water (Checkley & Barth, 2009; Gentemann et al., 2017). In this region, giant kelp maintains a relatively low capacity to store nutrients (30 days) (Zimmerman & Kremer, 1986), and show reduced growth in as short as 14 days when using internal reserves only (Gerard, 1982). As a result, giant kelp growth can be limited during these occurrences of naturally low DIN.

Beginning in January 2014 and continuing through August of 2016, a MHW (sometimes referred to as "the blob") brought anomalously warm water conditions to the California Current System (CCS) (Di Lorenzo & Mantua, 2016), significantly impacting kelp forest ecosystems in the SCB (Jacox et al., 2016). During this period, sea surface temperatures (SSTs) showed a 6.2 degree C maximum anomaly within the SCB, and spring upwelling was suppressed (Gentemann et al., 2017), creating challenging conditions for kelp growth. In the summer and fall of 2015, rapid declines in kelp forest canopy area were detected

along the entire coastline of the SCB (Cavanaugh et al., 2019). Response and subsequent recovery to the heat and nutrient stress during this period, however, showed significant variation. Understanding the factors behind this variability, including the potential utilization of anthropogenic nutrients, is critical to predictions of kelp ecosystems in the face of climate change (Filbee-Dexter et al., 2020; Nepper-Davidsen et al., 2019).

In the SCB, natural DIN sources are supplemented by anthropogenic inputs from wastewater outfalls and river runoff. Many kelp studies in this region have approximated nutrient availability by using the strong correlation between SST and nitrate (Cavanaugh et al., 2011; Bell et al., 2015; Bell & Siegel, 2022; Snyder et al., 2020), an approach which relies on observations, often sparse during periods of marine layer which seasonally affect the SCB. Even with observations, this methodology misses finer scale anthropogenic inputs, and does not allow for the separation of anthropogenic from natural nutrient sources. The recent development of comprehensive high-resolution biogeochemical models of the SCB provides an opportunity to assess the distribution of nutrients encompassing both natural and anthropogenic sources in this coastal region. Inputs of nutrient-rich effluent, accurately represented by these models (Kessouri et al., 2021b), is not episodic in nature like upwelling, and is the largest continuous source of anthropogenic DIN to the coastline in highly urbanized regions of the SCB ranging from Santa Monica Bay, to San Pedro Bay, and the Orange County coastlines. This supply of anthropogenic DIN, predominantly in the form of ammonium, can provide more DIN than upwelling in periods of non upwelling and low riverine flows (Howard et al., 2014; Kessouri et al., 2021a). Additional sources of DIN such as urea and ammonium from the sediment (captured by in-situ measurements) have been observed to provide DIN to kelp forests during periods of limited nitrate supply by summer upwelling in the Santa Barbara Channel (Smith et al., 2018; Brzezinksi et al., 2013). These studies indicate that alternative sources of DIN play a critical role during large reductions in the supply of nitrate via upwelling such as the MHW of 2015-2016. However, they could not quantify the importance of anthropogenic nutrient sources. Observations have also found high concentrations of kelp sporophytes (visible phase of the life cycle) in areas characterized by anthropogenic nutrient enrichment around Catalina Island (Deysher & Dean, 1986). Although it is apparent that alternative sources

of DIN are important to kelp forests in the SCB, and that human activity supplies large quantities of DIN to coastal waters in this region, the influence of anthropogenic nutrients on kelp forests, especially during MHWs, remains unclear.

Here, we focus on the interplay between anthropogenic nutrients and kelp forest canopy resilience during the 2015-2016 MHW in the SCB. By combining output from a high-resolution biogeochemical model with remotely sensed kelp canopy area measurements we address: 1) The extent of nutrient limitation in kelp forest canopy areas during the 2015-2016 MHW, 2) The influence of anthropogenic DIN sources, and 3) The relationship between anthropogenic DIN and kelp forest canopy resilience. By exploring the interplay of anthropogenic nutrient sources with kelp forest canopy resilience during the MHW, we highlight the utility of realistic ocean biogeochemical models in understanding kelp patterns, and underscore the challenges and opportunities that lie ahead for ensuring the continued health of this keystone species and the ecosystems it supports.

3.2 Methods

3.2.1 Study Area

The SCB is a coastal embayment that stretches from the US-Mexico border to Point Conception. Giant kelp is a prolific keystone species throughout this region (Buschmann et al., 2007). For our analysis, we subdivide the SCB into five sub-regions, consisting of North Mainland, Middle Mainland, Southern Mainland, Northern Channel Islands, and Southern Channel islands (Fig. 3.1).

3.2.2 Kelp canopy dataset

We use Landsat satellite imagery to quantify kelp canopy area and its change over time. The dataset provides estimates of canopy area of kelp on a 30 x 30 m grid. Data are derived from Landsat 5 Thematic Mapper (TM), Landsat 7 Enhanced Thematic Mapper Plus (ETM+), and Landsat 8 Operational Land Imager (OLI) satellite imagery and is detailed further by

LTER et al. (2022) and Bell et al. (2020a). The data span the period from January 1984 to December 2021, and is provided as seasonal averages of kelp canopy area per grid point (or pixel), in units of m^2.

For analysis over larger kelp forest areas, we combine the individual 30 m grid points (n = 75554) into larger 2 km by 2 km (i.e., 4 km^2) cells (Fig. 3.1), for a total of 520 4 km^2 analysis cells across the SCB.

In addition to the primary analysis conducted on the 4 km^2 cells, we performed a parallel analysis using the 30 m original pixels, to capture finer-scale variations within these ecosystems, with the results presented in the Supplementary Materials. This complementary approach allows for a more complete understanding of spatial heterogeneity, which may be obscured when averaging data over larger spatial scales. The methodology for interpolating nutrient values to the 30 m grids and their subsequent integration into the larger 4 km^2 analysis cells is outlined in Section 3.2.3 (see Supplementary Materials for detailed 30 m grid analysis).

3.2.2.1 Normalized MHW area

To asses the resilience of kelp to the MHW, we employed a method of normalization and compared the average kelp canopy area through the MHW to a reference baseline period. We use as the baseline (pre-MHW) a ten year average of all seasonal observations from 2003-2012, to ensure robustness and minimize noise from short-term (i.e., seasonal to interannual) variability.

The MHW started in the summer of 2014 and lasted until spring 2016. However, the kelp response to this event was delayed until the fall, as shown by canopy data and further detailed in Cavanaugh et al. (2019). To capture the most relevant impact of the MHW, we use the kelp canopy area from Winter 2015 to Fall 2016.

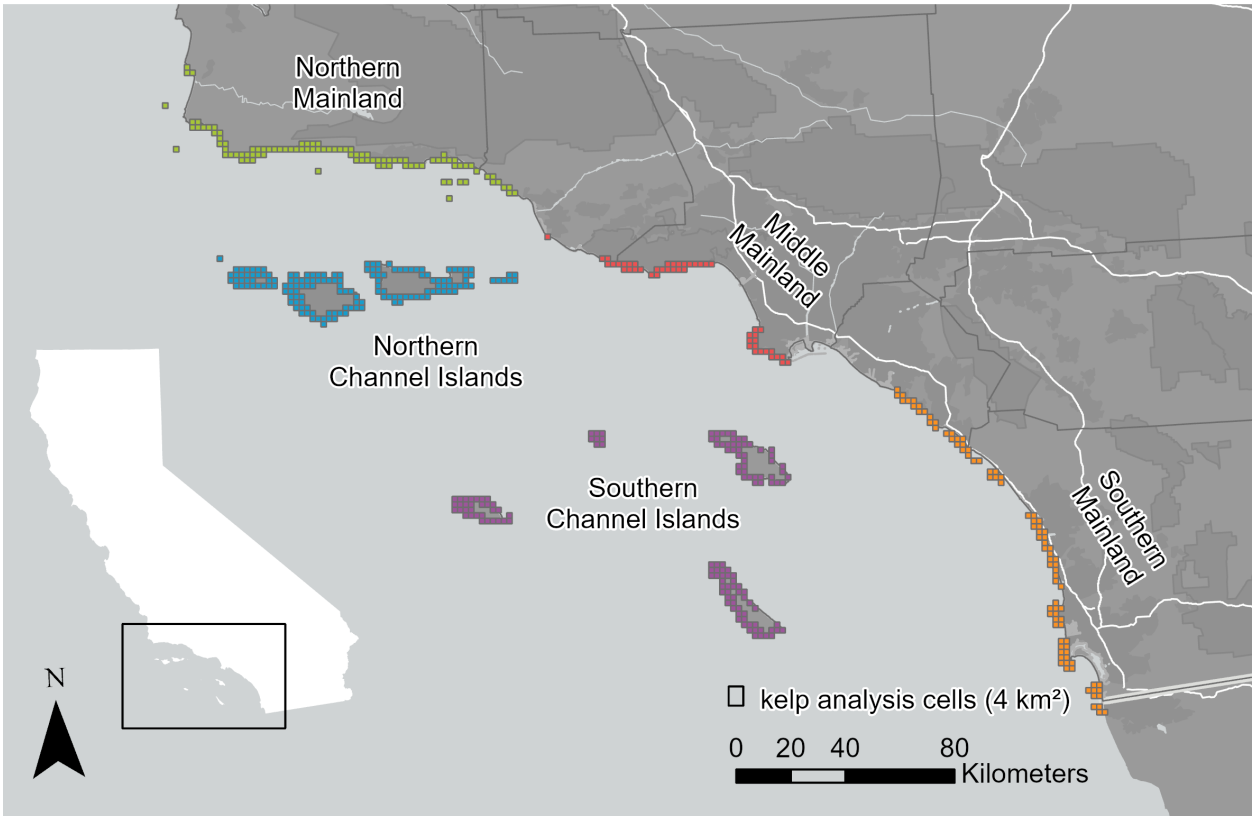

Figure 3.1: Giant kelp forest analysis cells and regions.

3.2.3 Physical-biogeochemical model

We take advantage of a realistic, validated, high-resolution physical-biogeochemical model to determine DIN values in the SCB, using scenarios that either include or exclude anthropogenic influences. The model output offers a higher resolution (300 m), horizontally and vertically, compared to previous assessments of the SCB which correlate SST with nitrate (1 km) (Snyder et al., 2020). Furthermore, models allow for differentiation of ammonium and nitrate, and inclusion of terrestrial sources of nutrients.

The numerical model used in this study, the Regional Ocean Modeling System (ROMS), is a widely adopted regional ocean model with a long history of application to the California Current System (CCS) (Capet et al., 2008a,b,c; Renault et al., 2021; Deutsch et al., 2021) and specifically the SCB (Dong et al., 2009; Dong & McWilliams, 2007; Kessouri et al., 2020, 2021b). The physical model is coupled to the Biogeochemical Elemental Cycling model (BEC) (Moore et al., 2013, 2004; Deutsch et al., 2021), which simulates the cycles of nutrients (nitrogen, phosphorus, silicon, iron), carbonate chemistry, oxygen, three phytoplankton groups (small phytoplankton, diatoms and diazotrophs) and one zooplankton group. The validation provided by Kessouri et al. (2021b) shows that the model captures observed biogeochemical gradients driven both by natural processes and by anthropogenic influences. The model is currently used to study the effects of terrestrial inputs on the coastal zone and water quality (Kessouri et al., 2021a, 2023; Ho, 2023). The model is run at a horizontal resolution of 300-m, with 60 terrain-following vertical levels. Although the baseline simulation spans the period from 1997 to 2017, our study focuses on the years 2012 to 2016. The time-step of the model is 30 s; output is saved as 1 day averages. We refer the reader to Kessouri et al. (2021b) for details on the model rationale, setup, boundary conditions, and forcings.

We average nutrient values from the model a MHW period (2015-2016). Model values are interpolated to the 30 m kelp area cells by matching the center of each cell to the 300 m nutrient model cell it was within. The 30 m kelp and nutrient values were then merged to the 4 km^2 analysis cell by averaging the 30 m cells within the 4 km^2 cell.

3.2.3.1 Anthropogenic nutrients

The magnitude of anthropogenic influence in the SCB is calculated via the difference of DIN in two model scenarios. The "control" (CTRL) scenario simulates the SCB without the influence of land-based anthropogenic inputs. The "full" (ANTH) scenario simulates the SCB by including the influence of land-based anthropogenic nutrients, consisting of large publicly owned treatment works (POTWs), small POTWs, rivers, and atmospheric deposition. Wastewater effluent and river discharge data are gathered from monitoring observations, and incorporates also include surface storm-water flow (Sutula et al., 2021a). Nutrient inputs by aerosol atmospheric deposition are generated from the Community Multiscale Air Quality model (Skamarock & Klemp, 2008). We determine the extent of anthropogenic influence by comparing the full and control scenarios, specifically focusing on nitrogen influences (hereon referenced as anthropogenic DIN).

3.2.4 DIN limitation days metric

To identify regions that would experience limited nutrients in the absence of anthropogenic influence, we draw upon metrics of previous studies of giant kelp in the SCB. We use established nutrient thresholds, defining the storage capacity of kelp in the SCB as two weeks (Gerard, 1982; Dean & Jacobsen, 1986). Concentrations below 1 μmol L^{-1} over the top 15 m in the control (CTRL) were considered to be DIN limited (Gerard, 1982). Accordingly, if an area is DIN limited over a period of 14 days, it is below the necessary requirements to reach the ideal growth rate of giant kelp (Bell & Siegel, 2022). Combining these factors, the instances of 14+ days of limitation in the control scenario are identified as "limitation days" and are summed throughout the year. This is done by taking a 14 day moving mean of DIN ($d(t)$) (Equation 3.1), wherein any mean below 1 μmol L^{-1} is considered a limitation day ($l(t)$)(Eq. 3.2). The sum of limitation days for each canopy grid point is taken over 2015-2016 to find the total DIN limitation days (l_{tot}) (Equation 3.3).

$$d(t) = \frac{1}{14} \sum_{i=0}^{13} x(t-i) \tag{3.1}$$

$$l(t) = \begin{cases} 1 & \text{if } d(t) < 1\,\mu mol\mathrm{L}^{-1} \\ 0 & \text{otherwise} \end{cases} \tag{3.2}$$

$$l_{tot} = \sum_{t=1}^{365} l(t) \tag{3.3}$$

3.2.5 Anthropogenic influence days metric

Days when DIN in the control (CTRL) model is below 1 μmol L^{-1} (DIN limited) and the full (ANTH) model is above 1 μmol L^{-1} are defined as "anthropogenic influence days" ($i(t)$) (Equation 3.4).

$$i(t) = \begin{cases} 1 & \text{if } DIN_{CTRL}(t) < 1 \text{ and } DIN_{ANTH}(t) > 1 \\ 0 & \text{otherwise} \end{cases} \tag{3.4}$$

Values of influence days are summed throughout the period 2015-2016 to find the total number of anthropogenic influence days (i_{total}) (Equation 3.5).

$$i_{total} = \sum_{t=1}^{730} i(t) \tag{3.5}$$

3.2.6 Statistical analysis

3.2.6.1 Kruskal-Wallis test

To assess differences in the normalized MHW kelp canopy area across all regions and throughout the SCB, we utilize the Kruskal-Wallis (KW) test, a non-parametric alternative to one-way ANOVA. This choice is informed by the non-normal distribution of the data, substantiated by preliminary exploratory analyses (Kruskal & Wallis, 1952).

The kelp canopy area is categorized by region and throughout the entire SCB into three groups based on the quantiles of influence days: low, medium, and high. These categories are chosen as they represent natural breakpoints in our data distribution and allow for a clear distinction between low and high influence days. When conducting statistical analyses, we exclude areas of potential kelp restoration from our data by removing records with no kelp canopy area from 2003-2013. Outliers with 500% "Normalized MHW Area" are considered as outliers, and removed before conducting statistical analysis.

Our null hypothesis states that the medians of the normalized MHW area (see Normalized MHW Area) are not statistically different across these groups. Upon obtaining significant results from the KW test, pairwise comparisons are conducted using Dunn's test (Dunn, 1964). Dunn's post-hoc test, with a Sidak alpha level correction, identifies specific groups showing significant differences in normalized MHW area.

3.2.6.2 Density plots

For each region, we visualize relationships of MHW kelp canopy area and anthropogenic influence days with two dimensional histograms (heatmaps) for the individual kelp canopy area points. This is done using the 'histcounts2' function in MATLAB. Plots display the probability density of the occurrences in each bin relative to the entire data set.

We also conduct a correlation analysis on the heatmaps, by calculating the Pearson's correlation coefficient (ρ) and corresponding P-value between the two datasets, using the 'corr' function in MATLAB, and displaying the results on the corresponding density plots.

3.3 Results

3.3.1 Nutrient Limitation

The 2015-2016 MHW increased the sea surface temperature (SST) and decreased surface DIN levels in the SCB (Fig. B.1), reducing nutrient availability to kelp. Throughout the entire SCB, grid cells experienced an average of 510 limitation days across the 2015-2016

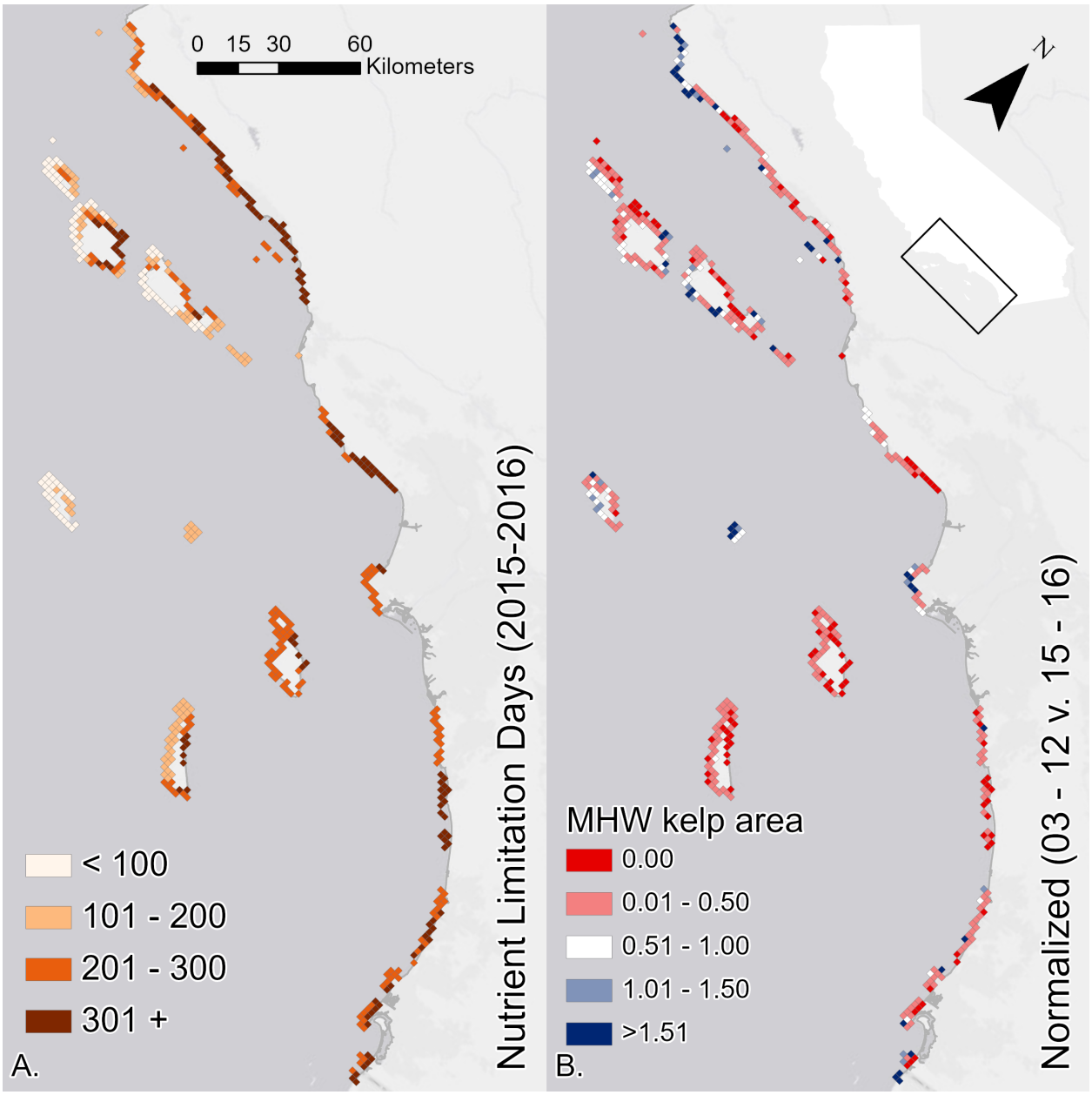

Figure 3.2: Comparative maps of kelp forest characteristics in the SCB from 2015 to 2016. A. Nutrient limitation days experienced by kelp forest areas. B. Normalized area of kelp forests during the 2015-2016 period relative to the average from 2003-2012. Increases are indicated in blue, minor change in white, and decreases are indicated in red.

time period, with the highest limitation days occurring in the Southern Mainland and Middle Mainland regions (Table B.1). A majority of the Mainland regions experienced more than 300 nutrient limitation days (Fig. 3.2 A.). These changes emphasize the profound effects of the MHW on nutrient availability, with the Mainland regions experiencing more limitation days than the Channel Islands during the same period.

The MHW event resulted in mixed responses in kelp areas across the SCB. A majority of the study region experienced large decreases throughout the MHW. However, some cells emerged where kelp area was preserved or increased (Fig. 3.2 B.). The Middle and Northern Mainland regions maintained the highest normalized area, with 53% and 33% of the long-term pre-heatwave average (Table B.1). The largest reductions in normalized area were experienced in the Southern Mainland (Table B.1), although some regions at the Southern edge showed a slight increase in area. Much of the Southern Channel Islands showed a decrease in kelp area, whereas some small pockets of the Northern Channel Islands showed a small increase (Fig. 3.2 B). This variable response in kelp area, with significant reductions in the Southern Mainland and pockets of increase in the Northern regions, highlights the heterogeneous impact of the MHW across the SCB.

3.3.2 Anthropogenic Nutrients

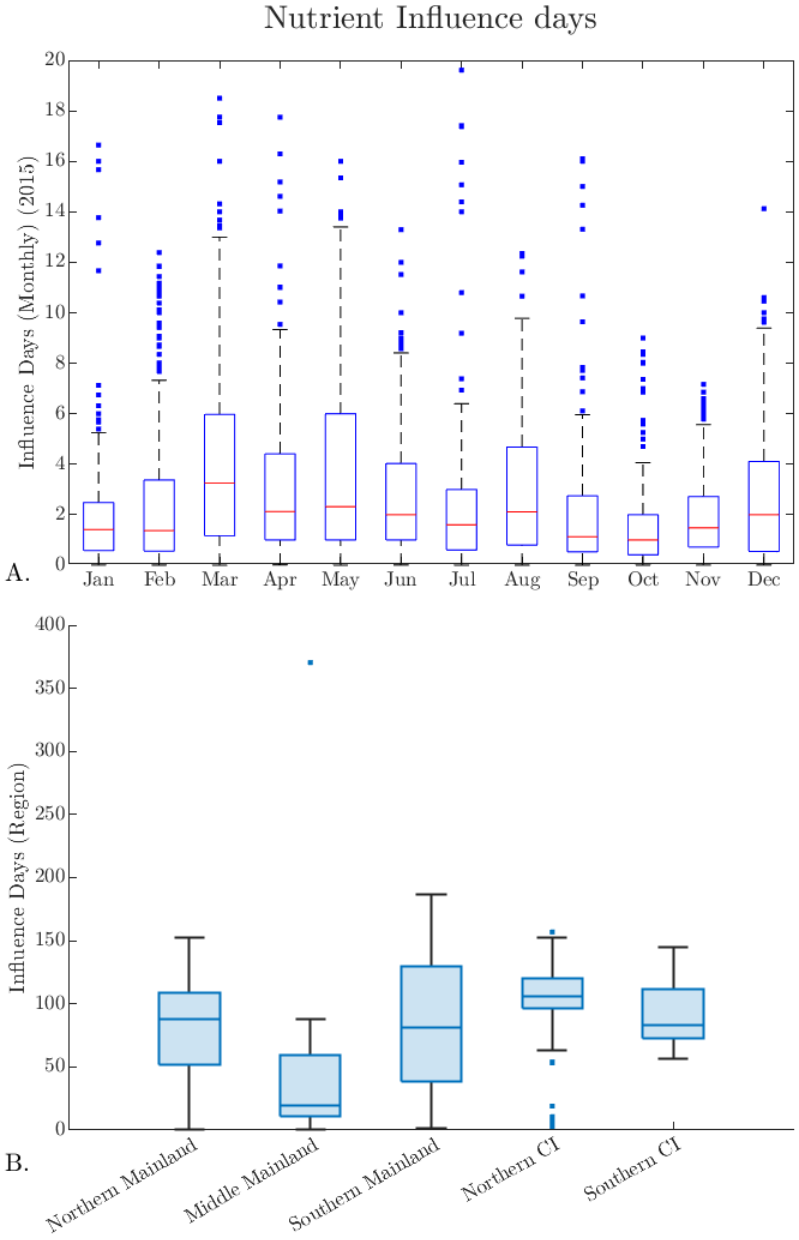

Figure 3.3: Box plots of average anthropogenic influence days for 2015 over the kelp forest cells within the SCB. (A.) Monthly distribution (B.) Regional distribution for the 2015-2016 event. Outliers are marked in blue

Anthropogenic influence days were experienced throughout kelp forests during the 2015-2016 period. The anthropogenic influence had no detectable seasonality in kelp forest areas, with influence days present in all seasons throughout the SCB (Fig. 3.3 A). By region, anthropogenic DIN had influence throughout the mainland and Channel Islands (Fig. 3.3 B). Over the entire SCB, there was an average of 88 influence days throughout the 2015-2016 period (Table B.1). Analysis on the individual canopy area points shows a greater spread of influence days within the Middle Mainland region, and a relatively similar spread throughout the remainder of the SCB (Fig. B.2). This widespread distribution of anthropogenic influence days, with a larger spread in the Mainland regions, suggests a consistent human impact on nutrients within kelp forests in the SCB.

3.3.3 Sustained Kelp Area

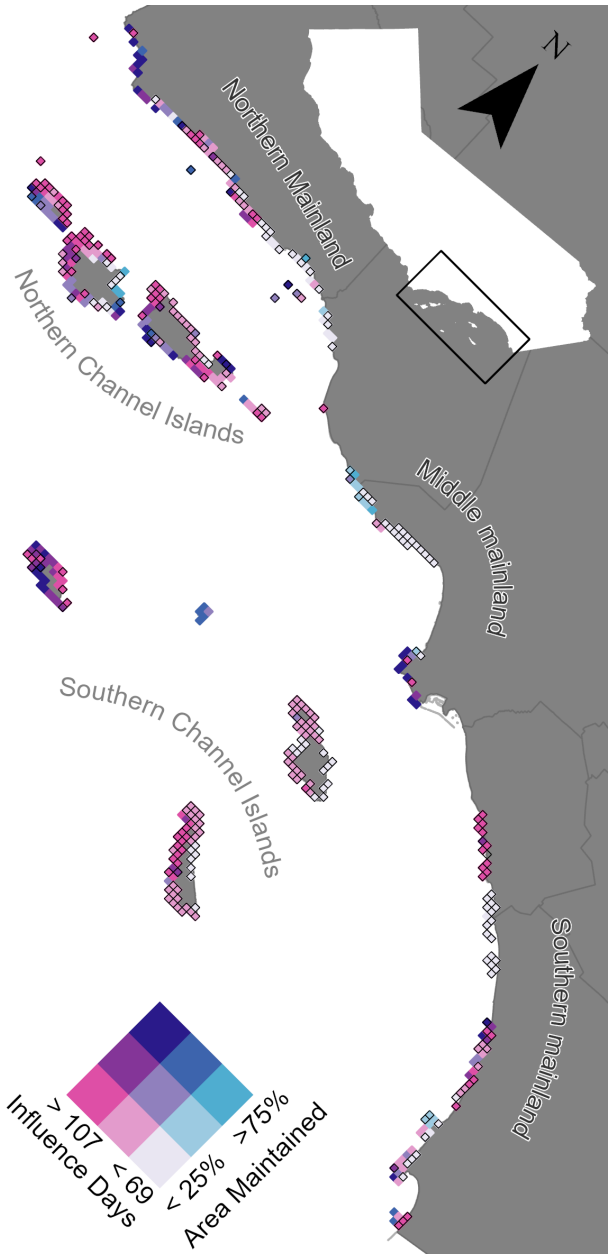

Figure 3.4: Map of anthropogenic influence days (pink) and area maintained throughout the MHW (2015-2016) normalized against pre-MHW (2003-2013) kelp forest area (blue). Influence days are grouped by quantile over the entire SCB. Regions which fit our qualification for statistical testing are outlined in black (see Section 3.2.6.1).

Analysis of anthropogenic influence days and normalized MHW kelp area reveals varying degrees of correlation across the SCB (Fig. 3.5). The entire SCB shows regions with high co-occurrence of influence days, and maintained kelp area in the Middle Mainland, Northern Channel Islands, and Northern Mainland (Fig. 3.4). Kelp forest locations that maintained their pre-MHW area contained higher average influence days and anthropogenic DIN than those that maintained a smaller area (Table. B.2). These findings suggest that the ability of kelp forests to preserve their area during the MHW event is related to the amount of anthropogenic nutrient influence that they are subjected to.

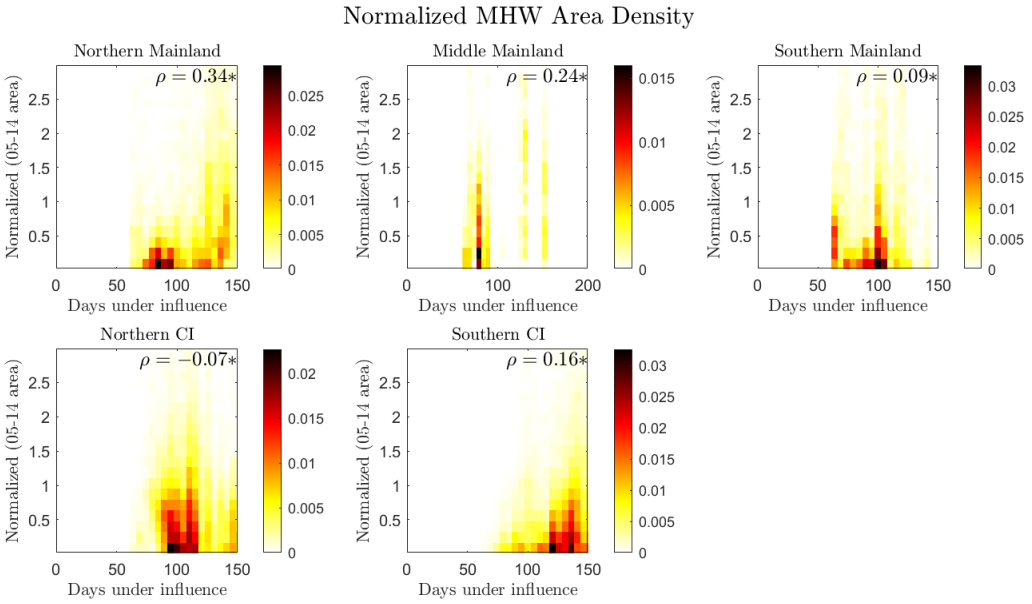

Figure 3.5: Density plots depicting the relationship between days under anthropogenic influence (x-axis) and the normalized MHW canopy area (y-axis) across the points within analysis regions. The Pearson correlation coefficient (ρ) is listed on the top right. The star (*) indicates statistical significance ($p < 0.1$). From left to right, top row: Northern Mainland, Middle Mainland, and Southern Mainland; bottom row: Northern Channel Islands and Southern Channel Islands. Color shades represent the density of data points.

We observed a significant positive relationship between normalized MHW canopy area and influence days across the SCB. Specifically, a significant positive linear relationship is

evident in all areas except the Northern Channel Islands (Fig. 3.5) among individual canopy location points. The correlation between anthropogenic influence days and normalized MHW area is most pronounced in Northern and Middle Mainland regions (Fig. 3.5). These patterns highlight the potential role of anthropogenic influence in sustaining kelp areas, especially the Mainland region, during the MHW event.

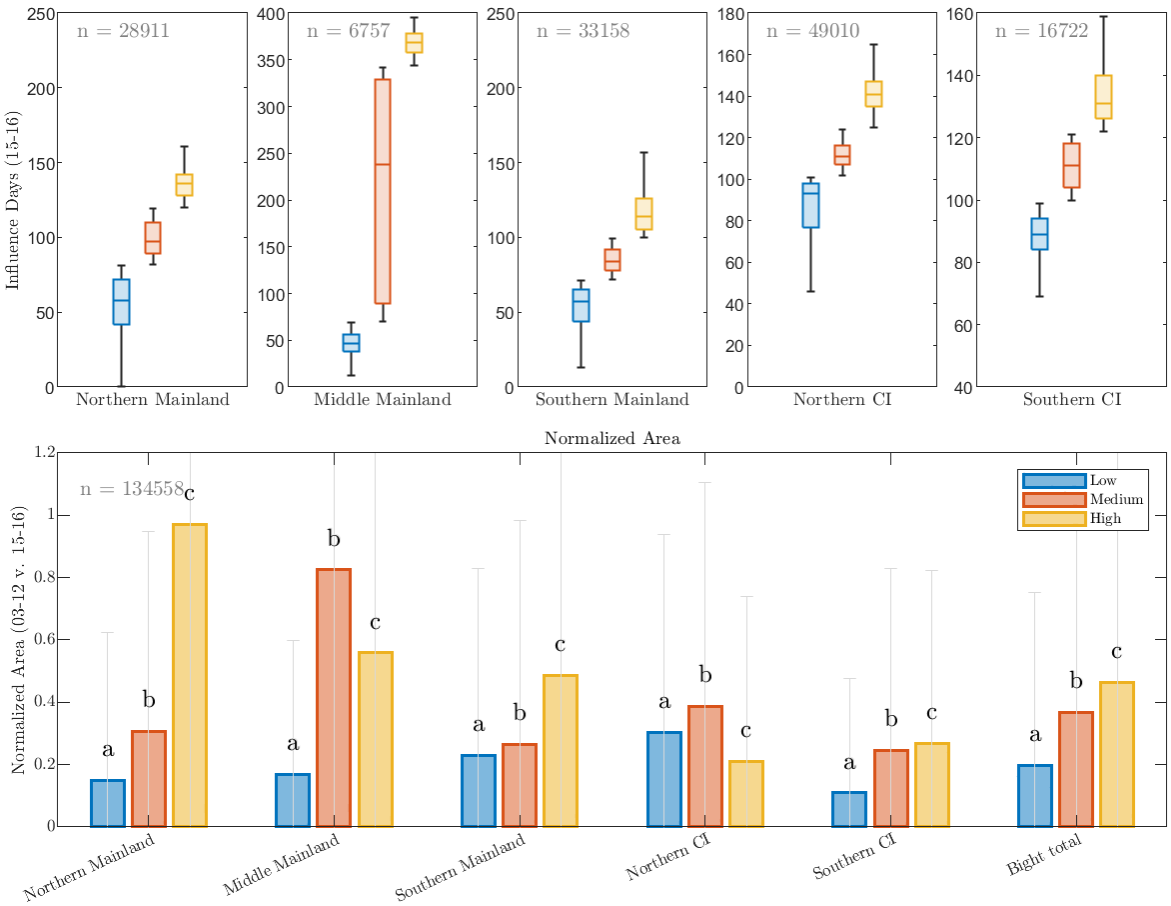

Figure 3.6: Comparative analysis of influence days against the normalized MHW area across various regions. Top panel: Box plots show the distribution of influence days categorized by the low, medium, and high quantiles for each region. Bottom panel: Bar charts show the normalized MHW area from 2015-2016 corresponding to the influence day quantiles (low, medium, high) for each region. Letters above bars indicate groups that are statistically different from one another ($p < 0.05$). The sample sizes in the right corner refer to the number of 4 km^2 boxes used in each analysis.

Kelp forests with higher anthropogenic influence maintain a greater normalized MHW area in regions of the SCB. Over the entire SCB, groups of anthropogenic influence show a statistically significant difference in normalized area ($p<0.05$), with the exception of the Northern Mainland (Table B.3). In the Middle Mainland, Southern Mainland, and Southern

Channel Islands regions, the kelp forest areas with low anthropogenic influence days show significantly lower normalized area compared to those with medium and high influence days (Fig. 3.6). The Northern Mainland and Northern Channel Islands do not show a statistical significance, however, in their relationship of kelp forest normalized area to influence days. Over the entire SCB, differences in normalized MHW area between the low anthropogenic influence days and medium and high categories are evident (Fig. 3.6). When the same analysis is carried out over the individual kelp canopy grid points (at the native 30 m resolution), we find that all groups are statistically different from one another in each region and throughout the SCB (Fig. B.3). These findings support the idea of a significant correlation across the SCB, and suggest that anthropogenic influence played a role in preserving canopy area in some of the major kelp forests of the SCB during the 2015-2016 MHW.

3.4 Discussion

We found evidence that anthropogenic inputs may have supported the resilience of kelp during the MHW. In order to quantify anthropogenic contributions, our study uses nutrient simulations from a validated physical-biogeochemical model of the SCB. This approach sets our research apart from previous kelp studies, which commonly rely on sea surface temperature as a proxy for nutrient availability and cannot directly quantify the influence of anthropogenic nutrients.

3.4.1 Anthropogenic influence correlated to MHW area

The positive correlation observed between anthropogenic nutrients and MHW area suggests that anthropogenic DIN may help explain post-MHW recovery patterns (Cavanaugh et al., 2019; Bell et al., 2023; Reed et al., 2016). Notably, areas with a higher influence from anthropogenic nutrients showed higher resilience during the MHWs, potentially benefiting from consistent nutrient availability even amidst stressful environmental conditions.

The link between kelp forest area and anthropogenic influence days was pronounced in Middle and Southern Mainland, aligning with previous finding indicating increased primary

production and phytoplankton biomass in these regions Kessouri et al. (2021a). The impact of wastewater point sources, such as major outfalls, was discernible in this region, positively contributing to net primary production. An exemplar case within the Middle Mainland region is the area surrounding the Palos Verdes peninsula. In the 1960s and 70s, large volumes of wastewater entering the Palos Verdes region led to reduced water clarity, thereby diminishing the photosynthetic radiation essential for kelp growth. However, with upgraded treatment standards, water clarity improved, enabling kelp populations to reclaim substantial areas, and potentially benefiting from increased DIN. This transformation highlights the pivotal role of enhanced outfall management in bolstering kelp health. Kelp forests in this region have also experienced significant decline due to purple urchin barrens (Williams et al., 2021). We note that ongoing restoration efforts involving urchin suppression began in central Palos Verdes forests around 2013 (House, Parker, 2018), possibly confounding our results in this specific region. However, the scale of this urchin removal (60 acres) is far less than the area where we observe significant correlations, and is not likely to explain the sustained kelp canopy in the entire region.

The Northern Mainland region exhibited sustained kelp growth during the MHW despite reduced nitrate levels, reminiscent of the findings by Smith et al. (2018) on kelp growth year-round in the Santa Barbara Channel. Our study suggests the presence of anthropogenic nutrients as a potential supplement to maintain kelp biomass beyond seasonal nutrient variations.

Further support for the influence of anthropogenic nutrients emerges in the Southern Channel Islands, where high correlation between kelp area and anthropogenic influence days aligns with recent modeling results suggesting nutrient transport from the mainland coast via eddies and subsequent increase in net primary production offshore Kessouri et al. (2023). Research on kelp populations surrounding Catalina Island demonstrated a higher growth rate and storage of internal nitrogen in young kelp populations that receive a regular supply of nitrogen (Zimmerman & Kremer, 1986), supporting our findings that anthropogenic nutrients can bolster kelp recovery during nutrient-limited periods.

Of the regions with less correlation between anthropogenic influence days and kelp canopy

area are the Northern Channel Islands and Southern Mainland, areas which experience differing responses and long term recovery patterns in the years following the MHW (Fig. B.5). Whereas the Northern Channel Islands has experienced large inter-annual variations over the past 20 years, the Southern Mainland experienced a large loss of canopy after the MHW, and is still recovering from this die off event, suggesting other factors, such as spore dispersal, may be influencing this area. As for the Northern Channel Islands, we note that this region has a higher ambient nutrient level, as seen from its lack of limitation days. This lack of relationship could be attributed to a smaller influence of local anthropogenic sources or factors not considered here such as significant wave height. Seeing as current data products that provide wave height over the entire SCB are coarse, and do not allow for analysis whithin the scales we study here, we do not dive further into this effect. Collectively, these observations highlight not just the pivotal role of anthropogenic nutrients, but also hint at the multifaceted and region-specific responses of kelp forests across different parts of the SCB.

3.4.2 Anthropogenic nutrient influence

We inferred influence of anthropogenic nutrients throughout the MHW, with anthropogenic influence days occurring in every season and region. Our spatial measurements indicated that anthropogenic nutrients were present in sufficient amounts to influence kelp growth rates in both the Mainland regions and the Channel Islands. While our findings focus on a specific MHW, it is crucial to acknowledge that anthropogenic DIN represents an ongoing and persistent nutrient source in the SCB (Sutula et al., 2021a).

This continuous supply of anthropogenic nutrients holds substantial implications for kelp forest dynamics beyond MHW events. Our observations prompt an examination of unknown drivers of kelp forest area fluctuations in non-MHW conditions (Bell et al., 2015). This is particularly significant as alternative sources of nitrogen have previously been shown to sustain kelp populations during periods of low ambient nitrate in the SCB (Brzezinksi et al., 2013; Zimmerman & Kremer, 1986; Fram et al., 2008). However, until now, the extent

of anthropogenic DIN influence throughout the entire SCB domain has remained poorly characterized.

While the distribution of anthropogenic nutrients nearshore is well characterized (Kessouri et al., 2021a), their offshore spread is less clear. This is due in part to the dynamic nature of the region's circulation and eddy field, which change with the seasons, driven by the influence of the California Current (Hickey, 1979). Eddies and fine-scale currents can unevenly distribute anthropogenic nutrients, carrying them from coastal areas to the remainder of the SCB Kessouri et al. (2023). Persistent eddies may thus be important in establishing the long-term patterns of nutrient influence, particularly for offshore kelp forests in the Channel Islands.

3.4.3 Caveats

Our study focuses on the roles of nutrient limitation and enrichment during a specific MHW. However, it does not encompass other complex factors influencing kelp distribution, such as waves, temperature stress, biological processes like dispersal and sea urchin predation, and human intervention like urchin removal in the Palos Verdes region. These factors significantly impact the kelp forest area in this region (Bell et al., 2020a). Furthermore we do not take into account the increased turbidity and reduced water quality often associated with anthropogenic outfalls, especially those in shallow regions. Although improvements have been made to water treatment in Southern California, anthropogenic runoff has negative impacts on kelp health in many circumstances. Furthermore, our analysis does not quantify the utilization rates of anthropogenic nutrients by kelp. Additional studies examining the competition between kelp and phytoplankton could shed light on how long anthropogenic nutrients persist in the SCB and their ultimate fate. Interpreting patterns of kelp loss during multiple MHWs over extended periods can be challenging, as the influence of anthropogenic nutrient loading both in the SCB and other kelp forests globally may have changed (Filbee-Dexter et al., 2020; Foster & Schiel, 2010). As human nutrient influence decreases and temperature increases, we expect to see a tighter coupling of kelp mortality to temperature

thresholds.

3.4.4 Outlook

This work offers an initial exploration into the anthropogenic influence on giant kelp in the SCB. Understanding the anthropogenic connection to natural kelp growth will inform conservation efforts for this keystone species, and further uses such as nutrient remediation and carbon offsetting. In addition to its significance as a keystone species and in providing valuable ecosystem services, giant kelp is increasingly affected by climate-related events such as MHW and El Niño (Wernberg et al., 2016; Laufkötter et al., 2020). Concurrently, the need to disentangle the impacts of nutrient stress from temperature stress becomes increasingly urgent. This distinction will enhance our understanding of the stressors affecting kelp in the SCB, and support more accurate predictions and management of species associated with kelp forests, in particular as their ranges range shift in a progressively warmer marine environment. By employing output from a high-resolution regional model, we have delineated the patterns of both natural and anthropogenic DIN with a resolution that surpasses the conventional estimations derived from SST satellite observations, while providing a distinction of nutrient source. The results indicate a correlation between anthropogenic nutrient influence and sustained kelp forest area throughout a major MHW in a highly urbanized coastal region, shedding light on some of the intricate dynamics that shape human-kelp forest interactions.

CHAPTER 4

Navigating Coastal Complexities: Advanced GIS Analysis for Kelp Aquaculture Suitability in the Southern California Bight

4.1 Introduction

Macroalgae (seaweed) aquaculture is the fastest growing component of global food production (Duarte et al., 2017), and has been recognised as a critical component in reaching the UN's sustainable development goals (SDG's) (Ferdouse et al., 2018). In the past 100 years, use of seaweed has expanded beyond food consumption into industrial services such as use in medicines, fertilizers, bio-plastics, textiles, and bio-fuel (Buschmann et al., 2017; Frieder et al., 2022; Kinley et al., 2020; Nabti et al., 2017). Demand for seaweed cultivation has also developed as a tool for anthropogenic nutrient remediation (Buschmann et al., 2017; Neori et al., 2004) as well as a mechanism for carbon dioxide sequestration (Duarte et al., 2017; Froehlich et al., 2019; Raven, 2017) and even suggested as form of protection from coastline erosion (Zhu et al., 2021). The utility of kelp has made it a key focus for the development of a blue economy. Despite the growing global demand for macroalgal farming, successful large-scale development beyond Asia has lagged (Bostock et al., 2010).

This lack of macroalgal farming development in many areas can be partially attributed to the increased demand on the coastal ocean for commerce, resource, and livelihood (Duarte et al., 2017). Identifying regions suitable to seaweed cultivation with minimal impact on existing ocean uses is crucial for the sustainable utilization of these ocean ecosystems (Scharin et al., 2016). In high demand coastal areas, site selection is further complicated by exten-

sive regulations, with multiple governing bodies regulating the coastal ocean (Morris Jr, 2021; Wickliffe et al., 2024). Site selection and permitting have impeded the growth of the macroalgal farming industry, and solutions are needed in order to expedite its development.

In order to establish and upscale macroalgal farming, it is necessary to develop an analytical framework that can accommodate commercial demands on the coastal ocean while promoting sustainability (Grebe et al., 2019; Gentry et al., 2017). Locational factors such as distance to a commercial port, shipping traffic, and depth influence site selection. However the relative importance of these variables may differ between farms. In addition to the aforementioned factors, suitable locations should experience a sufficient supply of nutrients to ensure healthy, consistent, and sustainable farm growth without the use of fertilizers. Consistent nutrient supply is crucial for the health of macroalgae, which has a relatively low capacity for carbon storage (Dean & Jacobsen, 1984). Introduction of fertilizers, however, is well known to trigger eutrophication and cascading detrimental effects in the marine environment (Boesch, 2019; Duarte & Krause-Jensen, 2018). Identification of ample, consistent nutrient supply ensures macroalgal growth and negates the need for additional nutrient input (Xu et al., 2023). A flexible framework for macroalgal site selection must allow for variations on relative importance of each of these factors while still providing concrete answers on what locations are most suitable.

In this research, we create a GIS framework for selecting suitable oceanic macroalgal farming locations and apply it to a case study in the Southern California Bight (SCB). The SCB has grown increasing attention in the past decade as a potential hotspot for aquaculture development (Morris Jr, 2021; Lester et al., 2018), and specifically macroalgal farming (Bell et al., 2020b; Snyder et al., 2020), and has well documented nutrient dynamics across remote sensing, observational, and modeling platforms. Previous efforts to asses suitability, such as the NOAA Aquaculture Opportunity Atlas (Morris Jr, 2021), provide a baseline evaluation of where kelp farming could be suitable in the SCB. This assessment, however, gives variables equal weights, and does not identify contributions of anthropogenic nutrients. Our macroalgal farm suitability framework builds upon this work by implementing multiple iterations of an analytical hierarchy process (AHP) in order to accommodate for differing

views on influence of different parameters. This framework incorporates the use of a high resolution biogeochemical model, which allows for a robust evaluation of nutrients, including an analysis on anthropogenic contributions, incoming solar radiation, and temperature in site selection. Through these model iterations, we identify hotspots to illuminate key site selections for farmers - experiencing conditions optimal for kelp growth while being within a suitable location to conduct macroalgae cultivation.

4.2 Methods

4.2.1 Study Domain

Our study domain covers the Southern California Bight (SCB), stretching from the US/ Mexico border to Point Conception, from 34°30' to 32°28' latitude and -121°to -117°longitude (Fig 4.1). A large scale equatorward flow from the California Current System (CCS) influences the SCB year round (Checkley & Barth, 2009). Additionally equatorward winds strengthen in spring and drive coastal upwelling. Stratification develops in the summer as the alongshore winds decrease and sea surface temperature rises in the euphotic zone (Dong et al., 2009).

Seasonal upwelling in this region supplies cold nitrate rich water which supports a robust giant kelp (*Macrocystis pyrifera*) population (Bell et al., 2020a; Krumhansl et al., 2016). Giant kelp in this region is primarily affected by temperature, nitrate availability, large wave events, and decadal climate cycles (Cavanaugh et al., 2011; Bell et al., 2015). Kelp canopies around the exposed regions of the Channel Islands experience more frequent disturbance due to large wave events (Edwards, 2019), but can support large canopy areas when unperturbed. Among the more protected nearshore southern California regions, nitrate availability often limits kelp canopy area (Bell et al., 2015).

The study area in total covers 38,765 km^2. State waters extend to 3 nautical miles offshore, including the areas around the Channel Islands. Within our domain (exclusion areas removed) approximately 6,103 km^2 (16%) is within state waters, while 32,103 km^2

(84%) is within federal waters.

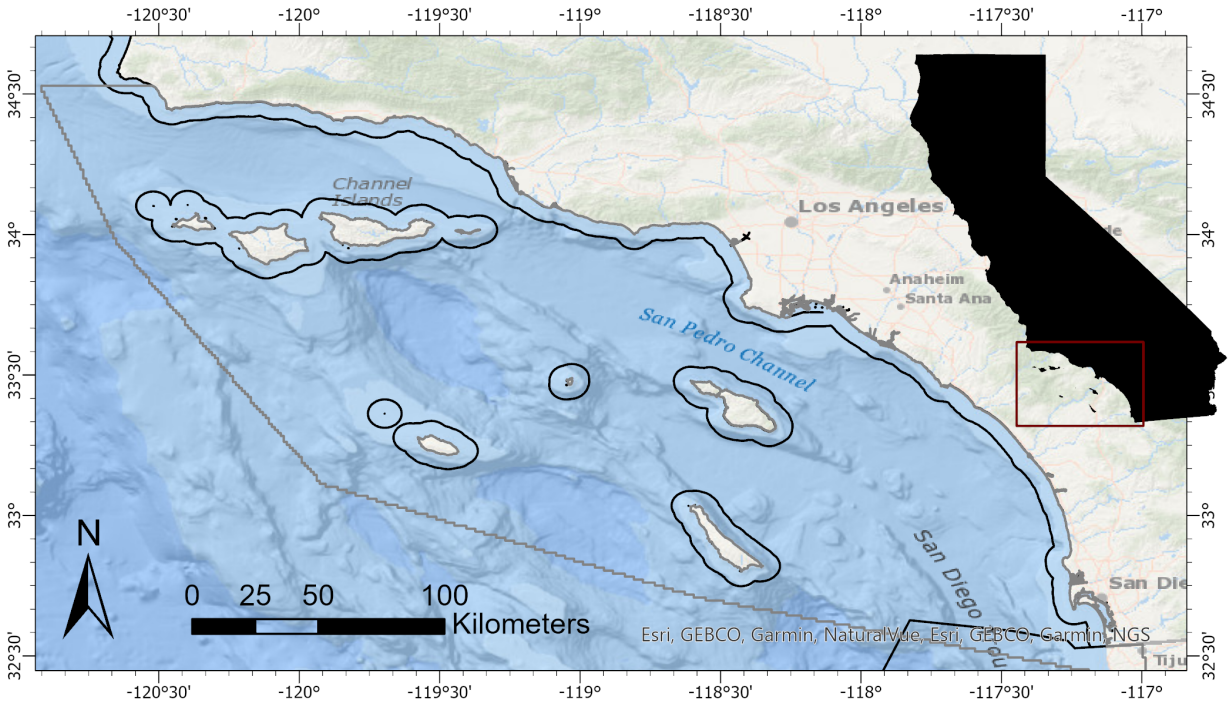

Figure 4.1: Domain of the suitability analysis. The grey outline takes into account the entire study region . The black line indicates the distinction between state and federal waters.

4.2.2 Data Description and Sources

Nutrients, light, and temperature are the primary determinants of kelp growth in Southern California (Gerard, 1982; Dean & Jacobsen, 1984; Cavanaugh et al., 2019; Deysher & Dean, 1986; Zimmerman & Kremer, 1984; Rodriguez et al., 2016; Bell et al., 2015). In this region, nutrients are primarily in the form of nitrate supplied by seasonal upwelling and ammonium supplied by anthropogenic sources such as river runoff and sewage outflow (Sutula et al., 2021a; Howard et al., 2014). To accommodate for both forms we use total dissolved inorganic nitrogen (DIN) in our analysis.

Optimal growth conditions for kelp involve ample dissolved inorganic nitrogen and light, and lower temperatures. In southern California, optimal DIN is above 1 μmol L^{-1} (Gerard, 1982), photosynthetic active radiation (PAR) is 3-9 W m^{-2} (Dean & Jacobsen, 1984), and

temperature is 14-20 °C (Gerard, 1982).

For this study, we extract DIN, photosynthetic active radiation (PAR), and seawater temperature from a coupled physical-biogeochemical modeling system, ROMS-BEC (Shchepetkin & McWilliams, 2005; Moore et al., 2004). Here, we use a downscaled solution for the SCB region with a 300 x 300 m resolution which has been extensively validated in previous studies (Kessouri et al., 2021b). DIN, PAR, and seawater temperature data is averaged from fall to spring to reflect the optimal growing season of seaweed aquaculture (Fieler et al., 2021; Snyder et al., 2020) and is integrated over the top 20 m of the water column and averaged.

Location and exclusion zone variables are informed by previous analysis on aquaculture within this domain (Morris Jr, 2021). Data is gathered from state and federal sources (see Table 4.2.2).

Category	Variable	Scale*	Source
Nutrients	DIN	MS Large	ROMS BEC[1]
	PAR	MS Large	ROMS BEC[1]
	Water temperature	MS Large	ROMS BEC[1]
Location	depth	semi-binary (20-60 m = 1, 60-200 m = 0.5)	NOAA NCEI[2]
	distance to dock	linear	US DOT[3]
	ship density	MS small	Marine Cadastre[4]
Exclusion Zones	shipping lanes	binary	U.S. Coast Guard[5]
	Marine Protected Areas (MPA's)	binary	California Department of Fish and Wildlife[6]
	Offshore oil and active gas leases	binary	NOAA[7]
	Military safety zones	binary	California Department of Fish and Wildlife[8]
	Wastewater outfall pipes	binary	NOAA[9]
	Submarine cable area	binary	NOAA[10]
	OCS Oil and gas pipelines	binary	BOEM[11]
	Ferry routes	binary	Department of Transportation [12]

Table 4.1: Data sources for classification. See section 4.2.3.2 for detailed scaling methodology.[1] (Kessouri et al., 2021b). [2] (National Geophysical Data Center, 2012). [3] (Bureau of Transportation Statistics, 2022). [4] (Office for Coastal Management (OCM), 2024). [5] (U.S. Coast Guard). [6] (California Department of Fish and Wildlife, 2016). [7] (National Oceanographic and Atmospheric Administration (NOAA), 2024). [8] (California Department of Fish and Wildlife, 2024). [9] (National Oceanographic and Atmospheric Administration (NOAA) Marine Cadastre, 2024). [10] (National Oceanographic and Atmospheric Administration (NOAA) Office for Coastal Management, 2024).[11] (Bureau of Ocean Energy Management, 2024). [12] (Bureau of Transportation Statistics (BTS), 2020).

4.2.3 Model description

Our suitability model assigns a score between 0 and 100 to each of the 1 km^2 cells within the domain.

The model can be applied to various types of aquaculture systems. In this case study we assume a longline farm design, similar to those described in Frieder et al. (2022). Alteration of suitability parameters could accommodate other farm designs such as artificial reefs and elevator systems (Navarrete et al., 2021).

The objective of this model is to provide a preliminary estimate of where farming and cultivation of giant kelp would be ideal. Our suitability model is a combination of two sub-models: location and kelp growth.

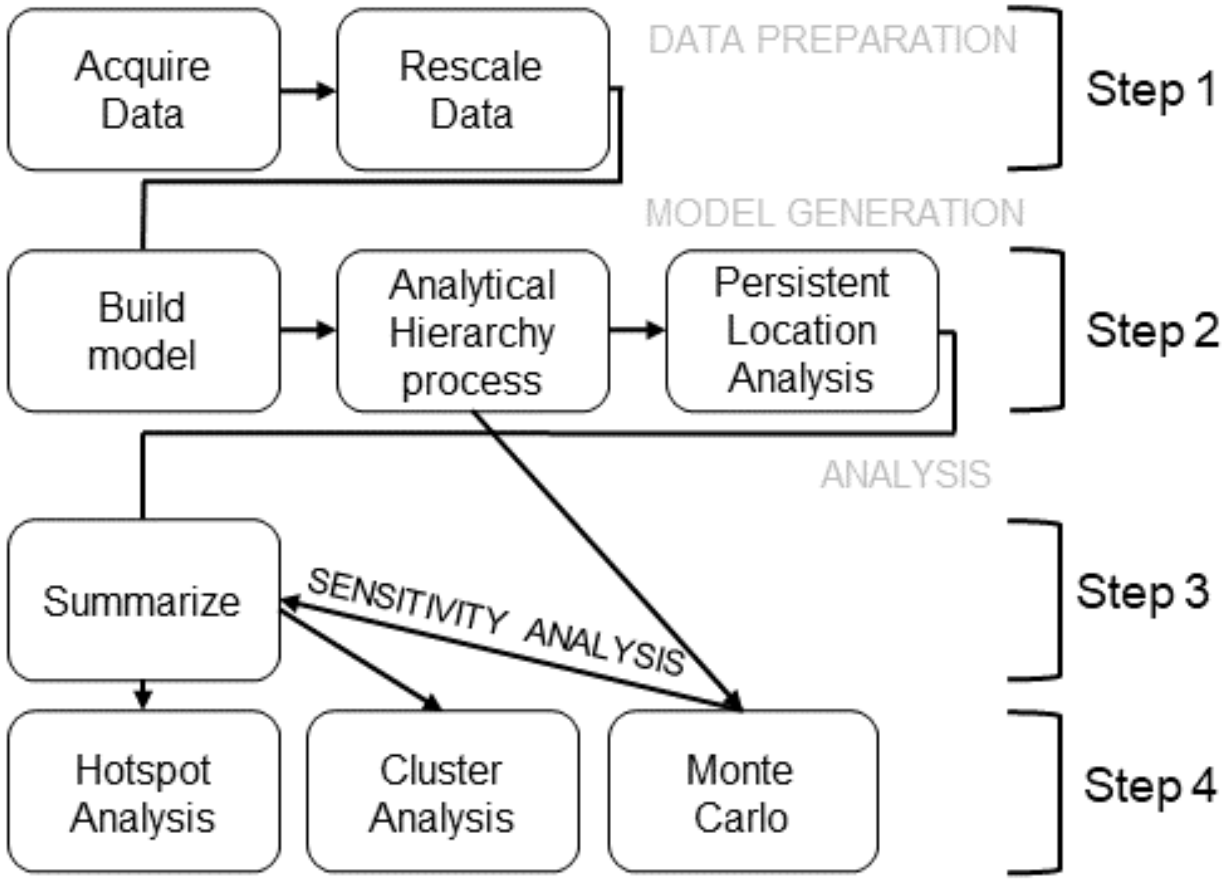

Figure 4.2: Workflow for the suitability model.

4.2.3.1 Sub-models

The location sub-model takes into account three criteria: depth, distance to port, and amount of shipping traffic. The kelp growth model takes into account DIN, PAR, and seawater temperature. With the output of the two sub-models, the suitability analysis was run with three different weight regimes. The three different sub-model weight regimes (kelp growth and location, respectively) are as follows: 0.4 and 0.6 (location more important), 0.5 and 0.5 (kelp growth and location equal importance) and 0.6 and 0.4 (kelp growths more important).

The result of the suitability analysis is a spatially continuous raster of 1 km^2 cells.

4.2.3.2 Scaling

Before variables are used within the model they are scaled to fit a 0-1 scheme. We use two resampling techniques to distinguish between continuous variables with non linear distributions: mean and standard deviation small (MS small) and mean and standard deviation large (MS large.) Fuzzy membership is used to resample discreet data to a continuous function. DIN, and PAR are re-scaled using a MS large scheme (Eq 4.2), which favors larger raster values. Ship density is rescaled using the MS small scheme (Eq 4.1), which favors smaller raster values.

For $x > a \cdot m$:

$$u_s(x) = \frac{b \cdot s}{x - (a \cdot m) + (b \cdot s)} \tag{4.1}$$

$$u_l(x) = 1 - \frac{b \cdot s}{x - (a \cdot m) + (b \cdot s)} \tag{4.2}$$

where m is the mean, s is the standard deviation, a is a multiplier of the mean, b is a multiplier of the standard deviation. The a and b multipliers are input parameters.

When $x \leq a \cdot m$:

$$u(x) = 0 \tag{4.3}$$

Depth we rank as semi binary, with optimum (score of 1) depth being 20 - 60 m, depths at which current macroalgal farming practice is most common (Frieder et al., 2022; Lester et al., 2018), and semi optimal (score of 0.5) depth at 60 - 200 m where technology is moving but still not fully adopted (Chen et al., 2023a; Arzeno-Soltero et al., 2022; Navarrete et al., 2021). Beyond 200 m depth is non optimal (score of 0) (Table 4.2.2). Temperature and distance to port are linearly rescaled to a 0-1 scale without altering the distribution.

4.2.3.3 Model weighting

Within the kelp growth and location submodels, each variable is assigned a weight. For the the kelp growth submodel we assign equal weights to all three variables, being that all three variables are necessary in the basic equation for algal growth (Behrenfeld & Falkowski, 1997).

Importance of the variables in the location submodel (depth, distance to port, and shipping traffic) is highly subjective. In order to generate weights for location sub-model variables, we create potential ranks of importance for siting farms by utilizing the Analytical Hierarchy Process (AHP) methodology. Development of the AHP involves ranking the importance of the factors (1-3) (Saaty, 2008). Ranks are informed based upon previous kelp aquaculture literature (Bodycomb et al., 2023; Rugiu et al., 2021; Buschmann et al., 2017; Frieder et al., 2022). From here we created a pairwise comparison matrix (Eq. 4.4) using the ranking, such that element a_{ij} represents the importance of element i over element j.

$$\mathbf{A} = \begin{bmatrix} 1 & a_{12} & a_{13} \\ \frac{1}{a_{12}} & 1 & a_{23} \\ \frac{1}{a_{13}} & \frac{1}{a_{23}} & 1 \\ \end{bmatrix} \tag{4.4}$$

From the pairwise comparison matrix (A), we compute eigenvectors (v) and values (λ) on the matrix, and finally normalize the principle eigenvector to derive the weights (w).

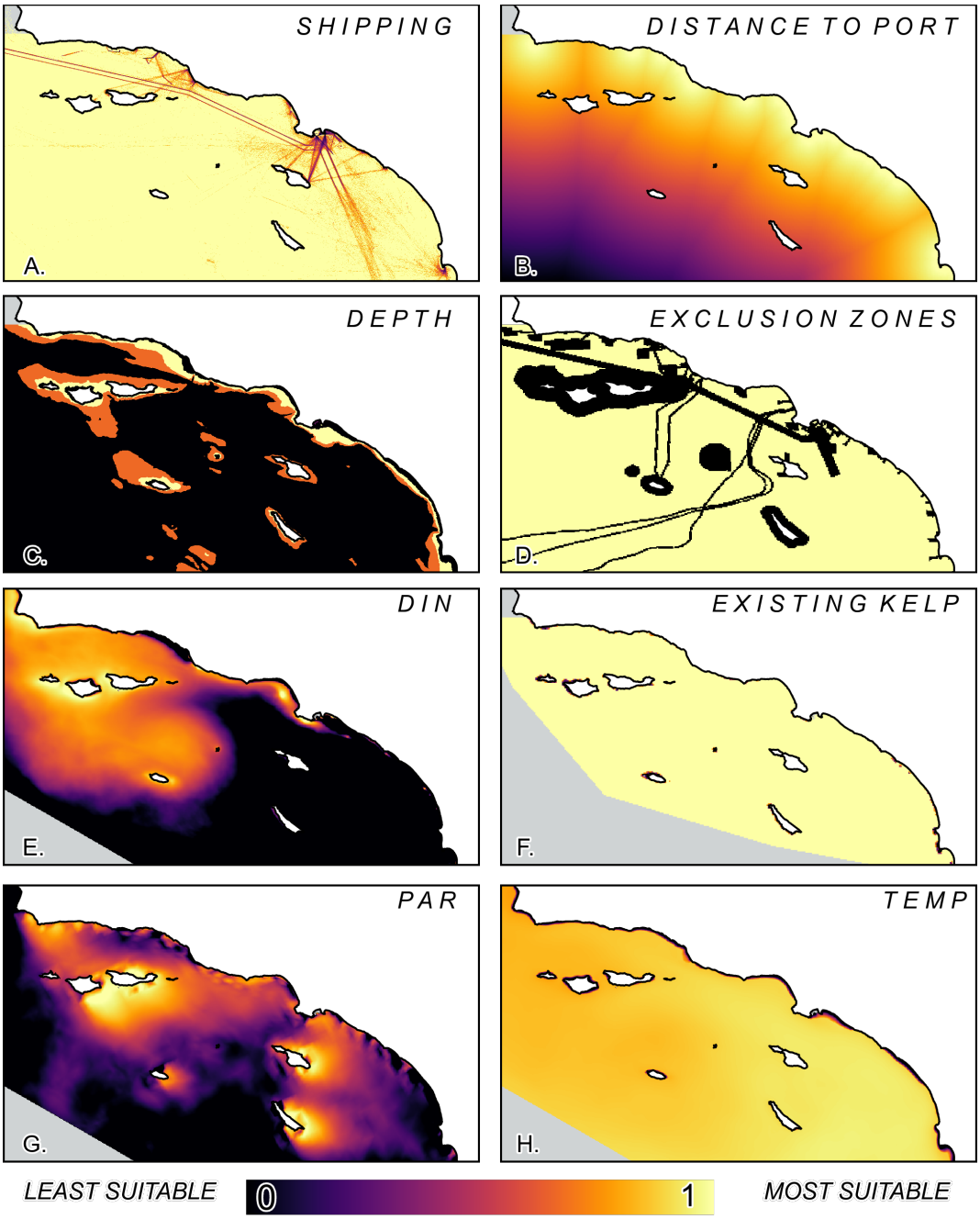

Figure 4.3: Re-scaled values of model variables, shipping (A.), distance to port (B.), depth (C.), exclusion zones (D.), integrated (0-20 m) average DIN (E.), existing kelp biomass (F.), integrated (0-20 m) average PAR (G.), and integrated (0-20 m) average temperature (H.)

$$\mathbf{Av} = \lambda \mathbf{v} \tag{4.5}$$

$$\mathbf{w} = \frac{\mathbf{v}}{\sum_{i=1}^{n} v_i} \tag{4.6}$$

To assess its robustness, our model is run with small perturbations to the initial pairwise comparison values. The comparison values are adjusted incrementally by 0.25 up to a max difference of 0.5. Each AHP scenario is computed 8 times, each with a small perturbation to one of the values. The average of these 8 perturbations is found to give the suitability for one specific AHP scenario.

4.2.3.4 Model Iterations

Three scenarios of AHP are run to represent possible interpretations of highest location suitability for macroalgal farming (Table C.1). These three location suitability scenarios are combined with the three sub-model weighting scenarios (see Section 4.2.3.1) to create nine total AHP suitability model scenarios. The combination and comparison of these we refer to as our Persistent Location Analysis (Fig. 4.2).

Our nomenclature for AHP gives rank comparisons in order of distance to port to depth, distance to port and shipping traffic, and depth to shipping traffic. For example AHP (2,3,1) indicates that distance to port is slightly more important than depth and more important than shipping traffic, and depth and shipping are of equal importance when compared to one another.

4.2.3.5 Sensitivity Analysis

Our model's sensitivity is tested by a Monte Carlo statistic. Here we use stochastic perturbations of the locational weights (detailed in Sec. 4.2.3.3) and apply them to the suitability model. These perturbations represent potential alternative ranks of location variable importance. The simulations were run over 20 random AHP iterations.

To compare the difference in the average of the 9 suitability models and Monte Carlo simulations we employ a Kolmogorov-Smirnov (K-S) test (Lilliefors, 1967). A K-S test is a non-parametric test that compares the distributions of two datasets and tests the null hypothesis that the two datasets are from the same distribution. We find a small p-value between the summary of our model and the summary of the Monte Carlo model, indicating the distributions are significantly different.

4.2.4 Model analysis

Results presented are summaries of all 9 AHP models (See sec. 4.2.4.1). In order to determine the most consistent combination of weights for an individual suitability model, we select the AHP model with the least skew.

From the suitability model outputs, which scaled from 0-100, we classify the results as follows (Table 4.2):

Score Range	Suitability	Abbreviation
0-20	Non-Suitable	NS
21-40	Less Suitable	LS
41-60	Suitable	S
61-80	Highly Suitable	HS
81-100	Very Highly Suitable	VHS

Table 4.2: Suitable range and classification

4.2.4.1 Hotspot analysis

We identify hotspots in our entire suitability analysis with the average across all 9 AHP scenarios. With this average of suitability scores, we run a Getis-Ord Gi* statistic (Getis & Ord, 1992). This statistic takes into account the value of a feature in relation to the neighboring features surrounding it. The z-score helps interpret the value of the feature (high value a positive z score) and the p-value indicates whether the feature is in a statistically

significant group of features (low value indicating a significant group).

The Getis-Ord local statistic is given as:

$$G_i^* = \frac{\sum_{j=1}^{n} w_{i,j}x_j - \bar{X}\sum_{j=1}^{n} w_{i,j}}{\sqrt{\frac{\sum_{j=1}^{n} w_{i,j}^2}{n-1}\left(\sum_{j=1}^{n} x_j^2\right) - \left(\frac{\sum_{j=1}^{n} w_{i,j}x_j}{n-1}\right)^2}} \tag{4.7}$$

where x_j is the attribute value for feature j, $w_{i,j}$ is the spatial weight between feature i and j, n is equal to the total number of features and:

$$\bar{X} = \frac{\sum_{j=1}^{n} x_j}{n} \tag{4.8}$$

$$S = \sqrt{\frac{\sum_{j=1}^{n} x_j^2}{n} - \left(\bar{X}\right)^2} \tag{4.9}$$

4.2.4.2 Location analysis

From the average results of the 9 AHP scenarios, we identify the locations of high score farming with their suitability scores. We identify the locations of eight neighboring 1 km^2 features and present the top 10 farming locations in our analysis. This size follows the aquaculture opportunity areas identified by NOAA (Morris Jr, 2021), which have a maximum size of 809 Ha (8 km^2).

The process to identify and evaluate these locations is as follows: For each cell $g_i \in G$, we identify all adjacent cells to form potential locations. A spatial function $A(g_i, G, sindex) \rightarrow \{g_j | g_j \text{ is adjacent to } g_i\}$ is employed, where $sindex$ aids in efficiently locating these adjacent cells. Once potential locations are identified, we evaluate them by calculating the average suitability score, $\bar{s}_C$, for the cells comprising each location:

$$\bar{s}_C = \frac{1}{|C|}\sum_{g_i \in C} s_i, \tag{4.10}$$

where $|C|$ is the number of cells in the location, and s_i is the suitability score of cell g_i.

After calculating the average scores for all identified locations, we rank them in descending order of their $\bar{s}_C$.

4.3 Results

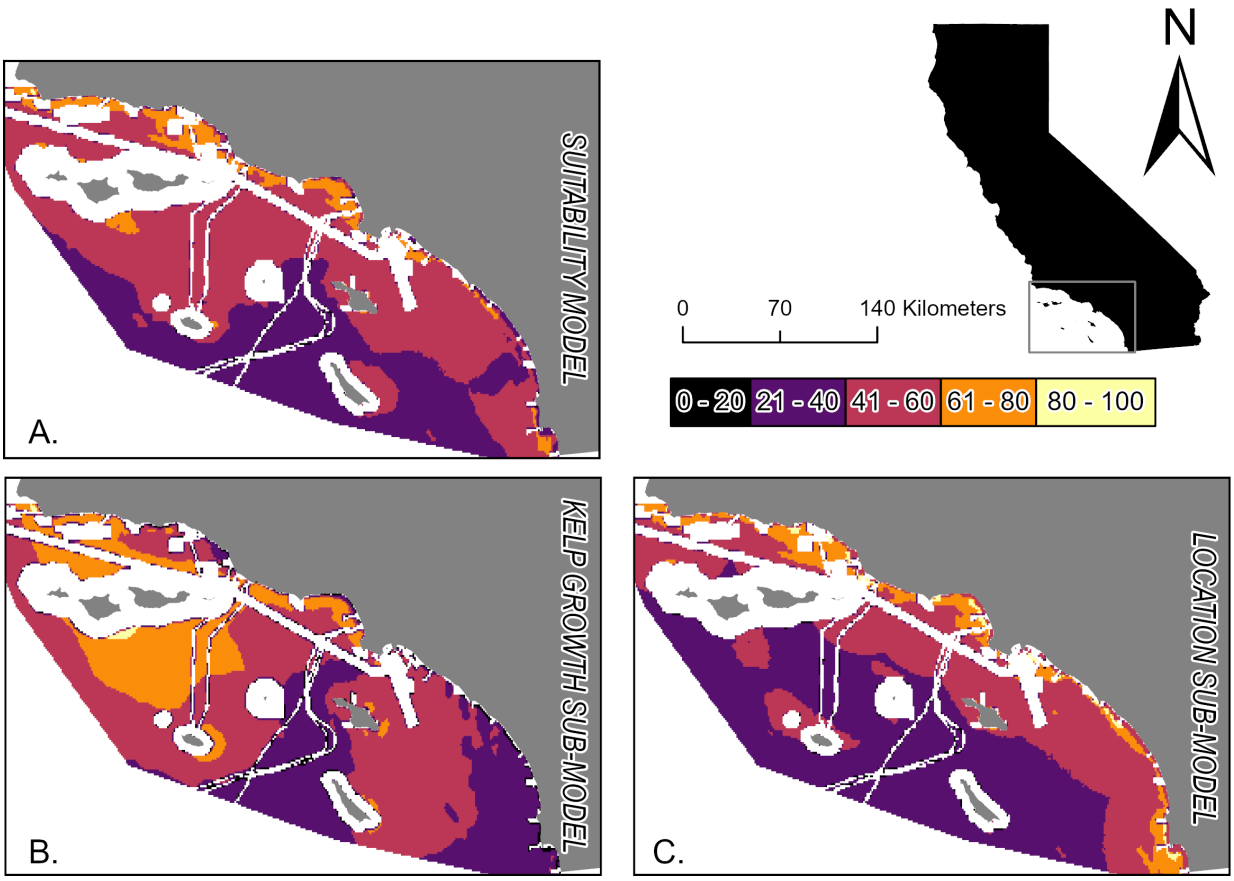

Figure 4.4: Maps of the suitability model (A.), kelp growth sub-model (B.), and location sub-model (C.) results for the lowest skew iteration.

Our model identified a substantial area - 2,289 km^2 - of high suitability (60-80) area within the study region (Fig. 4.4), underscoring the potential of macroalgal farming within the SCB.

Within the suitability model, the kelp growth sub-model showed a higher variation over

the Bight than the location sub-model. Highest scores of kelp growths were concentrated near Santa Monica Bay and surrounding the Northern Channel Islands (Fig. 4.4 A.). Location scores were highest along the mainland coastline, within closer proximity to ports. Both location and kelp growth sub-models had very highly suitable (VHS)(81-100) areas (0.07% and 0.01%) (Table. C.2) there was no overlap between the two, resulting in a max total suitability model score of 80.8. Highly suitable (HS)(61-80) regions were more common in the kelp growth sub-model (12%) versus the location model (5%) Excluded area comprised 9150 km^2 of our study region.

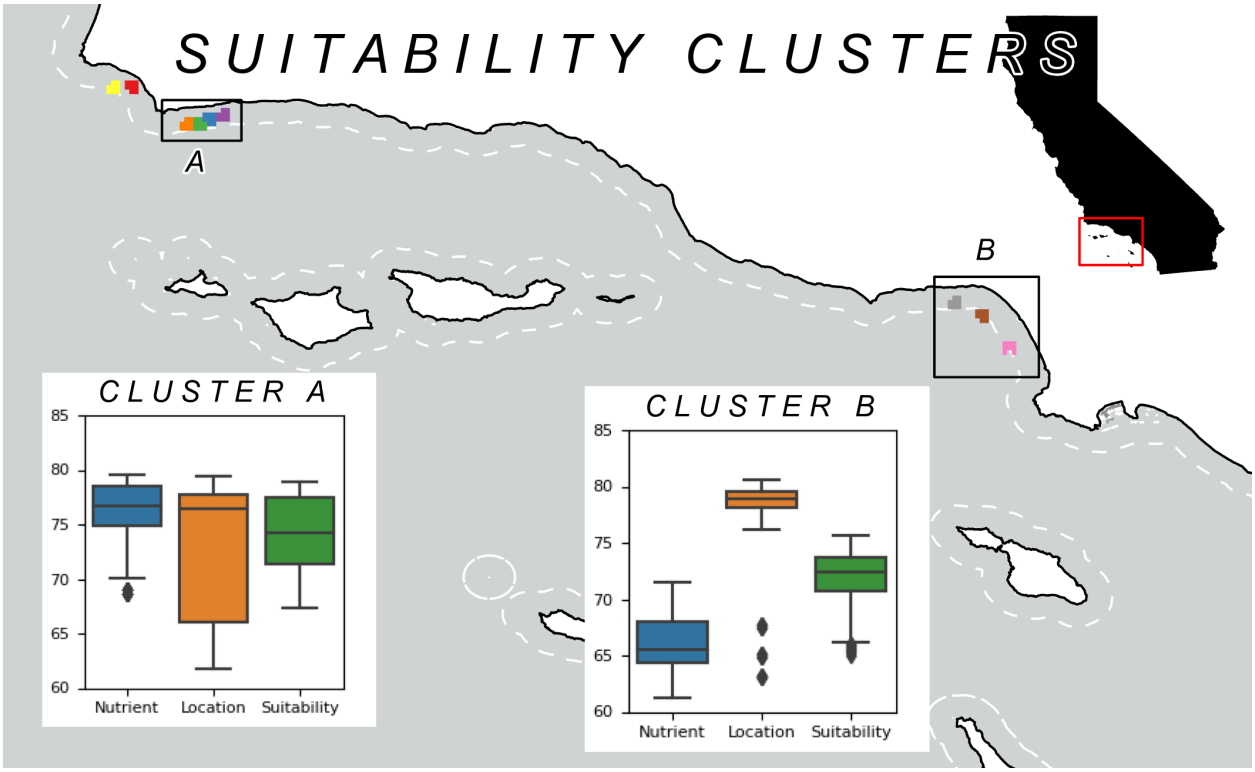

Figure 4.5: Suitability clusters. The top 9 suitable farming locations of 8 km^2. Box plots represent the kelp growth, location, and total suitability scores of the two clusters of highest suitability locations, A and B. White dashed line indicates the distinction between state and federal waters

Our detailed location analysis (see sec 4.2.4.2), identified two clusters, A and B, each characterized by multiple high suitability locations, highlighting distinct areas for potential

development.

Cluster A sits offshore in Santa Barbara County, just south east of Point Conception, 56 km from Santa Barbara Harbor. This cluster has a mean kelp growth score of 76 (Fig. 4.5). The locations scores are slightly lower, and have a broader range than the kelp growth scores. The total suitability for Cluster A is 74. The average depth in this location is 51.11 m, average temp is 15.69 °C, average PAR is 75.28 W m^{-2}, DIN is 40.67 mMol N m^{-3}.

Cluster B is within Los Angeles County, offshore of Santa Monica, 6km from Marina Del Ray. This region has a higher location score than kelp growth score (78 v. 66) (Fig. 4.5). The total suitability for this region is 73. The average depth in this location is 53.4 m, average temp is 14.7 C, average PAR is 75.63 W m^{-2}, DIN is 35.38 mMol N m^{-3}, anth DIN is 0.56 mMol N m^{-3}.

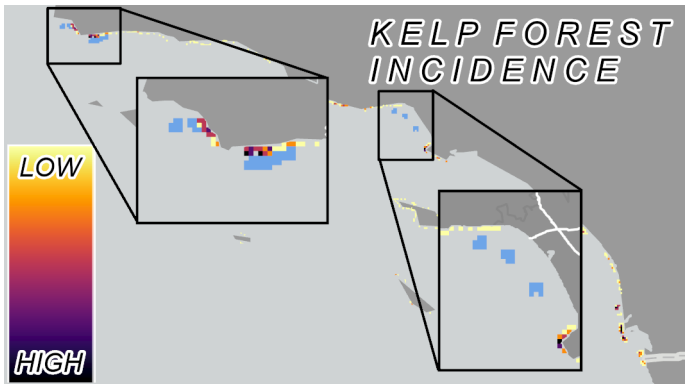

Figure 4.6: Incidence of natural kelp canopies over the past 20 years overlapping with suitable kelp farming locations. Darker cells indicate a higher coincidence of kelp canopy biomass and model suitability.

A consideration for the results of our suitability analysis was potential interference with current kelp forest locations, particularly noted in portions of the Santa Barbara Channel. Of the suitable locations, cluster A within Santa Barbara County experiences 3 km^2 of overlap within the footprint of recent (past 20 years) kelp canopies (Fig. 4.6). When accounting for a 1 km^2 buffer around current kelp forests to allow for spore dispersal, 12.8 km^2 of suitable area overlaps. Cluster B within the Santa Monica bay experiences no overlap with current forests or within a 1 km^2 buffer. When accounting for potential interference with current

kelp forests, Cluster B in Santa Monica is most ideal.

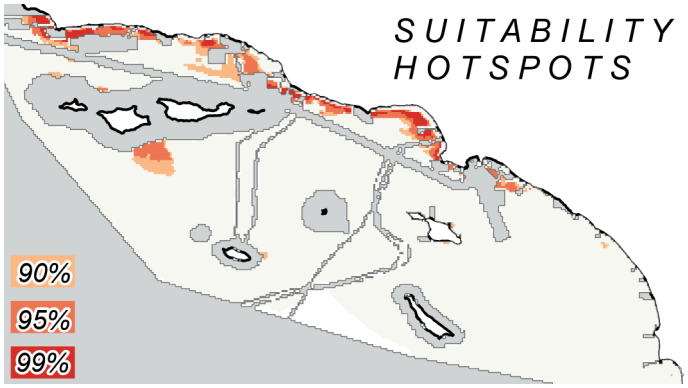

Figure 4.7: Suitability hotspot analysis. Getis-Ord Gi* hotspot analysis results from all suitability model iterations. Red locations indicate hotspots (frequently high suitability with high suitability neighbors) and blue locations indicate cold spots.

A consensus across our 9 AHP model iterations pinpointed the northern and central nearshore region as consistently high suitability hotspots, demonstrating alignment in identifying prime kelp farming locations. From the Palos Verdes region to Point Conception we see frequently high suitability with high suitability neighbors (Fig 4.7). A majority of these hotspots sit within state waters, however another hotspot emerges south of the Northern Channel Islands.

4.4 Discussion

Our evaluation of kelp farming in the SCB found the most suitable locations in the Santa Monica Bay and between Point Conception and Santa Barbara, and high (61-80) suitability throughout the coastline of the northern and central SCB. Of the high suitability sites, those between Point Conception and Santa Barbara have the highest possibility of interaction with current kelp forest areas.

In this suitability analysis we identify two regions optimal for development of farmed giant kelp. Demand for kelp farming has grown in the SCB, and our favorable suitability results within the Santa Barbara region align with other recent studies. Lester et al. (2018)

identified 325 1 km^2 sites 'highly suitable' for macroalgal cultivation, primarily concentrated offshore of Santa Barbara. Their analysis compares the feasibility of macroalgal cultivation alongside mussel farming and finfish aquaculture, and cites the Santa Barbara region as the most suitable for macroaglae among the three potential aquaculture industries. In addition, results from Snyder et al. (2020) support a high likelihood of healthy kelp aquaculture in Santa Barbara, finding this region to experience the least amount of kelp stress (over 21 consecutive days with nutrients below 1 μ mol $L^{-}1$) compared to the rest of the SCB. As of publication, Ocean Rainforest (ORI), a macroalgal cultivation contractor is set to scale giant kelp farming in Santa Barbara with ARPA-E funding under their project MacroSystems.

Our suitability results in Santa Monica Bay show agreement with previous suitability studies. The NOAA Aquaculture Opportunity Atlas cites Santa Monica Bay as a region of development for a 1000 acre (4.05 km^2) and 500 acre (2.02 km^2) sites (Morris Jr, 2021). The aquaculture opportunity atlas makes significant progress in identifying suitable areas within federal waters of the SCB. The atlas was created to provide a streamlined analysis for decision-makers and potential farmers in order to expedite aquaculture development. Our analysis improves upon this by catering specifically to macroalgae through simplifying variables and catering weights more specifically. Although there is a high concentration of sailing and pleasure craft in this region, Santa Monica Bay experiences high concentrations of natural and anthropogenic DIN (Kessouri et al., 2021a), low density of cargo traffic, and a close proximity to ports. These factors produce a high score within the location sub-model in this region.

Our methodology expands in the field of kelp suitability analysis by incorporating advanced biogeochemical models for nutrient estimates, allowing for a higher resolution than sea surface temperature (SST) to nitrate approximation methods (Chen et al., 2023b). Unlike these remote sensing methods that assume a negative correlation of SST to nitrate, our model outputs incorporate sources of anthropogenic DIN beyond nitrate that cannot be detected with temperature correlations alone. An example of these sources include wastewater outfalls and rivers (Snyder et al., 2020), which are critical in coastal regions where anthropogenic sources of DIN, predominantly in the form of ammonium (Sutula et al., 2021a), can

surpass the supply of upwelling derived nitrate periodically (Howard et al., 2014).

Building on this advancement in nutrient resolution, we differentiate our work by developing a flexible model structure which accommodates differing views of variable importance in the suitability analysis. Employing multiple versions of the AHP to asses and rank variables in siting suitability of macroalgae and other aquaculture, combines, and highlights locations most frequently suitable among scenarios, a method which expands upon traditional methods such as using fuzzy sets (Tarunamulia & Sammut, 2023; Gimpel et al., 2015), and the work of Radiarta et al. (2008) who averages the results from two AHP scenarios. This nuanced approach not only prevents over or underestimation for suitability, but also harnesses environmental variables from a validated biogeochemical model which provides continuous four dimensional information on PAR, temp, and DIN, going beyond the resolution of suitability analyses over large spatial domains (Gimpel et al., 2015; Snyder et al., 2020). This provides a horizontal resolution surpassing other suitability studies for aquaculture in the coastal zone, which frequently uses a large number of variables, up to 48 in some cases (Dapieve et al., 2023), however are limited by the resolution and quality of the variable data used.

In the Santa Monica Bay, a notable portion of DIN originates from anthropogenic sources, introducing complexities for analyzing kelp growth suitability. (Duarte et al., 2021) cites the benefit of choosing areas already enriched in nutrients in order to create the greatest environmental benefit from seaweed farms. They warn, however, targeting areas with solely anthropogenic nutrients and eutrophication can be at risk of epiphytes, which would damage the kelp stock. Further accompanying the nutrient dynamics in the SCB, Kessouri et al. (2023) note the importance of eddies in the northern portions of the SCB and the Channel islands. These eddies engage in cross shore transport of natural and anthropogenic sources of DIN, and can retain phytoplankton and nutrients offshore. These oceanographic variations accompanied by influence from terrestrial sources of nutrients underscore the nuances of analyzing kelp growth suitability in this dynamic region.

It is important to ensure sites selected do not interfere with the health of current kelp communities (Alberto et al., 2010). Although kelp spores can travel thousands of meters in the SCB, in order to produce a kelp frond they must settle within close (mm) proximity of

another spore (Reed et al., 2006). Reed et al. (2008) site that this settling of spores likely only happens within 1 km of a current forest. Of our suitable locations we find that portions of cluster A near Santa Barbara are within 1 km of kelp forests, and in some instances overlapping on an edge. Cluster B, however, sits within Santa Monica Bay, with historically low or non-present kelp forests.

It is worth noting that this model is not a comprehensive view of all suitable aquaculture area in the SCB. Our study is focused on updating suitability analysis to include high resolution biogeochemical variables within state and federal waters. This analysis does not include variables pertaining to cultural resources, current fishing and aquaculture, or national security. We note that the spatial domain does not take into account waters under municipal jurisdiction such as ports and harbors. These regions, however, still demand a thorough siting process and suitability analysis such as those by Wickliffe et al. (2024). Comparing multiple AHP scenarios as we present here would be beneficial to these smaller regions. Recent development of aquaculture in ports in the SCB such as San Diego and Ventura, demonstrates a demand for small scale macroalgal farming development (**?**). Programs such as these eliminate the high cost of transport and have a lower barrier to entry for emerging macroalgal companies, who may not be able to wait the four to ten years typical of attaining the appropriate lease and permits (Green Wave, 2018). We use limited key environmental variables, and do not include others which vary on a smaller scale, include wave action. This exclusion of wave action, however, is accounted for as most current technologies which keep kelp longlines slightly subsurface (10 m) where wave action is dissipated. As more technologies develop, such as depth cycling farms presented in Navarrete et al. (2021), analysis would benefit from more specific parameters to optimize for the farming method. In light of these factors it is important to interpret these analysis as a 'pre-selection process' for giant kelp suitability within state and federal waters of the SCB.

As macroalgal farming technologies advance, so must our suitability models. Integrated kelp forest models within biogeochemical models which allow us to analyze the impact of kelp forests on the biogeochemistry of the region have been validated on an individual farm scale (Frieder et al., 2022). Deploying this model within the suitable regions found here

would provide decision makers a comprehensive view of how the surrounding environment would be affected by macroalgal farming. Furthermore, studies are underway to estimate the anthropogenic nutrient remediation of suitable kelp farms (Frieder et al., personal communication). Analysis like these will allow decision makers to quantify the benefit of these farms to the biogeochemistry of the coastal zone, and are of particular interest to the SCB where there is a proven influence of anthropogenic nutrients (Kessouri et al., 2021a).

This macroalgal farming suitability analysis catered to giant kelp provides an estimate of which regions are most suitable for development in the Southern California Bight. Our study identified two clusters for highly suitable farms, one 56 km to the west of Santa Barbara Harbor, one within the Santa Monica Bay, 6 km from Marina Del Ray. Our model was run over multiple iterations with different ranks on variables to account for multiple views on optimal site location. We analyze our results in the context of existing kelp forests, and find that overlap could be possible with optimal locations near Santa Barbara. This analysis should be interpreted as a preliminary test of a framework for siting optimal kelp farming locations, within the Southern California Bight or elsewhere. Relevant interactions with other aquatic species ranges must be taken into consideration when making a final site selection.

CHAPTER 5

Conclusions

The goal of this dissertation was to improve our understanding of the interactions of primary producers with the anthopogenic nutrient sources within the southern California Bight (SCB). We accomplish this by first understanding the mechanisms of wastewater utilization in Chapter 2. We then shift our focus to giant kelp. In Chapter 3, we investigate the impacts of anthropogenic nutrients within kelp forests during the 2014-2016 MHW. Finally we identify the regions most suitable for cultivation of giant kelp within the SCB in Chapter 4.

5.1 Summary of Chapter 2

Chapter 2 we aimed to deepen our understanding of how the physical and chemical components of wastewater influence net primary production (NPP) in the SCB. To achieve this, we employed a series of coupled physical biogeochemical models, each performing a different perturbation to either the physical characteristics (concentrating volume), and/or chemical characteristics (inputting DIN as solely nitrate or ammonium). This research is novel as it enhances our understanding of the mechanisms through which anthropogenic nutrients impact coastal environments. Such impacts are increasingly relevant as concern over detrimental impacts of nutrient influence such as harmful algal blooms, anoxic zones, and eutrophication grows (Cloern, 2001; Breitburg et al., 2018; Kessouri et al., 2021a; Cai et al., 2011). Additionally, our research on wastewater is timely, as Los Angeles, Orange, and San Diego counties have made commitments to improving the treatment of wastewater to make these municipalities more resilient to drought (Boxall & Pt, 2021; Quinn, 2019; noa, 2019; Choi, 2018). It is essential to understand how these modifications may alter biogeo-

chemical cycling in the coastal zone. By comparing net primary production (NPP) between our five model scenarios and the control, we sought to find the influence of buoyancy and nutrient form within wastewater have on productivity. This analysis provides perspective on how changes to wastewater management could potentially mitigate or exacerbate ecological changes in coastal environments.

In scenarios with more concentrated wastewater inputs, the lower volume of freshwater restricts the dispersion of nutrient-rich wastewater (Fig. 2.5). This in turn results in more intense blooms that remain closer to the emission points, horizontally and vertically, with increases in NPP further subsurface (Fig. 2.3). These concentrated blooms could lead to a higher risk of enhanced eutrophication in the adjacent nearshore regions.

The concentrated discharge results suggest potential challenges for coastal management. As municipalities conduct more freshwater reclamation, thereby reducing the volume of wastewaters from outfalls, our model results suggest that there could be unintended shifts in the location and intensity of local eutrophication. This could lead to a decrease in water quality and adverse effects to marine life. Careful consideration of discharge strategies are necessary to manage localized impacts. Numerical models appear to be an increasingly valuable tool for these endeavours.

The influence of wastewater is not static, but varies seasonally. Wastewater plumes reach the surface more efficiently in the winter and spring season, when the water column is less stratified (Fig. 2.3). In all scenarios, even those with a higher wastewater buoyancy, the increased NPP from anthropogenic inputs has a less significant impact in the coastal zone (Fig. 2.3). In stratified seasons the impact of all wastewater scenarios reaches a minimum.

The seasonal variability highlights the complexity of managing nutrients in the coastal zone. These findings suggest that stakeholders and managers could consider seasonal changes in water column stratification while implementing wastewater management strategies. Adjusting outfall strategies according to seasonal stratification patterns could optimize the outcomes of wastewater discharge, potentially reducing risk of eutrophication and minimizing impact to ecosystems.

Our investigations reveal that dissolved inorganic nitrogen form significantly impacts productivity. Outfall discharges that include abundant ammonium stimulate greater total changes in NPP than those with nitrate (Fig. 2.4). In addition, these changes in NPP are closer to discharge points than that of nitrate, owing to the generally faster uptake timescale of this nutrient. Despite this, the nitrate-dominated scenario still contributes a notable increase in NPP, albeit dispersed over a broader area.

The difference in biological uptake rates of DIN forms highlights an important consideration in wastewater treatment strategies. While our scenarios with ammonium generated more intense local eutrophication, those with nitrate stimulated less eutrophication within the coastal region. Excess nitrate, however, may reach further than ammonium, resulting in a broader, and less intense influence on NPP. Our results support the idea of converting ammonium to nitrate in an effort to reduce human influence on primary production within the 0-15 m coastal band. We note, however, that these treatment strategies will not only result in a reduction, but also a redistribution of human influence. Balancing these outcomes is crucial for effective coastal ecosystem management.

5.2 Summary of Chapter 3

Chapter 3 focuses on understanding the dynamics between giant kelp (*Macrocystis spp.*) forests in the SCB and anthropogenic nutrients. We focused on a natural nutrient limitation event, the 2014-2016 Marine Heat Wave (MHW) (Di Lorenzo & Mantua, 2016). Our study analyzed the kelp canopy cover before and during the MHW and the anthropogenic nutrient influence within these forested areas. To achieve this, we utilized historical Landsat kelp imagery data combined with high resolution biogeochemical model data, including anthropogenic nutrient sources from simulations comparable to those described in Chapter 2. This approach allowed us to quantify the frequency of nutrient limitation within the kelp canopy during the MHW, and to identify when anthropogenic nutrients prevented nutrient-limited conditions. To understand these interactions is crucial, as giant kelp is a keystone species whose health directly impacts hundreds of species in the SCB (Buschmann et al., 2017;

Schiel, 2015). Although the 2014-2016 MHW caused a significant loss of kelp biomass, the pattern of this loss was non-uniform (Bell et al., 2023; Cavanaugh et al., 2019). By integrating the perspective of a highly resolved physical biogeochemical model, we aimed to better understand the degree of nutrient limitation during this period and asses the amount which anthropogenic nutrients contributed to sustained kelp forest populations. Our findings detect nutrient limitation throughout the Bight and identify regions of growth that contained significant anthropogenic nutrients. This information will inform kelp forest management and mitigation of detrimental impacts from future nutrient limitations.

Our analysis revealed that kelp forest locations retaining their pre-MHW area had higher average days of anthropogenic influence and higher DIN levels compared to areas with reduced kelp coverage (Fig. 3.4). This correlation is most pronounced in Northern and Middle Mainland regions (Fig. 3.5). These findings suggest a significant role of anthropogenic nutrients in supporting kelp resilience during periods of nutrient limitation.

The discernible impact of wastewater point sources, especially in the Middle Mainland region, contributed to enhanced kelp production. The Northern Mainland region exhibited sustained kelp growth during the MHW, despite not having any major outfalls, potentially due to transport of anthropogenic sources of nutrients and minor outfalls. These results align with previous studies which found kelp growth year-round in the Santa Barbara Channel despite similar nutrient constraints. Conversely, the Northern Channel Islands and Southern Mainland showed a weaker correlation between anthropogenic influence days and kelp canopy resilience pointing to varied regional responses and patterns following the MHW.

Anthropogenic nutrients were detected in kelp forest areas through all seasons throughout the Bight (Fig. 3.3) affecting both the mainland and the Channel Islands. This widespread influence underscores the extensive impact of human derived nutrients to the SCB kelp ecosystem.

Our biogeochemical model results revealed anthropogenic nutrients sufficient to influence kelp growth rates in both the Mainland regions and the Channel Islands. The continual supply of anthropogenic nutrients holds substantial implications for kelp forest dynamics

not only during MHW events, but also under typical conditions. Our findings prompt an examination of unknown drivers of kelp forest area fluctuations in non-MHW conditions. By detailing the extent of anthropogenic DIN influence during the MHW, we contribute new, valuable knowledge to the understanding of human impacts in this highly urbanized coastal region.

5.3 Summary of Chapter 4

Chapter 4 identified the most ideal locations for cultivation of giant kelp (*Macrocystis spp.*) within the SCB. This study sought to build upon previous aquaculture suitability mapping efforts by incorporating high-quality, high-resolution nutrient data, and a specific focus on kelp. Our approach involved creating a GIS-based suitability modeling framework that utilized spatial statistics to identify two major criteria: areas environmentally conducive to kelp growth, and locations optimal for macroalgal development. We used high-resolution data from a biogeochemical model (ROMS-BEC) focusing on the primary growth variables for kelp, dissolved inorganic nitrogen (DIN), photosynthetic active radiation (PAR), and water temperature. The increasing demand for macroalgal cultivation - driven by its benefits as a food sources, bio-fuel, and a potential venue for carbon dioxide sequestration - underscored the importance of this study. In the SCB, macroalgal cultivation projects are underway, highlighting the timeliness and relevance of our research. Furthermore, our study identifies potential impact on current kelp forest area, ensuring marine biodiversity is preserved with the development of aquaculture. This study not only identifies the most ideal locations for kelp cultivation within the SCB, but also advances analysis techniques used in site suitability studies, providing a scaleable model for global efforts in macroalgal cultivation and management.

Our suitability model (Fig. 4.4) pinpointed two clusters of highly suitable farming locations. One cluster is located to the west of Santa Barbara, and another within Santa Monica Bay (Fig. 4.5). These locations were identified due to their optimal scores for kelp growth and locational submodels.

The results of our suitability analysis agree with other aquaculture studies in the SCB, corroborating the potential of these regions as prime areas for macroalgal cultivation. Previous studies have identified the Santa Barbara region as especially conducive to macroalgal farming due to its nutrient-rich waters. The Santa Monica Bay has been identified based on its ideal location to multiple ports and shallow depth. This agreement with existing research emphasises the reliability and accuracy of our spatial statistics and analysis methods, and strengthens the arguments for aquaculture development in these regions of the SCB.

Of our two ideal clusters, we find that the Santa Monica location holds the additional potential to mitigate anthropogenic nutrient loads. Furthermore, this location poses less risk of adversely affecting existing kelp beds (Fig. 4.6).

The potential for anthropogenic nutrient remediation represented by macroalgal development without any interference to existing kelp beds sets the stage for a sustainable pathway for aquaculture expansion. This aspect is significant as addresses concerns of human influence via eutrophication as well as habitat destruction.

5.4 Synthesis

This dissertation aims to generate a comprehensive understanding of the interaction between human activities and micro- and macro-algae in the SCB. Both Chapter 2 and 3 explore the effects and implications of anthropogenic nutrient discharges on different scales: Chapter 2 studies phytoplankton growth via net primary production (NPP) with model simulations of wastewater outfall discharges, while Chapter 3 examines the resilience of giant kelp by correlating observations with modeled anthropogenic nutrients. Together, Chapters 2 and 3 provide ecological insights on the impact of anthropogenic nutrients that inform the practical applications explored in Chapter 4, specifically, kelp farmings and potentially offsetting anthropogenic nutrient inputs. Chapter 3 and 4 focus on giant kelp, the most prolific macroalgae in the SCB. Chapter 4 identified ideal areas for giant kelp farming in Santa Monica Bay, a region identified as high anthropogenic influence in Chapter 2. In addition, highly resilient sites identified in Chapter 3 could be used to inform kelp cultivation

suitability through a nutrient limited event.

Across all studies in this thesis, the importance of the dynamic nutrient cycles within the coastal SCB shines through. The results from Chapter 2 and 3 quantify anthropogenic impact and its degree, shedding light on how physical and chemical components of wastewater have a varying influence on the spatial distribution in the SCB- a crucial factor for municipalities to consider as they adjust water treatment standards. Furthermore despite the year-round, relatively uniform discharge of wastewaters, we observe a highly seasonal variations in their impact. Chapter 3's findings can inform the management of wastewater outfall placement in the realm of kelp forest management. While anthropogenic nutrients often have detrimental impacts on coastal ecosystems, our results indicate that kelp may be resilient enough to utilize these nutrients effectively, although further research is necessary beyond the context of marine heatwaves. Chapter 4 expands on previous studies by mapping out larger domains of kelp farming suitability within the SCB, presenting areas that policymakers should prioritize for sustainable development.

5.5 Future research

Our study on wastewater scenarios in the SCB underscores to the need for high-resolution simulations of anthropogenic nutrients, and sparks questions about the broader ecological impacts of anthropogenic nutrients. Extensive longitudinal studies are crucial for refining our predictions and strategies for managing wastewater outfalls. Emerging research is beginning to reveal the significant offshore signals of these nutrients, complementing findings seen in the coastal zone. A deeper understanding of the fate of anthropogenic nutrients is vital for addressing eutrophication and its associated detrimental impacts globally. The SCB may serve as a model among highly urbanized coastal regions worldwide, where similar strategies could mitigate environmental challenges.

By uncovering a significant relationship between kelp and anthropogenic nutrients during the 2014-2016 MHW, our research highlights critical biogeochemical interactions under conditions of strong nutrient stress. Gaining a fuller understanding of the influence of an-

thropogenic nutrients on kelp likely necessitates a study of these factors outside of a MHW, and across a greater number of MHWs. The importance of understanding these influences on kelp growth cannot be understated. Kelp remains a prolific species worldwide, a keystone species supporting diverse marine habitats and species, with potential benefit for fisheries. Addressing other stressors such as habitat destruction, predation via urchins, diseases, and heat stress in conjunction with anthropogenic nutrient dynamics is also important, especially before considering kelp in remediation applications.

The increasing global demand for cultivated macroalgae underscores the importance of our initial suitability analysis for identifying optimal locations for kelp farming. Future suitability models would benefit from an integration of specific growth thresholds and environmental tolerances. Although our study assumes that higher DIN and PAR, and lower temperature are optimal, incorporating precise growth thresholds will enhance model accuracy. Advanced growth models for farmed kelp, pioneered by Frieder et al. (2022), are essential to understanding the specific nutrient impact in the surrounding environment. In addition, advanced growth models coupled to larger regional biogeochemical models would allow for a comprehensive estimate of the carbon sequestration and anthropogenic nutrient remediation potential that macroalgal farming could provide. This integration will not only improve the accuracy of our suitability assessment, but potentially support policy-making decisions, by demonstrating the environmental benefits of kelp and macroalgal cultivation.

APPENDIX A

Supporting Information for Chapter 2

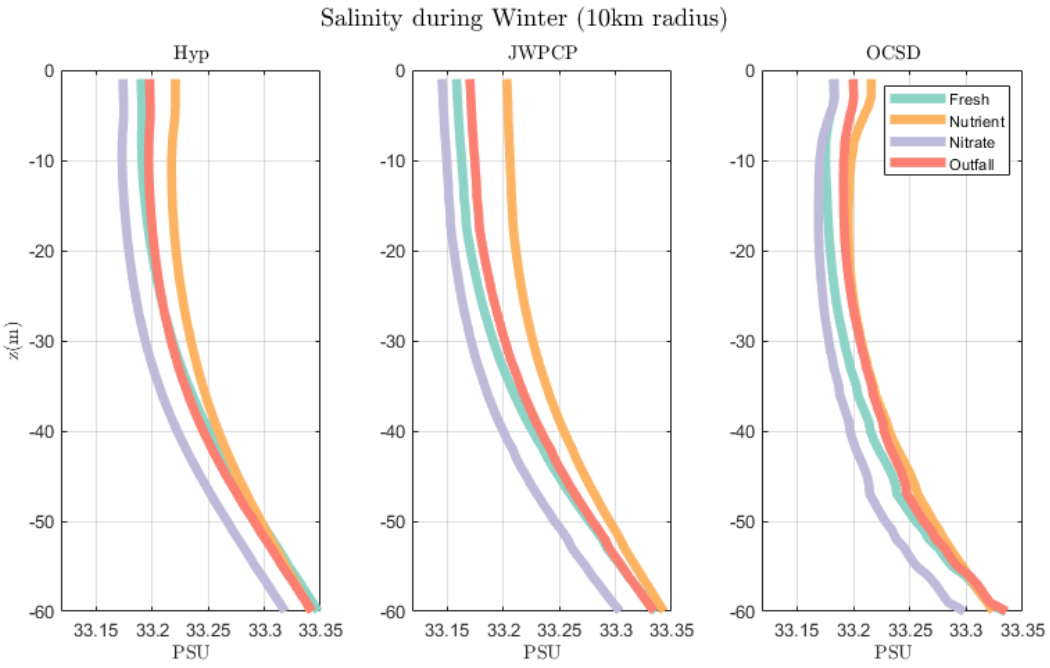

Figure A.1: Profiles of winter salinity for each model scenario for the Hyperion, JWPCP, and OCSD outfalls.

APPENDIX B

Supporting Information for Chapter 3

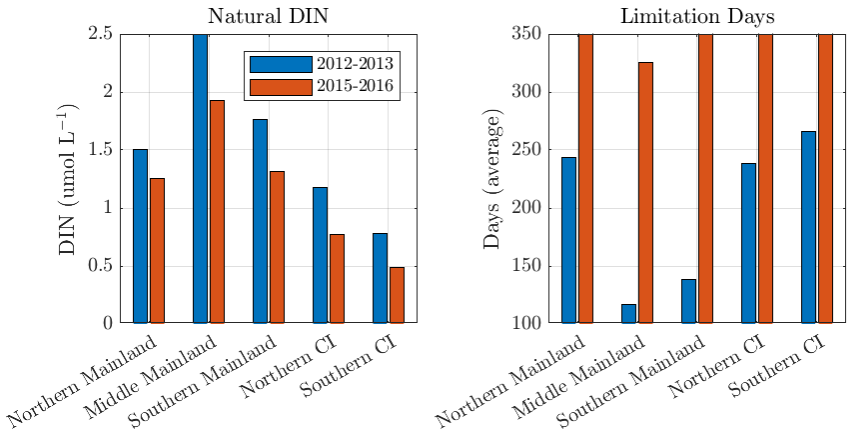

Figure B.1: Pre-MHW (2012-2013) values for average surface DIN (left) and limitation days (right) for the kelp regions in the SCB.

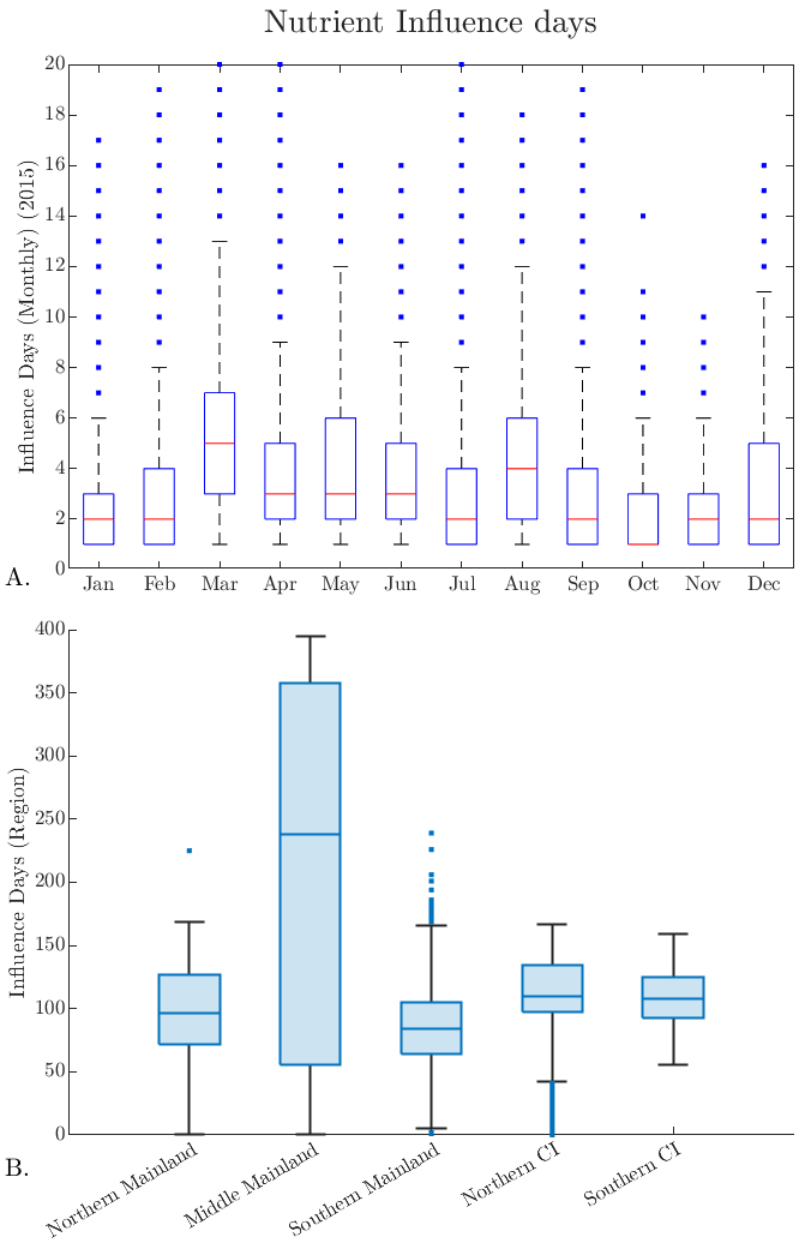

Figure B.2: Box plots of average anthropogeic influence days for 2015 over the kelp forest points within the Bight. (A.) Monthly distribution (B.) Regional distribution for the 2015-2016 event. Outliers are marked in blue (this figure is complementary to Fig. 3.3), using 30 m data.

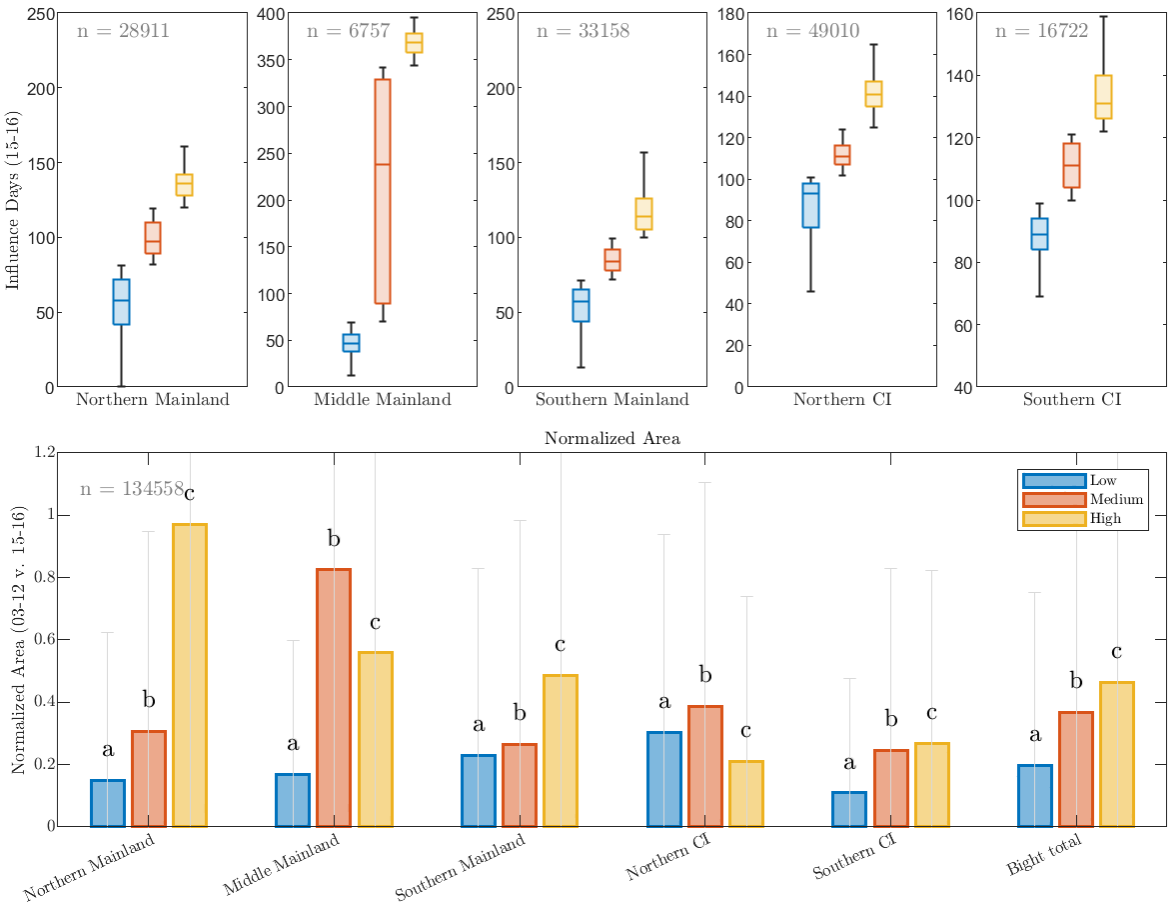

Figure B.3: Comparative analysis of influence days against the normalized MHW area across various regions. Top panel: Box plots represent the distribution of influence days categorized by the low, medium, and high quantiles for each region. Bottom panel: Bar charts displaying the normalized MHW area from 2015-2016 corresponding to the influence days' quantiles (low, medium, high) for each region. Letters above bars indicate groups that are statistically different from one another ($p < 0.05$). The sample sizes in the right corner refer to the number of 4 km^2 boxes used in each analysis (this figure is complementary to Fig. 3.6), using 30 m cells.

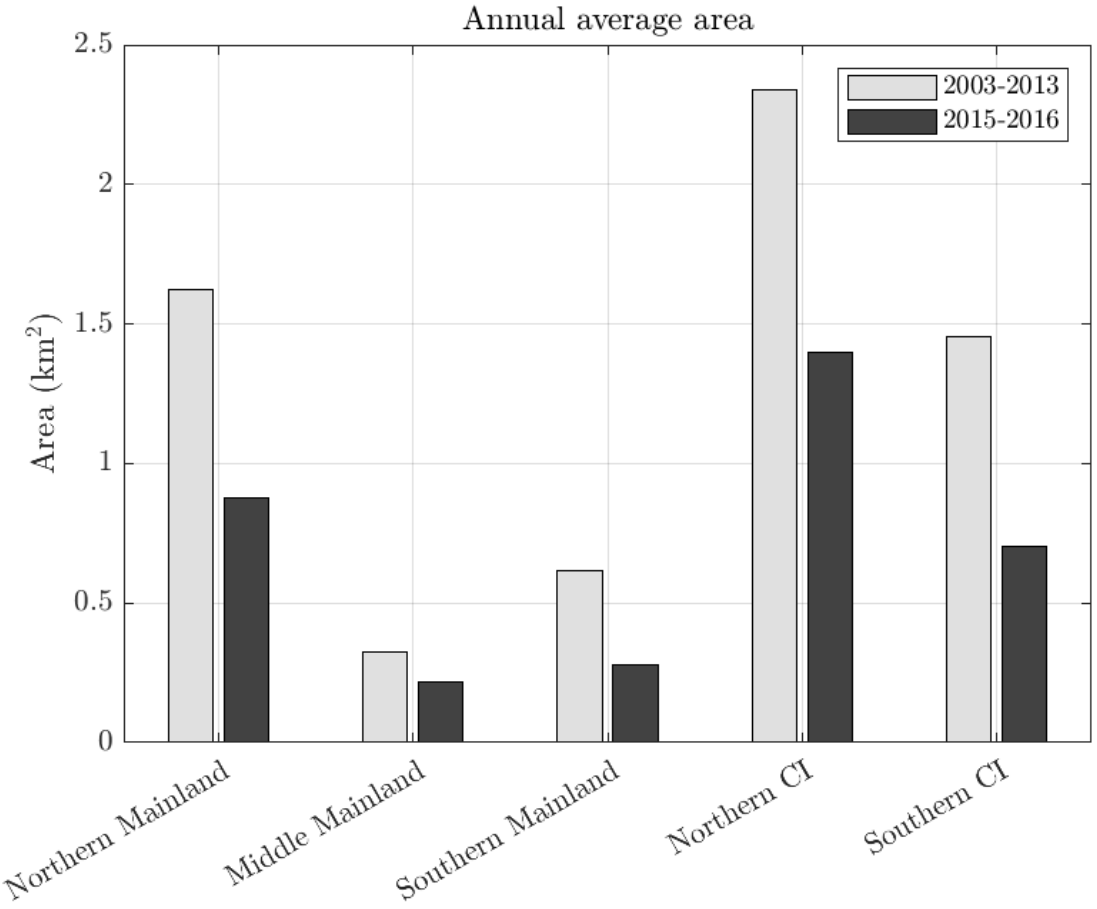

Figure B.4: Average area by region for the pre MHW (2003-2013) and MHW (2015-2016) periods

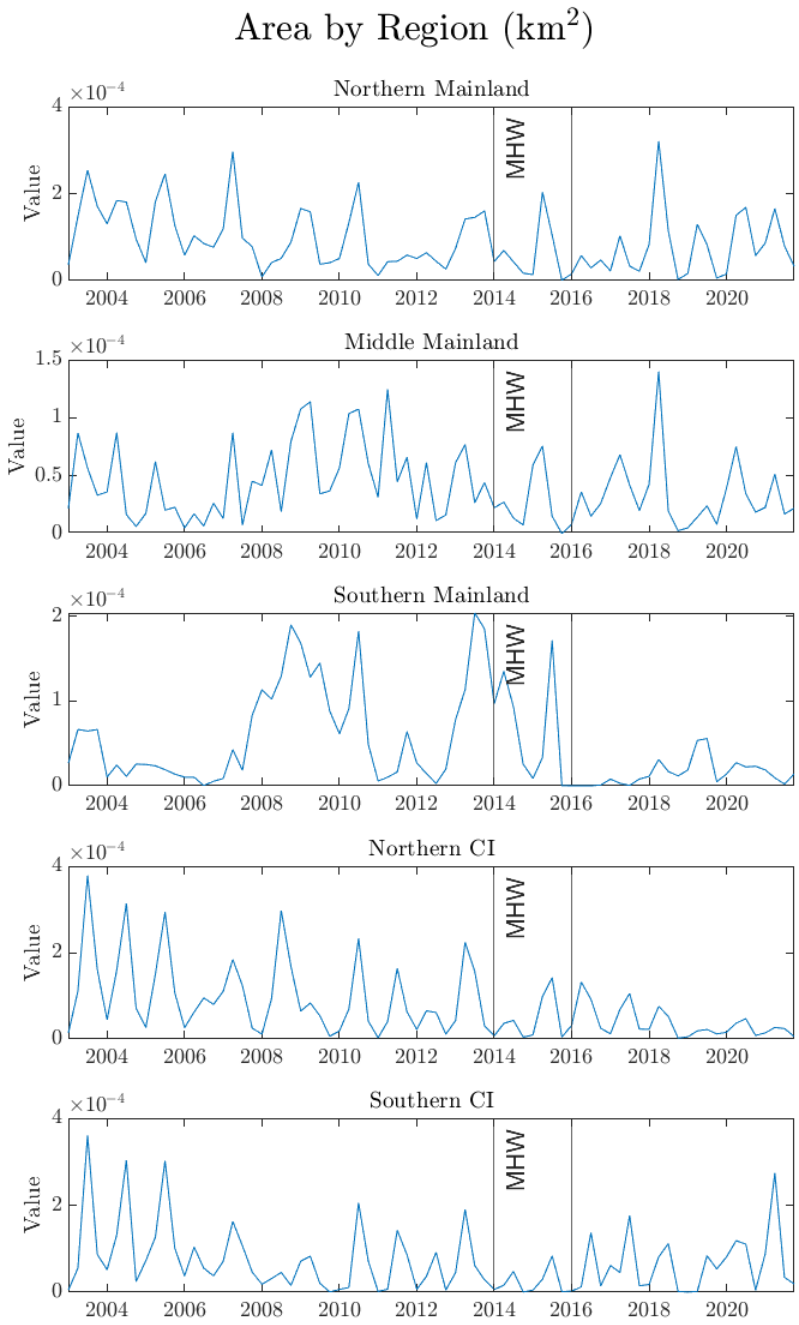

Figure B.5: Sum of kelp forest area by region from 2003 to 2021.

	Normalized Area	Anthropogenic DIN (μmol L^{-1})	Influence days	Limitation days (l_{tot})
Northern Mainland	0.33	0	94	540
Middle Mainland	0.53	0.77	210	570
Southern Mainland	0.20	0.020	82	620
Northern CI	0.25	0.060	110	330
Southern CI	0.21	0.050	120	400
Total Bight	0.21	0	88	510

Table B.1: Average domain values for normalized area, anthropogenic DIN, influence days, limitation days. Normalized area reflected the 2015-2016 average kelp area compared against the 2003-2012 average area, using 4 km^2 cells.

Area maintained (%)	Anthropogenic DIN (μmol L^{-1})	Influence days	Limitation days (l_{tot})
0.25	0.13102	124.82	395.75
0.5	0.15203	127.76	387.18
0.75	0.16563	131.06	387.44
1	0.1756	134.72	394.14

Table B.2: Averages by percent area maintained over kelp forests throughout the bight, using 4 km^2 cells.

Region	p-value	Quantiles		
		Q1 upper (low)	Q2 upper (middle)	Q3 upper (high)
Northern Mainland	0.3093	62	104	153
Middle Mainland	7.0339e-04	17	43	370
Southern Mainland	0.0057	46	121	187
Northern CI	0.0066	100	114	157
Southern CI	1.6066e-05	76	96	145
Total Bight	2.2813e-05	69	107	145

Table B.3: Kruskal-Wallis p-value results for all five regions and the Total bight, and quantiles derived by number of anthropogenic influence days (low, medium, and high)

APPENDIX C

Supporting Information for Chapter 4

	Depth	**Distance to Port**	**Shipping Traffic**
AHP	3	3	1
Weight	0.62	0.20	0.18
AHP	2	3	1
Weight	0.57	0.24	0.18
AHP	2	2	2
Weight	0.52	0.30	0.17

Table C.1: Summary of AHP rankings and resulting weights for the location sub model.

Area Ranges	Total suitability	Location	Nutrient
0-0	24.03	23.47	21.43
1-20	0.60	0.81	3.04
21-40	31.12	42.07	24.16
41-60	40.53	28.34	38.51
61-80	3.72	5.24	12.76
81-100	0	0.07	0.10

Table C.2: Percent of the Suitability model and location and nutrient sub models within score intervals

Interval	California km^2	California %	Federal km^2	Federal %
0 to 20	2307.80	37.81	4061.96	12.65
20 to 40	586.73	9.61	8594.40	26.77
40 to 60	1782.15	29.20	18583.06	57.88
60 to 80	1426.90	23.38	863.99	2.69
80 to 100	0.00	0.00	0.00	0.00

Table C.3: Area calculation by category and average intervals in square kilometers and percentages.

Interval	California (%)	Federal (%)
0 to 20	36.23	63.77
20 to 40	6.39	93.61
40 to 60	8.75	91.25
60 to 80	62.29	37.71
80 to 100	-	-

Table C.4: Percentage of area within score ranges for state or federal waters.

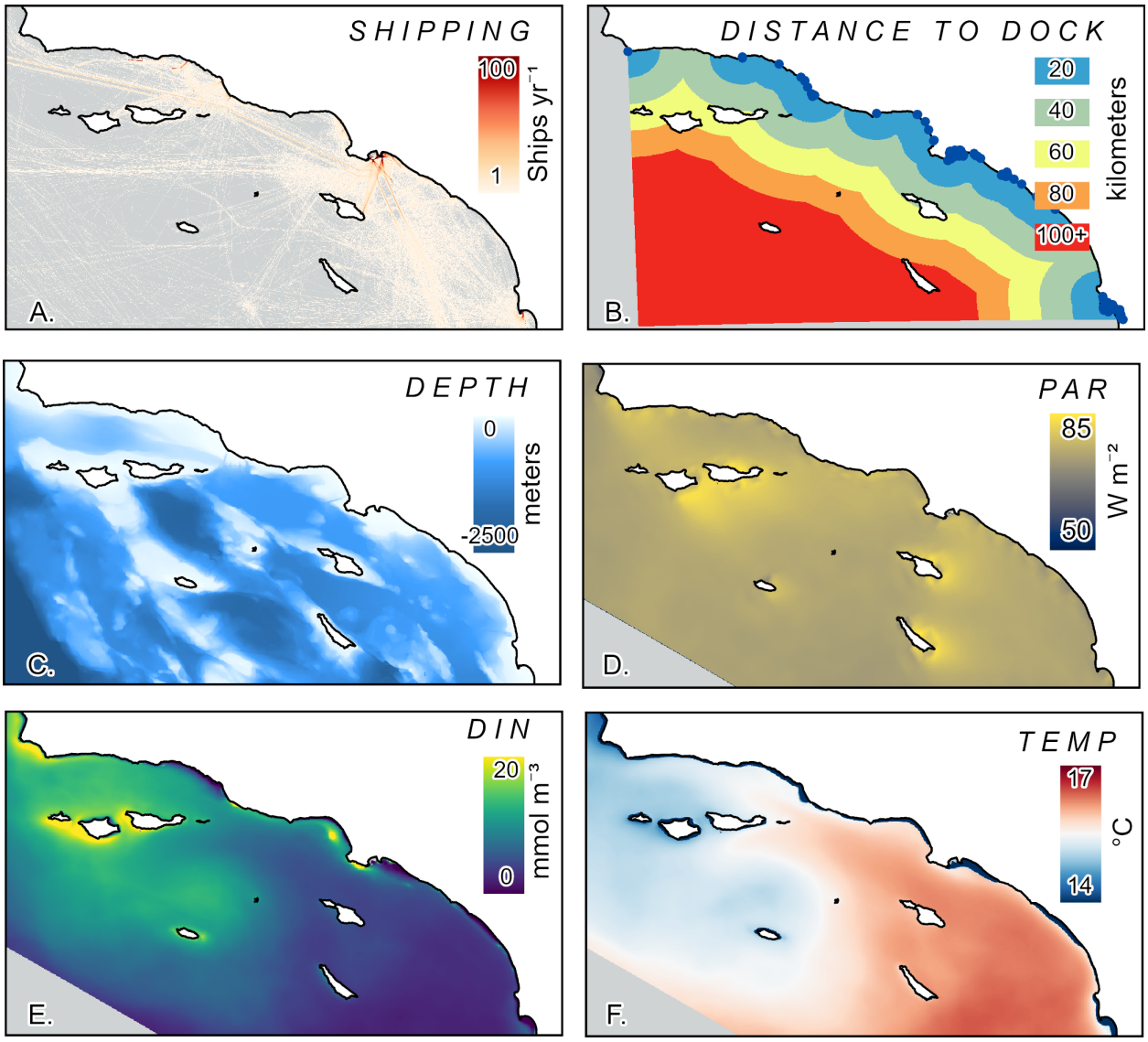

Figure C.1: Raw values of variables, shipping (A.), distance to dock (B.), depth (C.), and integrated (0-20 m) average PAR (D.), DIN (E.), and temp (F.).

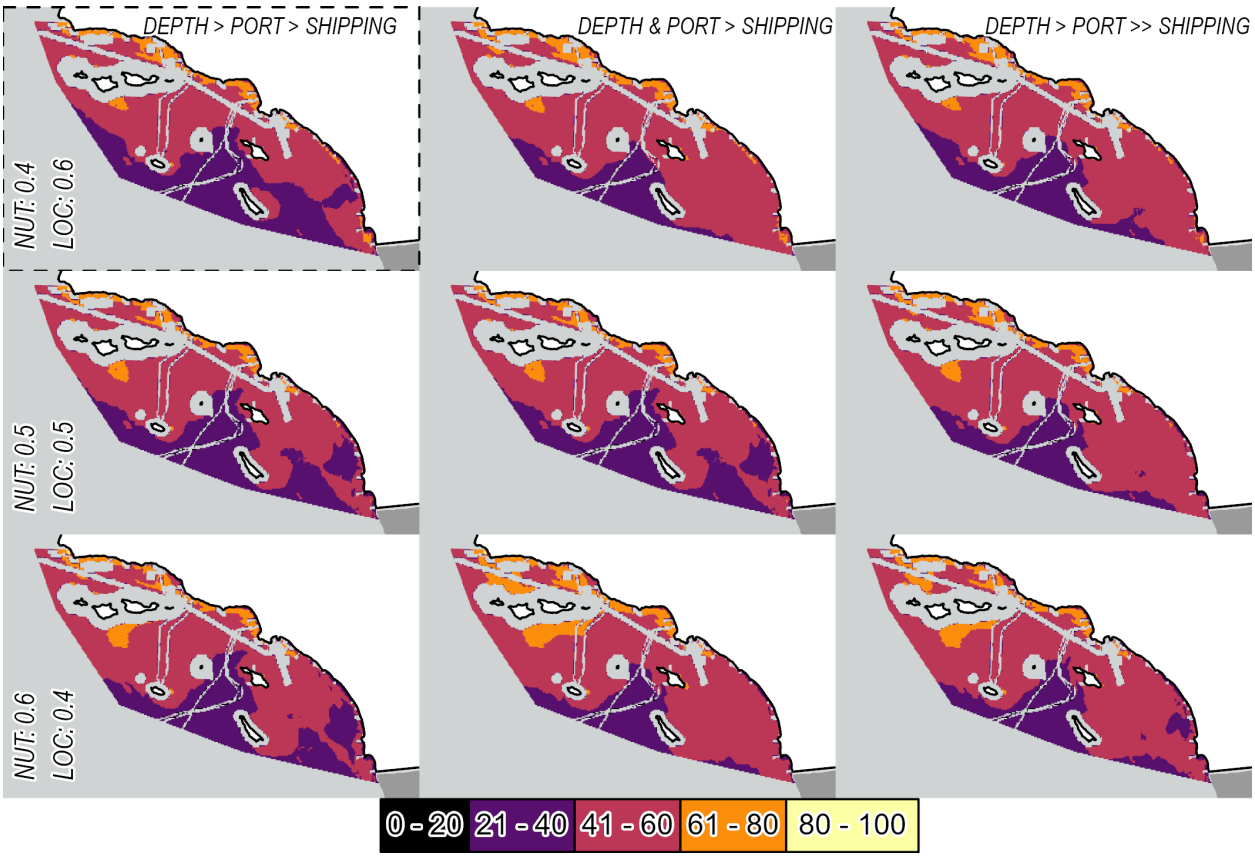

Figure C.2: Results from all 9 iterations of the suitability analysis. The dotted line indicates the map withe the least amount of skew.

Bibliography

(2019). Mayor Garcetti: Los Anglees will recycle 100% of citys wastewater by 2035. URL https://www.lamayor.org/mayor-garcetti-los-angeles-will-recycle-100-citys-wastewater-2035

Ahn, J. H., Grant, S. B., Surbeck, C. Q., DiGiacomo, P. M., Nezlin, N. P., & Jiang, S. (2005). Coastal Water Quality Impact of Stormwater Runoff from an Urban Watershed in Southern California. *Environmental Science & Technology*, *39*(16), 5940–5953. URL http://pubs.acs.org/doi/abs/10.1021/es0501464

Alberto, F., Raimondi, P. T., Reed, D. C., Coelho, N. C., Leblois, R., Whitmer, A., & Serrão, E. A. (2010). Habitat continuity and geographic distance predict population genetic differentiation in giant kelp. *Ecology*, *91*(1), 49–56. URL https://esajournals.onlinelibrary.wiley.com/doi/10.1890/09-0050.1

Arzeno-Soltero, I., Frieder, C., Saenz, B., Long, M., DeAngelo, J., Davis, S., & Davis, K. (2022). Biophysical potential and uncertainties of global seaweed farming. preprint, Biogeochemistry. URL http://eartharxiv.org/repository/view/3094/

Behrenfeld, M. J., & Falkowski, P. G. (1997). Photosynthetic rates derived from satellite-based chlorophyll concentration. *Limnology and Oceanography*, *42*(1), 1–20. URL https://aslopubs.onlinelibrary.wiley.com/doi/10.4319/lo.1997.42.1.0001

Bell, T. W., Allen, J. G., Cavanaugh, K. C., & Siegel, D. A. (2020a). Three decades of variability in California's giant kelp forests from the Landsat satellites. *Remote Sensing of Environment*, *238*, 110811. URL https://linkinghub.elsevier.com/retrieve/pii/S0034425718303171

Bell, T. W., Cavanaugh, K. C., Reed, D. C., & Siegel, D. A. (2015). Geographical variability in the controls of giant kelp biomass dynamics. *Journal of Biogeography*, *42*(10), 2010–

2021.

URL http://doi.wiley.com/10.1111/jbi.12550

Bell, T. W., Cavanaugh, K. C., Saccomanno, V. R., Cavanaugh, K. C., Houskeeper, H. F., Eddy, N., Schuetzenmeister, F., Rindlaub, N., & Gleason, M. (2023). Kelpwatch: A new visualization and analysis tool to explore kelp canopy dynamics reveals variable response to and recovery from marine heatwaves. *PLOS ONE*, *18*(3), e0271477.

URL https://dx.plos.org/10.1371/journal.pone.0271477

Bell, T. W., Nidzieko, N. J., Siegel, D. A., Miller, R. J., Cavanaugh, K. C., Nelson, N. B., Reed, D. C., Fedorov, D., Moran, C., Snyder, J. N., Cavanaugh, K. C., Yorke, C. E., & Griffith, M. (2020b). The Utility of Satellites and Autonomous Remote Sensing Platforms for Monitoring Offshore Aquaculture Farms: A Case Study for Canopy Forming Kelps. *Frontiers in Marine Science*, *7*, 520223.

URL https://www.frontiersin.org/articles/10.3389/fmars.2020.520223/full

Bell, T. W., & Siegel, D. A. (2022). Nutrient availability and senescence spatially structure the dynamics of a foundation species. *Proceedings of the National Academy of Sciences*, *119*(1), e2105135118.

URL http://www.pnas.org/lookup/doi/10.1073/pnas.2105135118

Bodycomb, R., Pomeroy, A. W. M., & Morris, R. L. (2023). Kelp Aquaculture as a Nature-Based Solution for Coastal Protection: Wave Attenuation by Suspended Canopies. *Journal of Marine Science and Engineering*, *11*(9), 1822.

URL https://www.mdpi.com/2077-1312/11/9/1822

Boesch, D. F. (2019). Barriers and Bridges in Abating Coastal Eutrophication. *Frontiers in Marine Science*, *6*, 123.

URL https://www.frontiersin.org/article/10.3389/fmars.2019.00123/full

Bond, B., Parsons, L., Barhydt, J. B., Jewett, F. R., Martinet, B., Hlavka, G. E., Isaacs, J. D., Lee, R. K. C., & Pearson, E. A. (1973). The ecology of the southern california bight: Implications for water quality managment. Technical Report 010, SCCWRP.

Bondur, V. G., Ivanov, V. A., & Fomin, V. V. (2018). Peculiarities of Polluted Water Spreading from a Submarine Source in Stratified Coastal Environment. *Izvestiya, Atmospheric and Oceanic Physics*, *54*(4), 386–393.
URL http://link.springer.com/10.1134/S0001433818040205

Booth, J. A. T., Woodson, C. B., Sutula, M., Micheli, F., Weisberg, S. B., Bograd, S. J., Steele, A., Schoen, J., & Crowder, L. B. (2014). Patterns and potential drivers of declining oxygen content along the southern California coast. *Limnology and Oceanography*, *59*(4), 1127–1138.
URL http://doi.wiley.com/10.4319/lo.2014.59.4.1127

Bostock, J., McAndrew, B., Richards, R., Jauncey, K., Telfer, T., Lorenzen, K., Little, D., Ross, L., Handisyde, N., Gatward, I., & Corner, R. (2010). Aquaculture: global status and trends. *Philosophical Transactions of the Royal Society B: Biological Sciences*, *365*(1554), 2897–2912.
URL https://royalsocietypublishing.org/doi/10.1098/rstb.2010.0170

Boxall, B., & Pt, A. (2021). L.A.'s ambitious goal: Recycle all of the city's sewage into drinkable water. *Los Angeles Times*, (p. 6).

Breitburg, D., Levin, L. A., Oschlies, A., Grégoire, M., Chavez, F. P., Conley, D. J., Garçon, V., Gilbert, D., Gutiérrez, D., Isensee, K., Jacinto, G. S., Limburg, K. E., Montes, I., Naqvi, S. W. A., Pitcher, G. C., Rabalais, N. N., Roman, M. R., Rose, K. A., Seibel, B. A., Telszewski, M., Yasuhara, M., & Zhang, J. (2018). Declining oxygen in the global ocean and coastal waters. *Science*, *359*(6371), eaam7240.
URL https://www.science.org/doi/10.1126/science.aam7240

Brzezinksi, M., Reed, D., Harrer, S., Rassweiler, A., Melack, J., Goodridge, B., & Dugan, J. (2013). Multiple Sources and Forms of Nitrogen Sustain Year-Round Kelp Growth on the Inner Continental Shelf of the Santa Barbara Channel. *Oceanography*, *26*(3), 114–123.
URL https://tos.org/oceanography/article/multiple-sources-and-forms-of-nitrogen-sustain-year-round-kelp-growth-on-th

Bureau of Ocean Energy Management (2024). OCS Oil & Gas Pipelines.
URL https://gis.boem.gov/arcgis/rest/services/BOEM_BSEE/MMC_Layers/MapServer/2

Bureau of Transportation Statistics (2022). Docks.

Bureau of Transportation Statistics (BTS) (2020). National Census of Ferry Operators (NCFO) Routes.
URL https://www.arcgis.com/sharing/rest/content/items/a52f38421635425098a7fcc6c455371e/info/metadata/metadata.xml?format=default&output=html

Buschmann, A., Graham, M., & Vasquez, J. (2007). Global Ecology of the Giant Kelp Macrocystis: from ecotypes to ecosystems. In R. Gibson, R. Atkinson, & J. Gordon (Eds.) *Oceanography and Marine Biology*, vol. 20074975, (pp. 39–88). CRC Press. Series Title: Oceanography and Marine Biology - An Annual Review.
URL http://www.crcnetbase.com/doi/abs/10.1201/9781420050943.ch2

Buschmann, A. H., Camus, C., Infante, J., Neori, A., Israel, , Hernández-González, M. C., Pereda, S. V., Gomez-Pinchetti, J. L., Golberg, A., Tadmor-Shalev, N., & Critchley, A. T. (2017). Seaweed production: overview of the global state of exploitation, farming and emerging research activity. *European Journal of Phycology*, *52*(4), 391–406.
URL https://www.tandfonline.com/doi/full/10.1080/09670262.2017.1365175

Cai, W.-J., Hu, X., Huang, W.-J., Murrell, M. C., Lehrter, J. C., Lohrenz, S. E., Chou, W.-C., Zhai, W., Hollibaugh, J. T., Wang, Y., Zhao, P., Guo, X., Gundersen, K., Dai, M., & Gong, G.-C. (2011). Acidification of subsurface coastal waters enhanced by eutrophication. *Nature Geoscience*, *4*(11), 766–770.
URL http://www.nature.com/articles/ngeo1297

California Department of Fish and Wildlife (2016). California State Marine Protected Areas.
URL https://map.dfg.ca.gov/metadata/MPA_CA_Existing_180905.html

California Department of Fish and Wildlife (2024). Military Safety Zones.

URL https://map.dfg.ca.gov/arcgis/rest/services/Project_Marine/Marine_Management/MapServer/20

Capet, X., McWilliams, J. C., Molemaker, M. J., & Shchepetkin, A. F. (2008a). Mesoscale to Submesoscale Transition in the California Current System. Part I: Flow Structure, Eddy Flux, and Observational Tests. *Journal of Physical Oceanography*, *38*(1), 29–43.
URL http://journals.ametsoc.org/doi/10.1175/2007JPO3671.1

Capet, X., McWilliams, J. C., Molemaker, M. J., & Shchepetkin, A. F. (2008b). Mesoscale to Submesoscale Transition in the California Current System. Part II: Frontal Processes. *Journal of Physical Oceanography*, *38*(1), 44–64.
URL http://journals.ametsoc.org/doi/10.1175/2007JPO3672.1

Capet, X., McWilliams, J. C., Molemaker, M. J., & Shchepetkin, A. F. (2008c). Mesoscale to Submesoscale Transition in the California Current System. Part III: Energy Balance and Flux. *Journal of Physical Oceanography*, *38*(10), 2256–2269.
URL http://journals.ametsoc.org/doi/10.1175/2008JPO3810.1

Carpenter, S. R., Caraco, N. F., Correll, D. L., Howarth, R. W., Sharpley, A. N., & Smith, V. H. (1998). Nonpoint Pollution of Surface Waters with Phosphorus and Nitrogen. *Ecological Applications*, *83*(3), 559–568.

Carvalho, J. L. B., Roberts, P. J. W., & Roldão, J. (2002). Field Observations of Ipanema Beach Outfall. *Journal of Hydraulic Engineering*, *128*(2), 151–160.
URL https://ascelibrary.org/doi/10.1061/%28ASCE%290733-9429%282002%29128%3A2%28151%29

Cavanaugh, K., Siegel, D., Reed, D., & Dennison, P. (2011). Environmental controls of giant-kelp biomass in the Santa Barbara Channel, California. *Marine Ecology Progress Series*, *429*, 1–17.
URL http://www.int-res.com/abstracts/meps/v429/p1-17/

Cavanaugh, K. C., Reed, D. C., Bell, T. W., Castorani, M. C. N., & Beas-Luna, R. (2019). Spatial Variability in the Resistance and Resilience of Giant Kelp in Southern and Baja

California to a Multiyear Heatwave. *Frontiers in Marine Science*, *6*, 413.
URL https://www.frontiersin.org/article/10.3389/fmars.2019.00413/full

Chai, Z. Y., Wang, H., Deng, Y., Hu, Z., & Zhong Tang, Y. (2020). Harmful algal blooms significantly reduce the resource use efficiency in a coastal plankton community. *Science of The Total Environment*, *704*, 135381.
URL https://linkinghub.elsevier.com/retrieve/pii/S0048969719353732

Checkley, D. M., & Barth, J. A. (2009). Patterns and processes in the California Current System. *Progress in Oceanography*, *83*(1-4), 49–64.

Chen, M., Yim, S. C., Cox, D. T., Yang, Z., Huesemann, M. H., Mumford, T. F., & Wang, T. (2023a). Modeling and Analysis of a Novel Offshore Binary Species Free-Floating Long-line Macroalgal Farming System. *Journal of Offshore Mechanics and Arctic Engineering*, *145*(2), 021301.
URL https://asmedigitalcollection.asme.org/offshoremechanics/article/145/2/021301/1146710/Modeling-and-Analysis-of-a-Novel-Offshore-Binary

Chen, S., Meng, Y., Lin, S., Yu, Y., & Xi, J. (2023b). Estimation of sea surface nitrate from space: Current status and future potential. *Science of The Total Environment*, *899*, 165690.
URL https://linkinghub.elsevier.com/retrieve/pii/S0048969723043139

Chenillat, F., Franks, P. J. S., Capet, X., Rivière, P., Grima, N., Blanke, B., & Combes, V. (2018). Eddy properties in the Southern California Current System. *Ocean Dynamics*, *68*(7), 761–777.
URL http://link.springer.com/10.1007/s10236-018-1158-4

Choi, A. S. (2018). Orange County's pioneering wastewater recycling system embarks on major expansion.

Cloern, J. E. (2001). Our evolving conceptual model of the coastal eutrophication problem. *Marine Ecology Progress Series*, *210*, 223–253.
URL http://www.int-res.com/abstracts/meps/v210/p223-253/

Corcoran, A. A., Reifel, K. M., Jones, B. H., & Shipe, R. F. (2010). Spatiotemporal development of physical, chemical, and biological characteristics of stormwater plumes in Santa Monica Bay, California (USA). *Journal of Sea Research*, *63*(2), 129–142.
URL https://linkinghub.elsevier.com/retrieve/pii/S1385110109001233

Crosset, K., Ache, B., Pacheco, P., & Haber, K. (2013). National Coastal Population Report: Population Trends from 1970 to 2020.
URL https://coast.noaa.gov/digitalcoast/training/population-report.html

Dailey, M. D., Reish, D. J., & Anderson, J. W. (Eds.) (1993). *Ecology of the Southern California Bight: a synthesis and interpretation*. Berkeley: University of California Press.

Damien, P., Bianchi, D., McWilliams, J. C., Kessouri, F., Deutsch, C., Chen, R., & Renault, L. (2023). Enhanced Biogeochemical Cycling Along the U.S. West Coast Shelf. *Global Biogeochemical Cycles*, *37*(1), e2022GB007572.
URL https://agupubs.onlinelibrary.wiley.com/doi/10.1029/2022GB007572

Dapieve, D. R., Maggi, M. F., Mercante, E., Francisco, H. R., Oliveira, D. D. D., & Luiz Junior, O. J. (2023). Use of geotechnologies for aquaculture site selection: suitability factors and constraints for production in ground-excavated ponds. *Latin American Journal of Aquatic Research*, *51*(2), 160–194.
URL http://www.lajar.cl/index.php/rlajar/article/view/vol51-issue2-fulltext-2981

Dauhajre, D. P., McWilliams, J. C., & Uchiyama, Y. (2017). Submesoscale Coherent Structures on the Continental Shelf. *Journal of Physical Oceanography*, *47*(12), 2949–2976.
URL https://journals.ametsoc.org/view/journals/phoc/47/12/jpo-d-16-0270.1.xml

Dean, T. A., & Jacobsen, F. R. (1984). Growth of juvenile Macrocystis pyrifera (Laminariales) in relation to environmental factors. *Marine Biology*, *83*(3), 301–311.
URL http://link.springer.com/10.1007/BF00397463

Dean, T. A., & Jacobsen, F. R. (1986). Nutrient-limited growth of juvenile kelp, Macrocystispyrifera, during the 1982-1984 "El Nifio" in southern California. *Marine Biology*, (90), 597–601.

Delaney, A., Frangoudes, K., & Ii, S.-A. (2016). Society and Seaweed. In *Seaweed in Health and Disease Prevention*, (pp. 7–40). Elsevier.
URL https://linkinghub.elsevier.com/retrieve/pii/B9780128027721000026

Deutsch, C., Frenzel, H., McWilliams, J. C., Renault, L., Kessouri, F., Howard, E., Liang, J.-H., Bianchi, D., & Yang, S. (2021). Biogeochemical variability in the California Current System. *Progress in Oceanography*, *196*, 102565.
URL https://linkinghub.elsevier.com/retrieve/pii/S0079661121000525

Deysher, E., & Dean, T. A. (1986). In situ recruitment of sporophytes of the giant kelp, Macrocystis pyrijkra (L.) C.A. Agardh: effects of physical factors. *Journal of Experimental Marine Biology and Ecology*, (p. 23).

Di Lorenzo, E. (2003). Seasonal dynamics of the surface circulation in the Southern California Current System. *Deep Sea Research Part II: Topical Studies in Oceanography*, *50*(14-16), 2371–2388.
URL https://linkinghub.elsevier.com/retrieve/pii/S0967064503001255

Di Lorenzo, E., & Mantua, N. (2016). Multi-year persistence of the 2014/15 North Pacific marine heatwave. *Nature Climate Change*, *6*(11), 1042–1047.
URL https://www.nature.com/articles/nclimate3082

Diaz, R. J., & Rosenberg, R. (2008). Spreading Dead Zones and Consequences for Marine Ecosystems. *Science*, *321*(5891), 926–929.
URL http://science.sciencemag.org/content/321/5891/926

DiGiacomo, P. M., Washburn, L., Holt, B., & Jones, B. H. (2004). Coastal pollution hazards in southern California observed by SAR imagery: stormwater plumes, wastewater plumes, and natural hydrocarbon seeps. *Marine Pollution Bulletin*, *49*(11-12), 1013–1024.
URL https://linkinghub.elsevier.com/retrieve/pii/S0025326X04002693

Doney, S. C., Ruckelshaus, M., Emmett Duffy, J., Barry, J. P., Chan, F., English, C. A., Galindo, H. M., Grebmeier, J. M., Hollowed, A. B., Knowlton, N., Polovina, J., Rabalais, N. N., Sydeman, W. J., & Talley, L. D. (2012). Climate Change Impacts on Marine Ecosystems. *Annual Review of Marine Science*, *4*(1), 11–37.
URL http://www.annualreviews.org/doi/10.1146/annurev-marine-041911-111611

Dong, C., Idica, E. Y., & McWilliams, J. C. (2009). Circulation and multiple-scale variability in the Southern California Bight. *Progress in Oceanography*, *82*(3), 168–190.
URL https://linkinghub.elsevier.com/retrieve/pii/S0079661109000573

Dong, C., & McWilliams, J. C. (2007). A numerical study of island wakes in the Southern California Bight. *Continental Shelf Research*, *27*(9), 1233–1248.
URL https://linkinghub.elsevier.com/retrieve/pii/S0278434307000209

Duarte, C. M., Bruhn, A., & Krause-Jensen, D. (2021). A seaweed aquaculture imperative to meet global sustainability targets. *Nature Sustainability*, *5*(3), 185–193.
URL https://www.nature.com/articles/s41893-021-00773-9

Duarte, C. M., & Krause-Jensen, D. (2018). Intervention Options to Accelerate Ecosystem Recovery From Coastal Eutrophication. *Frontiers in Marine Science*, *5*, 470.
URL https://www.frontiersin.org/article/10.3389/fmars.2018.00470/full

Duarte, C. M., Wu, J., Xiao, X., Bruhn, A., & Krause-Jensen, D. (2017). Can Seaweed Farming Play a Role in Climate Change Mitigation and Adaptation? *Frontiers in Marine Science*, *4*.
URL http://journal.frontiersin.org/article/10.3389/fmars.2017.00100/full

Dunn, O. J. (1964). Multiple Comparisons Using Rank Sums. *Technometrics*, *6*(3), 241–252.
URL http://www.tandfonline.com/doi/abs/10.1080/00401706.1964.10490181

Edwards, M. S. (2019). Comparing the impacts of four ENSO events on giant kelp (Macrocystis pyrifera) in the northeast Pacific Ocean. *ALGAE*, *34*(2), 141–151.
URL http://e-algae.org/journal/view.php?doi=10.4490/algae.2019.34.5.4

Fantom, L. (2023). Can Small Seaweed Farms Help Kelp Scale Up? *Civil Eats*. URL https://civileats.com/2022/03/16/can-small-seaweed-farms-help-kelp-scale-up/#

Ferdouse, F., Holdt, S. L., Smith, R., Murúa, P., & Yang, Z. (2018). *The global status of seaweed production, trade and utilization*. Rome: Food and Agriculture Organization of the United Nations. OCLC: 1078882988.

Fieler, R., Greenacre, M., Matsson, S., Neves, L., Forbord, S., & Hancke, K. (2021). Erosion Dynamics of Cultivated Kelp, Saccharina latissima, and Implications for Environmental Management and Carbon Sequestration. *Frontiers in Marine Science*, *8*, 632725. URL https://www.frontiersin.org/articles/10.3389/fmars.2021.632725/full

Filbee-Dexter, K., Wernberg, T., Grace, S. P., Thormar, J., Fredriksen, S., Narvaez, C. N., Feehan, C. J., & Norderhaug, K. M. (2020). Marine heatwaves and the collapse of marginal North Atlantic kelp forests. *Scientific Reports*, *10*(1), 13388. URL https://www.nature.com/articles/s41598-020-70273-x

Foster, M. S., & Schiel, D. R. (2010). Loss of predators and the collapse of southern California kelp forests (?): Alternatives, explanations and generalizations. *Journal of Experimental Marine Biology and Ecology*, *393*(1-2), 59–70. URL https://linkinghub.elsevier.com/retrieve/pii/S0022098110002510

Fram, J. P., Stewart, H. L., Brzezinski, M. A., Gaylord, B., Reed, D. C., Williams, S. L., & MacIntyre, S. (2008). Physical pathways and utilization of nitrate supply to the giant kelp, Macrocystis pyrifera. *Limnology and Oceanography*, *53*(4), 1589–1603. URL http://doi.wiley.com/10.4319/lo.2008.53.4.1589

Frieder, C. A., Yan, C., Chamecki, M., Dauhajre, D., McWilliams, J. C., Infante, J., McPherson, M. L., Kudela, R. M., Kessouri, F., Sutula, M., Arzeno-Soltero, I. B., & Davis, K. A. (2022). A Macroalgal Cultivation Modeling System (MACMODS): Evaluating the Role of Physical-Biological Coupling on Nutrients and Farm Yield. *Frontiers in Marine Science*,

9, 752951.

URL https://www.frontiersin.org/articles/10.3389/fmars.2022.752951/full

Froehlich, H. E., Afflerbach, J. C., Frazier, M., & Halpern, B. S. (2019). Blue Growth Potential to Mitigate Climate Change through Seaweed Offsetting. *Current Biology*, *29*(18), 3087–3093.e3.

URL https://linkinghub.elsevier.com/retrieve/pii/S0960982219308863

Gentemann, C. L., Fewings, M. R., & García-Reyes, M. (2017). Satellite sea surface temperatures along the West Coast of the United States during the 2014-2016 northeast Pacific marine heat wave: Coastal SSTs During "the Blob". *Geophysical Research Letters*, *44*(1), 312–319.

URL http://doi.wiley.com/10.1002/2016GL071039

Gentry, R. R., Lester, S. E., Kappel, C. V., White, C., Bell, T. W., Stevens, J., & Gaines, S. D. (2017). Offshore aquaculture: Spatial planning principles for sustainable development. *Ecology and Evolution*, *7*(2), 733–743.

URL https://onlinelibrary.wiley.com/doi/10.1002/ece3.2637

Gerard, V. A. (1982). Growth and Utilization of Internal Nitrogen Reserves by the Giant Kelp MacrocystispyHferain a Low-Nitrogen Environment. *Marine Biology*, *66*, 27–35.

Getis, A., & Ord, J. K. (1992). The Analysis of Spatial Association by Use of Distance Statistics. *Geographical Analysis*, *24*(3), 189–206.

URL https://onlinelibrary.wiley.com/doi/10.1111/j.1538-4632.1992.tb00261.x

Gimpel, A., Stelzenmüller, V., Grote, B., Buck, B. H., Floeter, J., Núñez-Riboni, I., Pogoda, B., & Temming, A. (2015). A GIS modelling framework to evaluate marine spatial planning scenarios: Co-location of offshore wind farms and aquaculture in the German EEZ. *Marine Policy*, *55*, 102–115.

URL https://linkinghub.elsevier.com/retrieve/pii/S0308597X15000238

Glibert, P. M., Wilkerson, F. P., Dugdale, R. C., Raven, J. A., Dupont, C. L., Leavitt, P. R., Parker, A. E., Burkholder, J. M., & Kana, T. M. (2016). Pluses and minuses of ammonium and nitrate uptake and assimilation by phytoplankton and implications for productivity and community composition, with emphasis on nitrogen-enriched conditions. *Limnology and Oceanography*, *61*(1), 165–197.
URL https://onlinelibrary.wiley.com/doi/10.1002/lno.10203

Graham, M. H. (2004). Effects of Local Deforestation on the Diversity and Structure of Southern California Giant Kelp Forest Food Webs. *Ecosystems*, *7*(4).
URL http://link.springer.com/10.1007/s10021-003-0245-6

Grebe, G. S., Byron, C. J., Gelais, A. S., Kotowicz, D. M., & Olson, T. K. (2019). An ecosystem approach to kelp aquaculture in the Americas and Europe. *Aquaculture Reports*, *15*, 100215.
URL https://linkinghub.elsevier.com/retrieve/pii/S2352513419300134

Green Wave (2018). Guide to Navigating Lease & Permit Approvals for Ocean Farming in California. Tech. rep., Green Wave.
URL https://static1.squarespace.com/static/6111d32a681aa003444ed7e1/t/61b8f59370fd950ae0421d42/1639511443831/GreenWave%2BGuide%2Bto%2BLease%2B%26%2BPermit%2BApprovals%2Bfor%2BOcean%2BFarming%2Bin%2BCalifornia%2B8.19.2018.docx.pdf

Halpern, B. S., Kappel, C. V., Selkoe, K. A., Micheli, F., Ebert, C. M., Kontgis, C., Crain, C. M., Martone, R. G., Shearer, C., & Teck, S. J. (2009). Mapping cumulative human impacts to California Current marine ecosystems. *Conservation Letters*, *2*(3), 138–148.
URL http://doi.wiley.com/10.1111/j.1755-263X.2009.00058.x

Hickey, B. M. (1979). The California current system—hypotheses and facts. *Progress in Oceanography*, *8*(4), 191–279.
URL https://linkinghub.elsevier.com/retrieve/pii/0079661179900028

Ho, M. (2023). Effect of ocean outfall discharge volume and dissolved inorganic nitrogen load on urban eutrophication outcomes in the Southern California Bight. preprint, Preprints.
URL https://essopenarchive.org/users/551180/articles/664388-effect-of-ocean-outfall-discharge-volume-and-dissolved-inorganic-nitrogen-load-on-urban-eutrophication-outcomes-in-the-southern-california-bight?commit=cd9dbc2c6c1835c9ff3e1ebecc79461da9046f03

Ho, M., Molemaker, J. M., Kessouri, F., McWilliams, J. C., & Gallien, T. W. (2021). High-Resolution Nonhydrostatic Outfall Plume Modeling: Cross-Flow Validation. *Journal of Hydraulic Engineering*, *147*(8), 04021028.
URL https://ascelibrary.org/doi/10.1061/%28ASCE%29HY.1943-7900.0001896

Hoel, P., Bianchi, D., Cavanaugh, K. C., & Freider, C. (2024a). Anthropogenic Nutrient Sources Influence Kelp Canopies During a Marine Heat Wave.
URL https://www.ssrn.com/abstract=4803306

Hoel, P., Bianchi, D., & Moreno, A. R. (2024b). Mechanisms controlling lower trophic ecosystem response to ocean outfall discharges: role of nitrogen form and freshwater volume. *This Thesis*.

House, Parker (2018). Kelp Restoration Year 5 Annual Report 2018. Tech. rep., The Bay Foundation.

Howard, M. D. A., Sutula, M., Caron, D. A., Chao, Y., Farrara, J. D., Frenzel, H., Jones, B., Robertson, G., McLaughlin, K., & Sengupta, A. (2014). Anthropogenic nutrient sources rival natural sources on small scales in the coastal waters of the Southern California Bight. *Limnology and Oceanography*, *59*(1), 285–297.
URL http://doi.wiley.com/10.4319/lo.2014.59.1.0285

Howarth, R., Chan, F., Conley, D. J., Garnier, J., Doney, S. C., Marino, R., & Billen, G. (2011). Coupled biogeochemical cycles: eutrophication and hypoxia in temperate estuaries and coastal marine ecosystems. *Frontiers in Ecology and the Environment*, *9*(1), 18–26.
URL http://onlinelibrary.wiley.com/doi/10.1890/100008/abstract

Hunt, C. D., Mansfield, A. D., Mickelson, M. J., Albro, C. S., Geyer, W. R., & Roberts, P. J. (2010). Plume tracking and dilution of effluent from the Boston sewage outfall. *Marine Environmental Research*, *70*(2), 150–161.
URL https://linkinghub.elsevier.com/retrieve/pii/S0141113610000565

Jacox, M. G., Hazen, E. L., Zaba, K. D., Rudnick, D. L., Edwards, C. A., Moore, A. M., & Bograd, S. J. (2016). Impacts of the 2015-2016 El Niño on the California Current System: Early assessment and comparison to past events: 2015-2016 El Niño Impact in the CCS. *Geophysical Research Letters*, *43*(13), 7072–7080.
URL http://doi.wiley.com/10.1002/2016GL069716

Jones, B. H., Noble, M. A., & Dickey, T. D. (2002). Hydrographic and particle distributions over the Palos Verdes Continental Shelf: spatial, seasonal and daily variability. *Continental Shelf Research*, *22*(6-7), 945–965.
URL https://linkinghub.elsevier.com/retrieve/pii/S0278434301001145

Kessouri, McWilliams, J. C., Bianchi, D., Sutula, M., Renault, L., Deutsch, C., Feely, R. A., McLaughlin, K., Ho, M., Howard, E. M., Bednaršek, N., Damien, P., Molemaker, J., & Weisberg, S. B. (2021a). Coastal eutrophication drives acidification, oxygen loss, and ecosystem change in a major oceanic upwelling system. *Proceedings of the National Academy of Sciences*, *118*(21), e2018856118.
URL http://www.pnas.org/lookup/doi/10.1073/pnas.2018856118

Kessouri, F., Bianchi, D., Renault, L., McWilliams, J. C., Frenzel, H., & Deutsch, C. A. (2020). Submesoscale Currents Modulate the Seasonal Cycle of Nutrients and Productivity in the California Current System. *Global Biogeochemical Cycles*, *34*(10).
URL https://onlinelibrary.wiley.com/doi/10.1029/2020GB006578

Kessouri, F., McLaughlin, K., Sutula, M., Bianchi, D., Ho, M., McWilliams, J. C., Renault, L., Molemaker, J., Deutsch, C., & Leinweber, A. (2021b). Configuration and Validation of an Oceanic Physical and Biogeochemical Model to Investigate Coastal Eutrophication in

the Southern California Bight. *Journal of Advances in Modeling Earth Systems*, *13*(12). URL https://onlinelibrary.wiley.com/doi/10.1029/2020MS002296

Kessouri, F., Sutula, M., Bianchi, D., Ho, M., Damien, P., McWilliams, J., Frieder, C., Renault, L., Frenzel, H., McLaughlin, K., & Deutsch, C. (2023). Importance of cross-shore transport and eddies in promoting large scale response to urban eutrophication. preprint, In Review.
URL https://www.researchsquare.com/article/rs-2693479/v1

Kim, H.-J., Miller, A. J., McGowan, J., & Carter, M. L. (2009). Coastal phytoplankton blooms in the Southern California Bight. *Progress in Oceanography*, *82*(2), 137–147.
URL https://linkinghub.elsevier.com/retrieve/pii/S0079661109000494

Kinley, R. D., Martinez-Fernandez, G., Matthews, M. K., De Nys, R., Magnusson, M., & Tomkins, N. W. (2020). Mitigating the carbon footprint and improving productivity of ruminant livestock agriculture using a red seaweed. *Journal of Cleaner Production*, *259*, 120836.
URL https://linkinghub.elsevier.com/retrieve/pii/S0959652620308830

Krumhansl, K. A., Okamoto, D. K., Rassweiler, A., Novak, M., Bolton, J. J., Cavanaugh, K. C., Connell, S. D., Johnson, C. R., Konar, B., Ling, S. D., Micheli, F., Norderhaug, K. M., Pérez-Matus, A., Sousa-Pinto, I., Reed, D. C., Salomon, A. K., Shears, N. T., Wernberg, T., Anderson, R. J., Barrett, N. S., Buschmann, A. H., Carr, M. H., Caselle, J. E., Derrien-Courtel, S., Edgar, G. J., Edwards, M., Estes, J. A., Goodwin, C., Kenner, M. C., Kushner, D. J., Moy, F. E., Nunn, J., Steneck, R. S., Vásquez, J., Watson, J., Witman, J. D., & Byrnes, J. E. K. (2016). Global patterns of kelp forest change over the past half-century. *Proceedings of the National Academy of Sciences*, *113*(48), 13785–13790.
URL http://www.pnas.org/lookup/doi/10.1073/pnas.1606102113

Kruskal, W. H., & Wallis, W. A. (1952). Use of Ranks in One-Criterion Variance Analysis.

Journal of the American Statistical Association, *47*(260), 583–621.
URL http://www.tandfonline.com/doi/abs/10.1080/01621459.1952.10483441

Kübler, J. E., Dudgeon, S. R., & Bush, D. (2021). Climate change challenges and opportunities for seaweed aquaculture in California, the United States. *Journal of the World Aquaculture Society*, *52*(5), 1069–1080.
URL https://onlinelibrary.wiley.com/doi/10.1111/jwas.12794

Laufkötter, C., Zscheischler, J., & Frölicher, T. L. (2020). High-impact marine heatwaves attributable to human-induced global warming. *Science*, *369*(6511), 1621–1625.
URL https://www.science.org/doi/10.1126/science.aba0690

Lawrence, M. (2023). Research Expanding Opportunities for Commercial Seaweed Production. Tech. rep., United States Department of Agriculture.
URL https://www.nifa.usda.gov/about-nifa/impacts/research-expanding-opportunities-commercial-seaweed-production

Lester, S. E., Stevens, J. M., Gentry, R. R., Kappel, C. V., Bell, T. W., Costello, C. J., Gaines, S. D., Kiefer, D. A., Maue, C. C., Rensel, J. E., Simons, R. D., Washburn, L., & White, C. (2018). Marine spatial planning makes room for offshore aquaculture in crowded coastal waters. *Nature Communications*, *9*(1), 945.
URL https://www.nature.com/articles/s41467-018-03249-1

L'Helguen, S., Maguer, J.-F., & Caradec, J. (2008). Inhibition kinetics of nitrate uptake by ammonium in size-fractionated oceanic phytoplankton communities: implications for new production and f-ratio estimates. *Journal of Plankton Research*, *30*(10), 1179–1188.
URL https://academic.oup.com/plankt/article-lookup/doi/10.1093/plankt/fbn072

Lilliefors, H. W. (1967). On the Kolmogorov-Smirnov Test for Normality with Mean and Variance Unknown. *Journal of the American Statistical Association*, *62*(318), 399–402.
URL http://www.tandfonline.com/doi/abs/10.1080/01621459.1967.10482916

LTER, S. B. C., Bell, T. W., Cavanaugh, K. C., & Siegel, D. A. (2022). SBC LTER: Time series of quarterly NetCDF files of kelp biomass in the canopy from Landsat 5, 7 and 8, since 1984 (ongoing).
URL https://portal.edirepository.org/nis/mapbrowse?packageid=knb-lter-sbc.74.16

Mantyla, A. W., Bograd, S. J., & Venrick, E. L. (2008). Patterns and controls of chlorophyll-a and primary productivity cycles in the Southern California Bight. *Journal of Marine Systems*, *73*(1-2), 48–60.
URL https://linkinghub.elsevier.com/retrieve/pii/S0924796307001650

Mateo-Sagasta, J., Raschid-Sally, L., & Thebo, A. (2015). Global Wastewater and Sludge Production, Treatment and Use. In P. Drechsel, M. Qadir, & D. Wichelns (Eds.) *Wastewater*, (pp. 15–38). Dordrecht: Springer Netherlands.
URL https://link.springer.com/10.1007/978-94-017-9545-6_2

McLaughlin, K., Howard, M. D. A., Robertson, G., Beck, C. D. A., Ho, M., Kessouri, F., Nezlin, N. P., Sutula, M., & Weisberg, S. B. (2021). Influence of anthropogenic nutrient inputs on rates of coastal ocean nitrogen and carbon cycling in the Southern California Bight, United States. *Elementa: Science of the Anthropocene*, *9*(1), 00145.
URL https://online.ucpress.edu/elementa/article/9/1/00145/118260/Influence-of-anthropogenic-nutrient-inputs-on

McLaughlin, K., Nezlin, N. P., Howard, M. D., Beck, C. D., Kudela, R. M., Mengel, M. J., & Robertson, G. L. (2017). Rapid nitrification of wastewater ammonium near coastal ocean outfalls, Southern California, USA. *Estuarine, Coastal and Shelf Science*, *186*, 263–275.
URL https://linkinghub.elsevier.com/retrieve/pii/S0272771416301512

Moore, J. K., Doney, S. C., & Lindsay, K. (2004). Upper ocean ecosystem dynamics and iron cycling in a global three-dimensional model: Global Ecosystem-Biogeochemical Model. *Global Biogeochemical Cycles*, *18*(4), n/a–n/a.
URL http://doi.wiley.com/10.1029/2004GB002220

Moore, J. K., Lindsay, K., Doney, S. C., Long, M. C., & Misumi, K. (2013). Marine Ecosystem Dynamics and Biogeochemical Cycling in the Community Earth System Model [CESM1(BGC)]: Comparison of the 1990s with the 2090s under the RCP4.5 and RCP8.5 Scenarios. *Journal of Climate*, *26*(23), 9291–9312.
URL https://journals.ametsoc.org/doi/10.1175/JCLI-D-12-00566.1

Morris Jr, J. A. (2021). An Aquaculture Opportunity Area Atlas for the Southern California Bight. Publisher: National Centers for Coastal Ocean Science (U.S.).
URL https://repository.library.noaa.gov/view/noaa/33303

Mulholland, M. R., & Lomas, M. W. (2008). Nitrogen Uptake and Assimilation. In *Nitrogen in the Marine Environment*, (pp. 303–384). Elsevier.
URL https://linkinghub.elsevier.com/retrieve/pii/B9780123725226000074

Nabti, E., Jha, B., & Hartmann, A. (2017). Impact of seaweeds on agricultural crop production as biofertilizer. *International Journal of Environmental Science and Technology*, *14*(5), 1119–1134.
URL http://link.springer.com/10.1007/s13762-016-1202-1

National Geophysical Data Center (2012). U.S. Coastal Relief Model - Southern California vers. 2. National Geophysical Data Center, NOAA.
URL https://www.ncei.noaa.gov/metadata/geoportal/rest/metadata/item/gov.noaa.ngdc.mgg.dem:4970/html#

National Oceanographic and Atmospheric Administration (NOAA) (2024). Offshore oil and active gas leases.
URL https://coast.noaa.gov/arcgis/rest/services/Hosted/OffshoreOilGasActiveLeases/FeatureServer/0

National Oceanographic and Atmospheric Administration (NOAA) Marine Cadastre (2024). Wastewater outfall pipes.
URL https://noaa.maps.arcgis.com/home/item.html?id=b81879061828467d88d2fac35077cdd2&sublayer=0

National Oceanographic and Atmospheric Administration (NOAA) Office for Coastal Management (2024). Submarine Cable Area.
URL https://coast.noaa.gov/arcgis/rest/services/Hosted/SubmarineCableAreas/FeatureServer/0

Navarrete, I. A., Kim, D. Y., Wilcox, C., Reed, D. C., Ginsburg, D. W., Dutton, J. M., Heidelberg, J., Raut, Y., & Wilcox, B. H. (2021). Effects of depth-cycling on nutrient uptake and biomass production in the giant kelp Macrocystis pyrifera. *Renewable and Sustainable Energy Reviews*, *141*, 110747.
URL https://linkinghub.elsevier.com/retrieve/pii/S1364032121000423

Neori, A., Chopin, T., Troell, M., Buschmann, A. H., Kraemer, G. P., Halling, C., Shpigel, M., & Yarish, C. (2004). Integrated aquaculture: rationale, evolution and state of the art emphasizing seaweed biofiltration in modern mariculture. *Aquaculture*, *231*(1-4), 361–391.
URL https://linkinghub.elsevier.com/retrieve/pii/S0044848603007841

Nepper-Davidsen, J., Andersen, D., & Pedersen, M. (2019). Exposure to simulated heatwave scenarios causes long-term reductions in performance in Saccharina latissima. *Marine Ecology Progress Series*, *630*, 25–39.
URL https://www.int-res.com/abstracts/meps/v630/p25-39/

Nezlin, N. P., Booth, J. A. T., Beegan, C., Cash, C. L., Gully, J. R., Latker, A., Mengel, M. J., Robertson, G. L., Steele, A., & Weisberg, S. B. (2016). Assessment of wastewater impact on dissolved oxygen around southern California's submerged ocean outfalls. *Regional Studies in Marine Science*, *7*, 177–184.
URL https://linkinghub.elsevier.com/retrieve/pii/S235248551630041X

Nezlin, N. P., McLaughlin, K., Booth, J. A. T., Cash, C. L., Diehl, D. W., Davis, K. A., Feit, A., Goericke, R., Gully, J. R., Howard, M. D. A., Johnson, S., Latker, A., Mengel, M. J., Robertson, G. L., Steele, A., Terriquez, L., Washburn, L., & Weisberg, S. B. (2018). Spatial and Temporal Patterns of Chlorophyll Concentration in the Southern California

Bight. *Journal of Geophysical Research: Oceans*, *123*(1), 231–245.
URL http://doi.wiley.com/10.1002/2017JC013324

Nissen, C., Vogt, M., Münnich, M., Gruber, N., & Haumann, F. A. (2018). Factors controlling coccolithophore biogeography in the Southern Ocean. *Biogeosciences*, *15*(22), 6997–7024.
URL https://www.biogeosciences.net/15/6997/2018/

Nixon, S. W., & Buckley, B. A. (2002). "A strikingly rich zone"—Nutrient enrichment and secondary production in coastal marine ecosystems. *Estuaries*, *25*(4), 782–796.
URL https://link.springer.com/article/10.1007/BF02804905

Office for Coastal Management (OCM) (2024). AIS Vessel Transit Counts 2015.

Paerl, H. W., Hall, N. S., Peierls, B. L., & Rossignol, K. L. (2014). Evolving Paradigms and Challenges in Estuarine and Coastal Eutrophication Dynamics in a Culturally and Climatically Stressed World. *Estuaries and Coasts*, *37*(2), 243–258.
URL http://link.springer.com/10.1007/s12237-014-9773-x

Piconi, P., Veidenheimer, R., & Chase, B. (2020). Edible Seaweed Market Analysis. Tech. rep., Islands Institute.

Quinn, T. (2019). City of Los Angeles Announces Bold Recycled Water Plan. *National Resoures Defense Council*, (p. 2).

Rabouille, C., Mackenzie, F. T., & Ver, L. M. (2001). Influence of the human perturbation on carbon, nitrogen, and oxygen biogeochemical cycles in the global coastal ocean. *Geochimica et Cosmochimica Acta*, *65*(21), 3615–3641.
URL http://www.sciencedirect.com/science/article/pii/S0016703701007608

Radiarta, I. N., Saitoh, S.-I., & Miyazono, A. (2008). GIS-based multi-criteria evaluation models for identifying suitable sites for Japanese scallop (Mizuhopecten yessoensis) aquaculture in Funka Bay, southwestern Hokkaido, Japan. *Aquaculture*, *284*(1-4), 127–135.
URL https://linkinghub.elsevier.com/retrieve/pii/S0044848608005437

Ramos, P., Neves, M., & Pereira, F. (2007). Mapping and initial dilution estimation of an ocean outfall plume using an autonomous underwater vehicle. *Continental Shelf Research*, *27*(5), 583–593.
URL https://linkinghub.elsevier.com/retrieve/pii/S0278434306003748

Raven, J. A. (2017). The possible roles of algae in restricting the increase in atmospheric CO $_2$ and global temperature. *European Journal of Phycology*, *52*(4), 506–522.
URL https://www.tandfonline.com/doi/full/10.1080/09670262.2017.1362593

Reed, D., Washburn, L., Rassweiler, A., Miller, R., Bell, T., & Harrer, S. (2016). Extreme warming challenges sentinel status of kelp forests as indicators of climate change. *Nature Communications*, *7*(1), 13757.
URL https://www.nature.com/articles/ncomms13757

Reed, D. C., Kinlan, B. P., Raimondi, P. T., Washburn, L., Gaylord, B., & Drake, P. T. (2006). A Metapopulation Perspective on the Patch Dynamics of Giant Kelp in Southern California. In *Marine Metapopulations*, (pp. 353–386). Elsevier.
URL https://linkinghub.elsevier.com/retrieve/pii/B9780120887811500133

Reed, D. C., Rassweiler, A., & Arkema, K. K. (2008). Biomass rather than growth rate determines variation in net primary production by giant kelp. *Ecology*, *89*(9), 2493–2505.
URL http://www.esajournals.org/doi/abs/10.1890/07-1106.1

Reed, D. C., Rassweiler, A., Carr, M. H., Cavanaugh, K. C., Malone, D. P., & Siegel, D. A. (2011). Wave disturbance overwhelms top-down and bottom-up control of primary production in California kelp forests. *Ecology*, *92*(11), 2108–2116.

Reifel, K. M., Corcoran, A. A., Cash, C., Shipe, R., & Jones, B. H. (2013). Effects of a surfacing effluent plume on a coastal phytoplankton community. *Continental Shelf Research*, *60*, 38–50.
URL https://linkinghub.elsevier.com/retrieve/pii/S027843431300112X

Renault, L., McWilliams, J. C., Kessouri, F., Jousse, A., Frenzel, H., Chen, R., & Deutsch, C. (2020). Evaluation of high-resolution atmospheric and oceanic simulations of the California

Current System. preprint, Ecology.
URL http://biorxiv.org/lookup/doi/10.1101/2020.02.10.942730

Renault, L., McWilliams, J. C., Kessouri, F., Jousse, A., Frenzel, H., Chen, R., & Deutsch, C. (2021). Evaluation of high-resolution atmospheric and oceanic simulations of the California Current System. *Progress in Oceanography*, *195*, 102564.
URL https://linkinghub.elsevier.com/retrieve/pii/S0079661121000513

Roberts, P. J. W., Salas, H. J., Reiff, F. M., Libhaber, M., Labbe, A., & Thomson, J. C. (2010). *Marine Wastewater Outfalls and Treatment Systems*. IWA Publishing.
URL https://doi.org/10.2166/9781780401669

Roberts, P. J. W., & Villegas, B. (2017). Modeling and Design of the Buenos Aires Outfalls. *Journal of Hydraulic Engineering*, *143*(2), 05016007.
URL https://ascelibrary.org/doi/10.1061/%28ASCE%29HY.1943-7900.0001244

Rodriguez, G. E., Reed, D. C., & Holbrook, S. J. (2016). Blade life span, structural investment, and nutrient allocation in giant kelp. *Oecologia*, *182*(2), 397–404.
URL http://link.springer.com/10.1007/s00442-016-3674-6

Rogers, L. A., Wilson, M. T., Duffy-Anderson, J. T., Kimmel, D. G., & Lamb, J. F. (2021). Pollock and "the Blob": Impacts of a marine heatwave on walleye pollock early life stages. *Fisheries Oceanography*, *30*(2), 142–158.
URL https://onlinelibrary.wiley.com/doi/10.1111/fog.12508

Rugiu, L., Hargrave, M. S., Enge, S., Sterner, M., Nylund, G. M., & Pavia, H. (2021). Kelp in IMTAs: small variations in inorganic nitrogen concentrations drive different physiological responses of Saccharina latissima. *Journal of Applied Phycology*, *33*(2), 1021–1034.
URL https://link.springer.com/10.1007/s10811-020-02333-8

Saaty, T. L. (2008). Decision making with the analytic hierarchy process. *International Journal of Services Sciences*, *1*(1), 83.
URL http://www.inderscience.com/link.php?id=17590

Salbitani, G., & Carfagna, S. (2021). Ammonium Utilization in Microalgae: A Sustainable Method for Wastewater Treatment. *Sustainability*, *13*(2), 956.
URL https://www.mdpi.com/2071-1050/13/2/956

Scharin, H., Ericsdotter, S., Elliott, M., Turner, R. K., Niiranen, S., Blenckner, T., Hyytiäinen, K., Ahlvik, L., Ahtiainen, H., Artell, J., Hasselström, L., Söderqvist, T., & Rockström, J. (2016). Processes for the sustainable stewardship of marine environments. *Ecological Economics*, *128*, 55–67.
URL https://linkinghub.elsevier.com/retrieve/pii/S092180091530450X

Schiel, D. (2015). *The biology and ecology of giant kelp forests*. Oakland, California : University of California Press.
URL https://search.library.ucla.edu/permalink/01UCS_LAL/17p22dp/alma9914806095306531

Schiff, K., McLaughlin, K., Moore, S., & Cao, Y. (2019). Southern California Bight. In *World Seas: an Environmental Evaluation*, (pp. 465–482). Elsevier.
URL https://linkinghub.elsevier.com/retrieve/pii/B9780128050682000231

Schwing, F., Murphree, T., deWitt, L., & Green, P. (2002). The evolution of oceanic and atmospheric anomalies in the northeast Pacific during the El Niño and La Niña events of 1995–2001. *Progress in Oceanography*, *54*(1-4), 459–491.
URL https://linkinghub.elsevier.com/retrieve/pii/S0079661102000642

Shchepetkin, A. F., & McWilliams, J. C. (2005). The regional oceanic modeling system (ROMS): a split-explicit, free-surface, topography-following-coordinate oceanic model. *Ocean Modelling*, *9*(4), 347–404.
URL https://linkinghub.elsevier.com/retrieve/pii/S1463500304000484

Siedlecki, S. A., Pilcher, D., Howard, E. M., Deutsch, C., MacCready, P., Norton, E. L., Frenzel, H., Newton, J., Feely, R. A., Alin, S. R., & Klinger, T. (2021). Coastal processes modify projections of some climate-driven stressors in the California Current System.

Biogeosciences, *18*(9), 2871–2890.
URL https://bg.copernicus.org/articles/18/2871/2021/

Skamarock, W. C., & Klemp, J. B. (2008). A time-split nonhydrostatic atmospheric model for weather research and forecasting applications. *Journal of Computational Physics*, *227*(7), 3465–3485.
URL https://linkinghub.elsevier.com/retrieve/pii/S0021999107000459

Smith, J. M., Brzezinski, M. A., Melack, J. M., Miller, R. J., & Reed, D. C. (2018). Urea as a source of nitrogen to giant kelp (*Macrocystis pyrifera*): Urea use by giant kelp. *Limnology and Oceanography Letters*, *3*(4), 365–373.
URL http://doi.wiley.com/10.1002/lol2.10088

Smith, V. H., Tilman, G. D., & Nekola, J. C. (1999). Eutrophication: impacts of excess nutrient inputs on freshwater, marine, and terrestrial ecosystems. *Environmental pollution*, *100*(1), 179–196.
URL http://www.sciencedirect.com/science/article/pii/S0269749199000913

Snyder, J. N., Bell, T. W., Siegel, D. A., Nidzieko, N. J., & Cavanaugh, K. C. (2020). Sea Surface Temperature Imagery Elucidates Spatiotemporal Nutrient Patterns for Offshore Kelp Aquaculture Siting in the Southern California Bight. *Frontiers in Marine Science*, *7*, 22.
URL https://www.frontiersin.org/article/10.3389/fmars.2020.00022/full

Steneck, R. S., Graham, M. H., Bourque, B. J., Corbett, D., Erlandson, J. M., Estes, J. A., & Tegner, M. J. (2002). Kelp forest ecosystems: biodiversity, stability, resilience and future. *Environmental Conservation*, *29*(4), 436–459.
URL https://www.cambridge.org/core/product/identifier/S0376892902000322/type/journal_article

Stull, J. (1995). Two Decades of Marine Biological Monitoring, Palos Verdes, California, 1972 to 1992. *Bulletin, Southern California Academy of Sciences*, *94*, 21–45.

Sutula, M., Ho, M., Sengupta, A., Kessouri, F., McLaughlin, K., McCune, K., & Bianchi, D. (2021a). A baseline of terrestrial freshwater and nitrogen fluxes to the Southern California Bight, USA. *Marine Pollution Bulletin*, *170*, 112669.
URL https://linkinghub.elsevier.com/retrieve/pii/S0025326X21007037

Sutula, M., Ho, M., Sengupta, A., Kessouri, F., McLaughlin, K., McCune, K., & Bianchi, D. (2021b). Dataset of terrestrial fluxes of freshwater, nutrients, carbon, and iron to the Southern California Bight, U.S.A. *Data in Brief*, *35*, 106802.
URL https://linkinghub.elsevier.com/retrieve/pii/S235234092100086X

Tarunamulia, & Sammut, J. (2023). Application of GIS and fuzzy sets to small-scale site suitability assessment for extensive brackish water aquaculture. *Annals of GIS*, *29*(4), 585–601.
URL https://www.tandfonline.com/doi/full/10.1080/19475683.2023.2255072

Tuholske, C., Halpern, B. S., Blasco, G., Villasenor, J. C., Frazier, M., & Caylor, K. (2021). Mapping global inputs and impacts from of human sewage in coastal ecosystems. *PLOS ONE*, *16*(11), e0258898.
URL https://dx.plos.org/10.1371/journal.pone.0258898

Uchiyama, Y., Idica, E. Y., McWilliams, J. C., & Stolzenbach, K. D. (2014). Wastewater effluent dispersal in Southern California Bays. *Continental Shelf Research*, *76*, 36–52.
URL https://linkinghub.elsevier.com/retrieve/pii/S0278434314000041

U.S. Coast Guard (????). Shipping Lanes and Regulations.
URL https://gis.charttools.noaa.gov/arcgis/rest/services/NavigationChartData/MarineTransportation/MapServer/0

Vitousek, P. M., Aber, J. D., Howarth, R. W., Likens, G. E., Matson, P. A., Schindler, D. W., Schlesinger, W. H., & Tilman, D. G. (1997). Human Alteration of the Global Nitrogen Cycle: sources and concequences. *Ecological Applications*, *7*(3), 737–750.
URL http://doi.wiley.com/10.1890/1051-0761(1997)007[0737:HAOTGN]2.0.CO;2

Wang, Y., He, X., Bai, Y., Tan, Y., Zhu, B., Wang, D., Ou, M., Gong, F., Zhu, Q., & Huang, H. (2022). Automatic detection of suspected sewage discharge from coastal outfalls based on Sentinel-2 imagery. *Science of The Total Environment*, *853*, 158374.
URL https://linkinghub.elsevier.com/retrieve/pii/S0048969722054730

Warrick, J., DiGiacomo, P., Weisberg, S., Nezlin, N., Mengel, M., Jones, B., Ohlmann, J., Washburn, L., Terrill, E., & Farnsworth, K. (2007). River plume patterns and dynamics within the Southern California Bight. *Continental Shelf Research*, *27*(19), 2427–2448.
URL https://linkinghub.elsevier.com/retrieve/pii/S0278434307001720

Washburn, L., Jones, B. H., Bratkovich, A., Dickey, T. D., & Chen, M. (1992). Mixing, Dispersion, and Resuspension in Vicinity of Ocean Wastewater Plume. *Journal of Hydraulic Engineering*, *118*(1), 38–58.
URL http://ascelibrary.org/doi/10.1061/%28ASCE%290733-9429%281992%29118%3A1%2838%29

Washburn, L., McClure, K. A., Jones, B. H., & Bay, S. M. (2003). Spatial scales and evolution of stormwater plumes in Santa Monica Bay. *Marine Environmental Research*, *56*(1-2), 103–125.
URL https://linkinghub.elsevier.com/retrieve/pii/S0141113602003276

Wernberg, T., Bennett, S., Babcock, R. C., De Bettignies, T., Cure, K., Depczynski, M., Dufois, F., Fromont, J., Fulton, C. J., Hovey, R. K., Harvey, E. S., Holmes, T. H., Kendrick, G. A., Radford, B., Santana-Garcon, J., Saunders, B. J., Smale, D. A., Thomsen, M. S., Tuckett, C. A., Tuya, F., Vanderklift, M. A., & Wilson, S. (2016). Climate-driven regime shift of a temperate marine ecosystem. *Science*, *353*(6295), 169–172.
URL https://www.science.org/doi/10.1126/science.aad8745

Wickliffe, L. C., Jossart, J. A., Theuerkauf, S. J., Jensen, B. M., King, J. B., Henry, T., Sylvia, P. C., Morris, J. A., & Riley, K. L. (2024). Balancing conflict and opportunity - spatial planning of shellfish and macroalgae culture systems in a heavily trafficked maritime

port. *Frontiers in Marine Science*, *10*, 1294501.
URL https://www.frontiersin.org/articles/10.3389/fmars.2023.1294501/full

Williams, J., Claisse, J., Pondella Ii, D., Williams, C., Robart, M., Scholz, Z., Jaco, E., Ford, T., Burdick, H., & Witting, D. (2021). Sea urchin mass mortality rapidly restores kelp forest communities. *Marine Ecology Progress Series*, *664*, 117–131.
URL https://www.int-res.com/abstracts/meps/v664/p117-131/

Wolter, K., & Timlin, M. S. (2011). El Niño/Southern Oscillation behaviour since 1871 as diagnosed in an extended multivariate ENSO index (MEI.ext). *International Journal of Climatology*, *31*(7), 1074–1087.
URL https://onlinelibrary.wiley.com/doi/10.1002/joc.2336

Xu, S., Yu, Z., Zhou, Y., Yue, S., Liang, J., & Zhang, X. (2023). The potential for large-scale kelp aquaculture to counteract marine eutrophication by nutrient removal. *Marine Pollution Bulletin*, *187*, 114513.
URL https://linkinghub.elsevier.com/retrieve/pii/S0025326X2201195X

Zhao, S.-J., Jiao, N.-Z., Shen, Z.-L., & Wu, Y.-L. (2005). Causes and Consequences of Changes in Nutrient Structure in the Jiaozhou Bay. *Journal of Integrative Plant Biology*, *47*(4), 396–410.
URL https://onlinelibrary.wiley.com/doi/10.1111/j.1744-7909.2005.00005.x

Zhu, L., Lei, J., Huguenard, K., & Fredriksson, D. W. (2021). Wave attenuation by suspended canopies with cultivated kelp (Saccharina latissima). *Coastal Engineering*, *168*, 103947.
URL https://linkinghub.elsevier.com/retrieve/pii/S0378383921001058

Zimmerman, R., & Kremer, J. (1986). In situ growth and chemical composition of the giant kelp, Macrocystis pyrifera: response to temporal changes in ambient nutrient availability. *Marine Ecology Progress Series*, *27*, 277–285.
URL http://www.int-res.com/articles/meps/27/m027p277.pdf

Zimmerman, R. C., & Kremer, J. N. (1984). Episodic nutrient supply to a kelp forest ecosystem in Southern California. *Journal of Marine Research*, *42*(3), 591–604.

URL http://www.ingentaconnect.com/content/jmr/jmr/1984/00000042/00000003/art00008